

Implementing the LWD for MoDOT Construction Acceptance of Unbound Material Layers



November 2022
Final Report

Project number TR202103
MoDOT Research Report number cmr 22-011

PREPARED BY:

Xiong Zhang, Ph.D., P. E.

Jenny Liu, Ph.D., P. E.

Beshoy Riad, Ph.D.

Chuanjun Liu

Missouri University of Science and Technology

PREPARED FOR:

Missouri Department of Transportation

Construction and Materials Division, Research Section

TECHNICAL REPORT DOCUMENTATION PAGE

1. Report No. cmr 22-011	2. Government Accession No.	3. Recipient's Catalog No.	
4. Title and Subtitle Implementing the LWD for MoDOT Construction Acceptance of Unbound Material Layers		5. Report Date June 2022 Published: November 2022	
		6. Performing Organization Code	
7. Author(s) Xiong Zhang, Ph.D., P. E. Jenny Liu, Ph.D., P. E. Beshoy Riad, Ph.D. Chuanjun Liu		8. Performing Organization Report No.	
9. Performing Organization Name and Address Department of Civil, Architectural and Environmental Engineering Missouri University of Science and Technology 1401 N. Pine St. Rolla, MO 65409		10. Work Unit No.	
		11. Contract or Grant No. MoDOT project # TR202103	
12. Sponsoring Agency Name and Address Missouri Department of Transportation (SPR-B) Construction and Materials Division P.O. Box 270 Jefferson City, MO 65102		13. Type of Report and Period Covered Final Report (October 2020-June 2022)	
		14. Sponsoring Agency Code	
15. Supplementary Notes Conducted in cooperation with the U.S. Department of Transportation, Federal Highway Administration. MoDOT research reports are available in the Innovation Library at https://www.modot.org/research-publications .			
16. Abstract Conventional density-based methods of compaction quality assurance (QA) using nuclear density gauges (NDG) have been the practice for many years. However, NDG testing becomes less desirable because of safety, regulatory, and cost concerns. In addition, density is not a direct input to the structural design of the pavements and is not directly linked to pavement performance. In recent years, modulus-based compaction QA of unbound materials is gaining attention, as it can not only result in a better constructed product but also provide the engineering properties critical for better understanding of the connection between pavement design and long-term pavement performance. Moisture content is one of the main factors influencing soil modulus and should also be performed concurrent with field modulus measurement. However, existing LWDs do not have the function to measure moisture content. In this study, a national survey on acceptance of LWD and a substantial literature review were firstly carried out to study the current status of LWD application. Then, four types of representative soils from two projects provided by MoDOT were selected to investigate the implementation of LWD for construction acceptance of unbound materials. Four LWD devices including three Zorn ZFG 2000 and one Zorn ZFG lab 3.0, were used in laboratory and field tests. Furthermore, two moisture content analyzers including Aggrameter and Ohaus MB120 were chosen to evaluate their practicability of quick moisture content measurement in the field. Based on the results of considerable laboratory and field tests, it was concluded that the modulus-based construction quality assessment method using LWD and moisture content analyzer Ohaus MB120 worked well at four construction sites. In addition, a guideline was created for the use of the modulus-based method in the appendix.			
17. Key Words Construction acceptance; LWD implementation; Unbound materials; Moisture content analyzer		18. Distribution Statement No restrictions. This document is available through the National Technical Information Service, Springfield, VA 22161.	
19. Security Classif. (of this report) Unclassified.	20. Security Classif. (of this page) Unclassified.	21. No. of Pages 128	22. Price

IMPLEMENTING THE LWD FOR MODOT CONSTRUCTION ACCEPTANCE OF UNBOUND MATERIAL LAYERS

Prepared for
Missouri Department of Transportation

By
Xiong Zhang, Ph.D., P. E.,
Jenny Liu, Ph.D., P. E.,
Beshoy Riad, Ph.D., and
Chuanjun Liu

Department of Civil, Architectural and Environmental Engineering
Missouri University of Science and Technology

June 22, 2022

COPYRIGHT PERMISSIONS

Authors herein are responsible for the authenticity of their materials and for obtaining written permissions from publishers or individuals who own the copyright to any previously published or copyrighted material used herein.

DISCLAIMER

The content of this report reflects the views of the authors, who are responsible for the facts and the accuracy of the data presented herein. The contents do not necessarily reflect the official view or policies of the Missouri Department of Transportation (MoDOT). This report does not constitute a standard, specification, or regulation.

ACKNOWLEDGMENTS

The authors are thankful for the MoDOT's sponsorship of this research project. They wish to express their appreciation to all project advisory committee members. They would also like to thank Eric Kopinski, Tabitha Locke, and Brendan Kuehn from the I-270 North project, as well as James Pflum and Ryan Kneib from the Buck O'Neil Bridge project, for their great help and collaboration during coordination and project visits.

Acknowledgment is extended to people from Missouri S&T, including graduate students Javad Galinmoghadam, Bo Lin, Hanli Wu, Xiaolong Xia, Sara Fayek, Farshad Saberi Kerahroudi, and Anyou Zhu, undergraduate student Andrew Mikes, and technicians Greg Leckrone, John Whitchurch, and Jeffrey P. Heniff for assistance during the lab and field work.

EXECUTIVE SUMMARY

Conventional density-based methods of compaction quality control/assurance (QC/QA) using nuclear density gauges (NDG) have been the practice for many years. However, NDG testing becomes less desirable because of safety, regulatory, and cost concerns. In addition, density is not a direct input to the structural design of the pavements and is not directly linked to pavement performance.

In recent years, modulus-based compaction QA of unbound materials is gaining attention. It can not only result in a better constructed product but also provide the engineering properties critical for better understanding of the connection between pavement design and long-term pavement performance. Several state DOTs have implemented modulus-based specifications using lightweight deflectometer (LWD). Missouri Department of Transportation (MoDOT) is interested in exploring the use of the LWD as replacement of the NDG and creating standards for acceptance of unbound material layers and some preliminary studies have been performed.

Although the findings from this prior research can be helpful, the LWD modulus-based QA specifications resulted from the previous studies may not be directly used due to the differences in typical unbound geomaterial types and equipment conditions in Missouri. More research is needed to evaluate the performances of LWDs before they are implemented as tools for construction acceptance for unbound material layers.

The objective of this project is to develop standards for the implementation of the Zorn LWD for the acceptance of unbound material layers on MoDOT projects.

A comprehensive literature review was first conducted to gather information on the current compaction QA practices to study the applicability of implementing a LWD for the construction acceptance of unbound granular materials. A survey was also conducted to inquire about highway agencies' construction acceptance specifications for unbound materials layers and their practices and experience using the LWD for compaction QC/QA. In total, 46 DOTs responded to the survey. Almost 94.0% of the state DOTs (43 DOTs) use the density-based specifications for compaction QC/QA of unbound materials. All these states use NDG to determine the in-situ density. Of these 43 DOTs, 11 are not specifying any field moisture content (MC) requirements. 6.5% of the responded state DOTs (3 DOTs - Nebraska, Indiana, and Minnesota) implemented and used the LWD for compaction QC/QA of unbound materials. 63.0% of the respondents are unfamiliar with the LWD and never used it, even for evaluation or demonstration purposes. The rest of the DOTs were evaluated (in-house or through a university/consultant) or demonstrated using LWD. The Nebraska DOT specifies only the LWD for compaction QC and QA purposes.

Four construction sites from the I-270 North and Buck O'Neil Bridge projects were selected to verify the proposed LWD modulus-based QA approach under field conditions. Four types of soils including a well graded sand (SW), a lean clay, a base aggregate, and

a silty clay, were tested in the field and laboratory to achieve the objectives of the proposed research.

A series of laboratory tests were performed on the four soils, including (1) basic physical soil property tests such as sieve analysis, Atterberg limits, modified Proctor compaction, and soil water characteristic curve tests, (2) LWD test on Proctor mold via Zorn ZFG Lab 3.0 LWD device, (3) evaluation of the efficiency of field moisture content measurement devices, and (4) repeated load triaxial test.

Repeated load triaxial test results were performed at a span of moisture contents for the four soils, which showed that resilient modulus (M_R) generally decreased with increasing the moisture contents and increased with increasing bulk stresses for all tested soils. Moreover, a new model was proposed based on the Mechanistic-Empirical Pavement Design Guide (MEPDG) model, in which the impact of the moisture content on the M_R was considered. Comparison of coefficients of determination between the new and MEPDG models revealed that the new model had better prediction reliability than the MEPDG model.

LWD tests were performed on Proctor mold to investigate the influences of the applied stress and moisture content on the LWD modulus. It was found that increases in the applied stress resulted in an increase in the LWD modulus, and the LWD modulus decreased with an increase in the moisture content. The LWD lab tests were used to perform regression analyses and provide coefficients for a two-variable quadratic equation to predict field LWD modulus, where the required inputs for the equation were the field applied stress and in-situ moisture content. Analyses results indicate that the equation can provide the best prediction for field LWD modulus for the well graded sand, while the predictions for the silty clay were better than those for the base aggregate, and the predicted results for the lean clay had the least accuracy with an R^2 of 0.7.

The moisture content is one of the main factors influencing soil modulus and should also be performed concurrent with field modulus measurement. However, existing LWDs do not have the function to measure moisture content. In this research project, two field moisture content measurement devices, e.g., the Ohaus MB120 and the Aggrameter, were evaluated as alternatives to the NDG for moisture content measurements. Results indicated that the Ohaus can produce moisture content measurements with high accuracy and precision for both the well graded sand and clay soils, and fair results for the base aggregate because of limited weight capacity. It was found that sometimes it was difficult to perform moisture content measurements using the Ohaus MB120 at site due to lack of a leveled ground and vibratory environment. It was also found that the Aggrameter is not suitable for moisture content measurements for the clayey soils and base aggregate, while for the well graded sand, the Aggrameter showed good practicality and accurate moisture content measurements in the field compared with the oven-dry method.

Field LWD tests were performed both immediately after the compaction and two hours after compaction. It was found that two hours after the compaction, the soil moisture normally decreased due to evaporation, and the LWD moduli increased slightly

accordingly. It was also found that the moisture content changed more in fine-grained soils than coarse-grained soils, mainly attributed to a higher unsaturated permeability in fine-grained soils.

Analyses of contours of moisture contents and field LWD moduli obtained from different devices (described in 3.1.1 Zorn LWDs) indicated that LWD moduli contours obtained from the three devices for the same test sections shared the same or similar patterns most of the time, indicating that all devices can correctly measure the trend of the LWD modulus. It was also found that the moisture content contours were closely related to the LWD modulus contours, but with larger variations at many cases. This can be attributed to the fact that the moisture content is an important influencing factor on the LWD moduli, but it is not the only influencing factor. Other factors such as degree of compaction also influence the LWD moduli.

It was found that all moisture contents at the lean clay and the silty clay sites were much higher than the acceptable moisture content ranges. Consequently, the compaction quality was not acceptable. The moisture contents at the well graded sand and the base aggregate sites were well-controlled in the acceptable ranges. The ratio of the field to target LWD modulus was used to evaluate whether the LWD modulus results were acceptable. It was found that the predictions from the three LWD devices were consistent. For example, among 47 points that all three devices tested at the base aggregate site, 20 points (42.6%) were predicted acceptable by all three devices, while for 14 points (29.8%), all three devices predicted unacceptable results. 13 points (27.7%) were considered unacceptable by one or two of the three LWD devices. It seems that LWD 4421 had a more lenient acceptance criterion.

Overall, the results obtained from this study indicated that all three LWD devices can provide reasonable and consistent results for QA/QC for field compaction. The devices were easy to use, and the tests can be performed rapidly in the field with less interference with the compaction process. Since the moisture content at neither the lean clay nor the silty clay site was fallen in the acceptable moisture content ranges, the conclusions obtained from this study are only applicable for coarse-grained soils. More study is needed to evaluate the performance of the LWD test for fine-grained soils in Missouri.

TABLE OF CONTENTS

Executive Summary	vi
Table of Contents	ix
List of Figures	xi
List of Tables	xiv
CHAPTER 1 Introduction.....	1
1.1 Problem Statement.....	1
1.2 Research Objectives.....	1
1.3 Research Methodology	2
CHAPTER 2 Literature Review	4
CHAPTER 3 Laboratory Testing.....	6
3.1 LWD and Moisture Content Testing Equipment	6
3.1.1 Zorn LWDs	6
3.1.2 Ohaus MB120	8
3.1.3 Aggrameter	9
3.2 Laboratory Testing for Collected Materials.....	12
3.2.1 Material Characterization.....	12
3.2.2 Compaction Test Results	17
3.2.3 LWD Testing on Proctor Mold	20
3.2.4 Determination of Regression Coefficients.....	35
3.3 Lab Moisture Content Measurements Using Field Moisture Content Devices	35
3.3.1 Field Moisture Content Devices Soil-Specific Calibration	35
3.3.2 Validation with the LWD Test on Proctor Mold Test	39
3.4 Resilient Modulus Testing	42
3.4.1 Developing a New Resilient Modulus Prediction Model	60
CHAPTER 4 Findings from Field Testing	64
4.1 Introduction.....	64
4.2 Field Projects and Testing Method	64
4.2.1 Introduction to Testing Sites.....	64
4.2.2 Testing Procedure	70
4.2.3 Determination of Field LWD Modulus.....	72
4.3 Evaluation of the Moisture Detection Devices in the Field.....	73
4.4 Evaluation of LWD Devices in the Field.....	77
4.5 Evaluation of Moisture Content-Modulus Correlation in the Field.....	80
4.5.1 Relationship Between Moisture Content and LWD Modulus Right After Compaction	80
4.5.2 Relationship Between Moisture and LWD Modulus Two Hours after Construction	93
4.6 Evaluation of Field Construction	95
4.6.1 Acceptance Criterion–Moisture Content	95

4.6.2 Acceptance Criterion–Field to Target LWD Modulus Ratio.....	97
CHAPTER 5 Conclusions.....	100
References.....	103
Appendix.....	A-1
A. Weather Condition of Four Sites During Testing	A-1
B. Guideline of Implementing LWD Devices on QC/QA for Unbound Material Layers B-	
1	

LIST OF FIGURES

Figure 3.1 Configurations of the LWD (Zorn ZFG 2000).....	7
Figure 3.2 Zorn equipment.	7
Figure 3.3 Ohaus MB120.....	8
Figure 3.4 Comparison of moisture content measurements by the Ohaus MB120 and oven for different soils.....	9
Figure 3.5 Aggrameter from the James Instruments.....	10
Figure 3.6 Aggrameter and acrylic test box.....	11
Figure 3.7 Aggrameter readings versus layer thickness.	11
Figure 3.8 Aggrameter readings versus compaction energy.....	12
Figure 3.9 Gradations of the four soils.	13
Figure 3.10 SWCCs for the four collected geomaterials.	17
Figure 3.11 Moisture-density relationships of the four soils.	19
Figure 3.12 Moisture content-density relationships for the lean clay along with the corresponding MCs for common relative compaction values (98%, 95%, and 90%).....	21
Figure 3.13 Moisture-density relationships for the well graded sand along with the corresponding MCs for common relative compaction values (98%, 95%, and 90%).....	22
Figure 3.14 Moisture-density relationships for the base aggregate along with the corresponding MCs for common relative compaction values (98%, 95%, and 90%).....	22
Figure 3.15 Moisture-density relationships for the silty clay and the corresponding MCs for common relative compaction values (98%, 95%, and 90%).....	23
Figure 3.16 Schematic plot for the single degree of freedom mechanism for the LWD-soil motion.	24
Figure 3.17 LWD test on Proctor mold.	25
Figure 3.18 Common time-deflection curves from LWD test (Fleming et al., 2009).	26
Figure 3.19 Time-deflection curves from LWD testing on the well graded sand and the lean clay for seating and measurement drops.	27
Figure 3.20 Time-deflection curves for low-quality tests.....	28
Figure 3.21 LWD testing on Proctor mold results for the lean clay.	31
Figure 3.22 LWD testing on Proctor mold results for the well graded sand.	32
Figure 3.23 LWD testing on Proctor mold results for the base aggregate.....	33
Figure 3.24 LWD testing on Proctor mold results for the silty clay.....	34
Figure 3.25 Ohaus MB120 calibration for the four soils.	38
Figure 3.26 Aggrameter calibration for the lean clay and well graded sand.	39
Figure 3.27 Steps for Aggrameter testing on a lean clay sample.....	40
Figure 3.28 Ohaus MB120 and Aggrameter moisture content versus oven moisture content for the lean clay.....	41
Figure 3.29 Ohaus MB120 and Aggrameter moisture content versus oven moisture content for the well graded sand.	41

Figure 3.30 Ohaus MB120 moisture content versus oven moisture content for the base aggregate.	42
Figure 3.31 Ohaus MB120 moisture content versus oven moisture content for the silty clay.	42
Figure 3.32 RLTT wave shape and terms: contact stress, cyclic axial stress, and maximum applied stress (AASHTO T 307, 1999).	43
Figure 3.33 MTS 858 load frame and used cells for M_R tests.	45
Figure 3.34 M_R test results at different confining pressures and different moisture contents for the lean clay.	48
Figure 3.35 M_R test results at different confining pressures and different moisture contents for the well graded sand.	50
Figure 3.36 M_R test results at different confining pressures and different moisture contents for the base aggregate.	53
Figure 3.37 M_R test results at different confining pressures and different moisture contents for the silty clay.	55
Figure 3.38 M_R changes with moisture content and bulk stress for the lean clay.	56
Figure 3.39 M_R changes with moisture content and bulk stress for the well graded sand.	57
Figure 3.40 M_R changes with moisture content and bulk stress for the base aggregate. ..	57
Figure 3.41 M_R changes with moisture content and bulk stress for the silty clay.	58
Figure 3.42 Comparison between the MEPDG and the proposed prediction model.	63
Figure 4.1 Location and field view of four tested sites.	66
Figure 4.2 Points distribution at the lean clay site.	67
Figure 4.3 Points distribution at the well graded sand site.	68
Figure 4.4 Points distribution at the base aggregate site.	69
Figure 4.5 Points distribution at the silty clay site.	70
Figure 4.6 Moisture content measurement comparison between the Ohaus MB120 and oven for the lean clay.	74
Figure 4.7 Moisture content measurement comparison between the Ohaus MB120, Aggrameter, NDG, and oven for the well graded sand.	75
Figure 4.8 Moisture content measurement comparison between the Ohaus MB120 and oven for the base aggregate.	76
Figure 4.9 Moisture content measurement comparison between the Ohaus MB120, NDG, and oven for the silty clay.	76
Figure 4.10 Correlations of LWD devices at the lean clay site.	78
Figure 4.11 Correlations of LWD devices at the well graded sand site.	78
Figure 4.12 Correlations of LWD devices at the base aggregate site.	79
Figure 4.13 Correlations of LWD devices at the silty clay site.	79
Figure 4.14 Moisture contents and LWD moduli spatial distribution at the lean clay site.	84

Figure 4.15 Moisture contents and LWD moduli spatial distribution of the well graded sand in section 1.....	85
Figure 4.16 Moisture contents and LWD moduli spatial distribution of the well graded sand in section 2.....	86
Figure 4.17 Moisture contents and LWD moduli spatial distribution of the base aggregate in section 1.	88
Figure 4.18 Moisture contents and LWD moduli spatial distribution of the base aggregate in section 2.	89
Figure 4.19 Moisture contents and LWD moduli spatial distribution of the base aggregate in section 3.	90
Figure 4.20 Moisture contents and LWD moduli spatial distribution at the silty clay site.	93
Figure 4.21 Instant and after-2h comparison of moisture contents and LWD moduli at the well graded sand site.	94
Figure 4.22 Instant and after-2h comparison of moisture contents and LWD moduli at the lean clay site.....	94
Figure 4.23 Moisture content range of testing points at the lean clay site.....	95
Figure 4.24 Moisture content range of testing points at the well graded sand site.....	96
Figure 4.25 Moisture content range of testing points at the base aggregate site.	96
Figure 4.26 Moisture content range of testing points at the silty clay site.	97
Figure 4.27 Field to target LWD modulus ratios of testing points at the well graded sand site.	98
Figure 4.28 Field to target LWD modulus ratios of testing points at the base aggregate site.	99

LIST OF TABLES

Table 3.1 Zorn LWDs configurations.....	8
Table 3.2 Material description.....	13
Table 3.3 Salt concentrations and corresponding suction.....	14
Table 3.4 Calibrated fitting parameters and R^2 for each collected unbound material.....	17
Table 3.5 OMCs and MDDs for the four collected soils.....	19
Table 3.6 Target values for the lean clay.....	20
Table 3.7 Target values for the well graded sand.....	20
Table 3.8 Target values for the base aggregate.....	21
Table 3.9 Target values for the silty clay.....	21
Table 3.10 Reduced LWD drop heights and the corresponding applied forces.....	24
Table 3.11 Typical Poisson's ratio values for different geomaterials from MEPDG.....	29
Table 3.12 Regression coefficients in the prediction model for four soils.....	35
Table 3.13 Ohaus MB120 and Aggrimeter calibration results.....	36
Table 3.14 Testing sequence for subgrade soils (AASHTO T 307, 1999).....	44
Table 3.15 Testing sequence for base/subbase soils (AASHTO T 307, 1999).....	44
Table 3.16 Regression parameters of the MEPDG model for the lean clay.....	59
Table 3.17 Regression parameters of the MEPDG model for the well graded sand.....	59
Table 3.18 Regression parameters of the MEPDG model for the base aggregate.....	60
Table 3.19 Regression parameters of the MEPDG model for the silty clay.....	60
Table 3.20 Calibrated parameters for the new model.....	61
Table 4.1 Filed visit date and construction soils.....	66
Table 4.2 Average of weather conditions and soil temperatures at four sites.....	66
Table 4.3 Properties of LWD devices used in the field.....	71
Table 4.4 Stress distribution factors for different types of soils.....	73
Table 4.5 R^2 for correlations between the three LWD devices.....	77

CHAPTER 1 INTRODUCTION

1.1 Problem Statement

The foundations of most roads and pavements are prepared by compacting unbound geomaterials under unsaturated conditions, where the unbound materials are usually solely graded soil, including gravel, sand, silt, and clay, without binder or cement material. Conventional density-based methods of compaction quality control/assurance (QC/QA) using nuclear density gauges (NDG) have been the practice for many years. However, the NDG testing becomes less desirable because of safety, regulatory, and cost concerns. In addition, the density is not a direct input to the structural design of the pavements and is not directly linked to the pavement performance.

The modulus is a fundamental material input required for the structural design of pavements. In recent years, modulus-based compaction QA of unbound materials is gaining attention since it will not only result in a better constructed product but also provide the engineering properties critical for better understanding of the connection between pavement design and long-term pavement performance. Several state DOTs have implemented modulus-based specifications using lightweight deflectometer (LWD), which is a portable device that can be used to measure the surface modulus of unbound layers directly in the field. MoDOT is interested in exploring the use of the LWD as replacement of the NDG and create standards for acceptance of unbound material layers. Recently MoDOT participated in a pooled fund project with Maryland DOT *“Standardizing Lightweight Deflectometer Modulus Measurements for Compaction Quality Assurance.”* The research findings led to two modulus-based QA procedures/specifications intended for practical implementation by state DOTs and engineers.

Although the findings from this prior research can be helpful in producing standards for the use of the LWD in Missouri, the LWD modulus-based QA specifications resulted from this pooled fund study may not be directly used due to the difference in typical unbound geomaterial types and equipment conditions in Missouri. More research is needed to evaluate the performances of LWDs before they are implemented as a tool for construction acceptance for unbound material layers. Moisture content (MC) is one of the main factors influencing soil modulus and should also be performed concurrent with field modulus measurement. However, existing LWDs do not have the function to measure moisture content. As a result, an appropriate rapid and accurate method of moisture content measurements must also be identified and included in the LWD modulus-based QA specifications.

1.2 Research Objectives

The principal objective of this project is to develop standards for the implementation of the Zorn LWD for the acceptance of unbound material layers on MoDOT projects, which includes the following elements:

- Literature review of existing applications of LWDs for modulus-based QA;

- Evaluation of moisture, stress states, and spatial variability on measured LWD modulus;
- Determining the target modulus range for the field through laboratory LWD tests on Proctor mold for samples of various soil types prepared at optimum and field conditions;
- Identification of rapid, reliable, and accurate field moisture content measurement alternatives to NDG;
- Correlating field target modulus with LWD field modulus and verification of the proposed LWD modulus-based QA approach under field conditions; and
- Drafting practical LWD modulus-based QA specifications, including recommendations on measuring moisture content in the field.

1.3 Research Methodology

To meet the objectives of this study, the following major tasks were accomplished:

- Task 1: Literature Review and Survey
- Task 2: Material Collection
- Task 3: Laboratory Testing
- Task 4: Field Testing
- Task 5: Draft Specifications and Standards

Task 1: Literature Review and Survey

A comprehensive literature review was conducted to gather information related to the state-of-the-art and current compaction QC/QA practices using different in-situ spot testing tools, including the usage of LWD, through published reports and research articles. The previous practices in implementing specifications for compaction quality control using the LWD in different states have been reviewed. Moreover, an online survey was distributed to all the state DOTs to collect information about the current compaction QA practices and their practical experience with LWD. In total, 46 DOTs responded to the survey. The survey consists of three main sections as follows:

- Current practices for compaction QA of unbound materials;
- Current LWD QA specifications and the practical use experiences, including the extent of LWD use in terms of the number of projects and soil types; and
- DOTs' practical experience related to field moisture content measurements.

The interim project report presents a full version of the comprehensive literature review and survey results. A summary of the main findings of the literature and the survey results were documented in Chapter 2.

Task 2: Material Collection

Four different types of geomaterials were collected from construction sites in Missouri. These materials covered a wide range of soils, from cohesive, fine-grained to cohesionless and coarse-grained soils. The materials are 1) the lean clay used for embankment construction, 2) the well graded sand (SW) used as a backfill material during the construction of mechanically stabilized earth (MSE) walls, 3) coarse aggregates used as a base course material, and 4) silty clay used for the construction of

bridge approaches. These materials are typically used for road construction purposes in Missouri.

Task 3: Laboratory Testing

A comprehensive laboratory testing program was conducted on the soil samples collected from the construction projects. The laboratory tests are listed as follows, and the experimental details are presented in Chapter 3.

- fundamental materials properties such as gradation sieve analysis based on ASTM D422, Atterberg limits as per ASTM D4318, and specific gravity testing as per ASTM D854-14 for fine-grained soils (size<4.75mm) and ASTM C127-15 for aggregates (size>4.75mm) (ASTM C127, 2016; ASTM D854, 2016; ASTM D4318, 2018; ASTM D7928, 2021);
- soil classification based upon both Unified and AASHTO soil classification system (AASHTO M 145, 1991; ASTM D2487, 2020);
- compaction tests to obtain the optimum moisture content (OMC) and maximum dry density (MDD) (ASTM D1557, 2021);
- LWD tests on top of the compaction mold using Zorn ZFG Lab-3 LWD;
- Moisture content tests using Ohaus MB120 Moisture Analyzer (Ohaus MB120 hereafter) and Aggrameter Moisture Detector (Aggrameter hereafter) devices and comparison with the moisture content measured by conventional oven; and
- repeated load triaxial tests as per AASHTO T307 at different compaction moisture contents (AASHTO T 307, 1999).

Task 4: Field Testing

Four field-testing campaigns were performed in this project. The tested soils were compacted well graded sand, compacted lean clay, compacted base aggregate, and compacted silty clay. Details of field-testing activities and analysis of test results are provided in Chapter 4, as well as an evaluation of moisture content and field to target LWD modulus ratio acceptance for each material.

Tasks 5: Draft Specifications and Standards

The draft “*Standard Method of Test for Laboratory Determination of Target Modulus Using LWD Drops on Compacted Proctor Mold*” and “*Standard Method of Test for Compaction Quality Control Using Light Weight Deflectometer*” was developed in a previous study (Schwartz et al., 2017). The study was used as references for lab and field testing in Tasks 3 and 4. Therefore, the research team revised and refined the documents to include the findings from this study. The revised documents were formatted into the guideline for implementing and using LWD testing specifically for projects in Missouri (e.g., available equipment – Zorn ZFG 2000 LWD, typical Missouri soil types). The field compaction QA procedure also included the associated field moisture content measurement device, identified from Task 3 and further verified in Task 4. The enhanced LWD specifications in designated format are provided in the appendix.

CHAPTER 2 LITERATURE REVIEW

A full version of the comprehensive literature review and survey results were presented in the interim project report (Beshoy et al., 2021). The main findings and recommendations from the literature and the survey results are summarized as follows.

The current density-based QC specifications are relatively simple and practical. The NDG is currently used by most of the state DOTs to assess the compaction quality for various types of unbound materials. Among all density-based devices, it is one of the few devices that can provide both moisture content and density measurements. However, NDG testing becomes less desirable because of safety, regulatory, and cost concerns. During the past decade, various non-radioactive devices for the field determination of density/moisture content have been proposed and evaluated. Their pros and cons were identified in past research studies, and more studies are needed for further evaluation. In addition, density-based QC specifications do not provide the engineering properties that can be used to ensure optimal performance of the tested material. Though efforts have been dedicated to correlating NDG measurements and the measured soil strength/stiffness, they were not successful. General research and engineering practices to develop stand-alone modulus-based specifications can be noticed and should be encouraged. This will result in better quality control, and therefore, a better-constructed product. Moreover, it will provide engineering properties that can be linked to pavement design and, in turn, long-term pavement performance.

With the growing interests in modulus-based compaction QA of unbound materials, several in situ test devices have been utilized to assess the mechanical properties of geomaterials, including but not limited to Briard compaction Device (BCD), Clegg Hammer (CH), Dynamic Cone Penetrometer (DCP), Soil Compaction Supervisor (SCS), Soil Stiffness Gauge (SSG), LWD, and Portable Seismic Property Analyzer (PSPA). Among these devices, the DCP, SSG, and LWD are the most studied and used devices among state DOTs in the United States. Internationally, the most commonly adopted techniques for compaction QC of unbound aggregate layers are the LWD, SSG, and surface seismic. However, SSG has not been implemented into any of the QC/QA specifications, nationally and internationally, and DOTs that evaluated it reported poor to fair accuracy and repeatability (Nazzal, 2014). Several state DOTs (e.g., Illinois, Indiana, Missouri, Minnesota, and Nebraska) have implemented modulus-based specifications using LWD and DCP. DCP had very good repeatability and accuracy, however, it cannot be used for oversized aggregates (>2 in, 51 mm) or soft clays. The LWD is a versatile and portable stiffness measuring tool. It has been increasingly used on a variety of unbound materials, including during construction and in-service around the world, and successfully used for broader applications related to the transportation industry compared to all other compaction QC devices. Studies recommended it for a modulus-based construction specification to accept compacted geomaterials but did indicate high degree of spatial variability and significant effect of moisture content on LWD modulus, which is one of the common challenges associated with modulus-based devices.

To facilitate further implementation of modulus-based QA specifications, it's strongly recommended to identify an accurate, rapid, and cost-effective field moisture content device included in the modulus-based QA specifications. Moisture content is one of the main factors influencing soil modulus and should be performed concurrently with field modulus measurement for compaction QA.

In addition, with the growing interests and increasing use of the LWD as replacement of the NDG, systematically investigation of important influencing factors on measured LWD modulus such as moisture, stress states, spatial variability, and development of reliable correlations with the NDG are needed to gain a better understanding of this relatively new technique. Other parameters such as types and makes of the LWD (e.g., target field values, the plate size and falling mass drop height) and pavement layer properties (e.g., Poisson's ratio, multi-layer or singly-layer system) should be considered as well to obtain consistent and reliable data for the purpose of developing LWD specifications. More research is needed to improve the repeatability and reproducibility of LWDs, including optimization of data analysis and local calibration protocols. A comparative study would be helpful to identify the most robust, accurate, and practical data analysis procedure to be implemented into LWD software for in-situ compaction evaluation. Proper training for field inspectors, contractors, and technicians is also needed for practical implementation by state DOTs and engineers.

CHAPTER 3 LABORATORY TESTING

This chapter consists of a description of the equipment used in this research. In addition, the laboratory testing details are provided, including the materials, characterization, specimen preparation, testing setup, and testing methods. Moreover, compaction testing results for every material and the corresponding MDD and OMC are shown. Details for the LWD test on Proctor mold are presented and discussed. Finally, repeated load triaxial tests were conducted to evaluate the collected materials' stress dependency properties and permanent deformation.

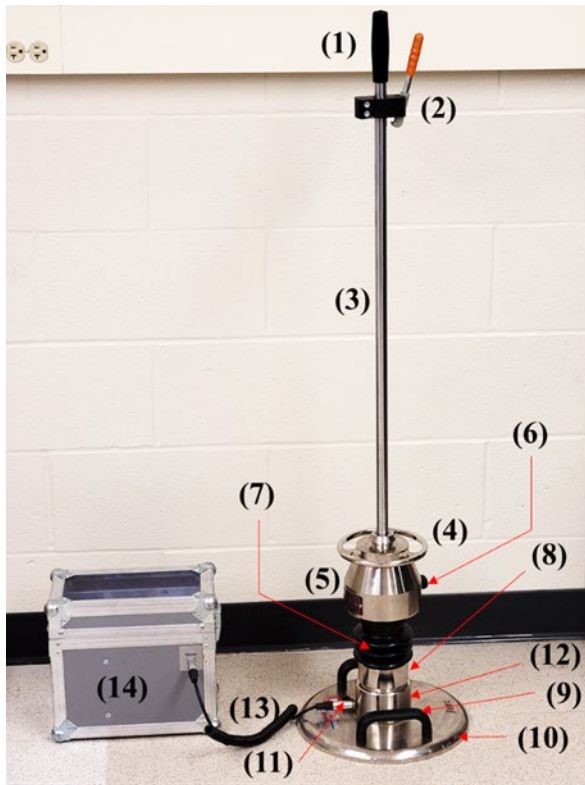
3.1 LWD and Moisture Content Testing Equipment

This section provides working principles and calibration procedures for the LWD project-related equipment, including Zorn ZFG 2000 and Zorn ZFG Lab-3 LWDs, Ohaus MB120, and Aggrameter.

3.1.1 *Zorn LWDs*

MoDOT owns four Zorn LWDs — two Zorn 2000-300mm (12 in) plate diameter versions, one Zorn-2000-200mm (8 in) plate diameter version, and one Zorn-Lab version with 6 in (150 mm) plate diameter. Figure 3.1 shows the configurations of Zorn ZFG 2000 LWD with 12 in (300 mm)-diameter loading plate. The Zorn device was developed based on extensive model calculations and parametric studies and is also prescribed in German specifications for road construction (TP BF-StB Part B 8.3, 2012). The applied load of Zorn ZFG 2000 is assumed to be constant and equal to 1589.40 lbf (7.07 kN). The deflection of the loading plate is calculated by double integrating the acceleration with measuring capacity ranges from 0.0079 to 1.1811 in (0.20 to 30 mm). This device is recommended for use on stiff cohesive soils, mixed soils, and coarse-grained soils having a maximum particle size of 2.48 in (63 mm). The Missouri S&T research team borrowed these LWDs for laboratory and field-testing purposes. Figure 3.2 shows these three different versions of Zorn LWDs, along with the corresponding data loggers and field transportation trolley.

Although four different Zorn LWDs are used, the testing principles are the same. The differences between them are the loading plate diameter and the applied load. Table 3.1 shows the different configurations for each LWD version.



- (1) grip;
- (2) top fix and release mechanism;
- (3) guide rod;
- (4) round grip;
- (5) falling weight;
- (6) lock pin;
- (7) set of steel springs;
- (8) anti tipping fixture;
- (9) plate carry grip;
- (10) loading plate;
- (11) socket for connection to electronic device;
- (12) adapter plate;
- (13) connection wire;
- (14) electronic data acquisition system

Figure 3.1 Configurations of the LWD (Zorn ZFG 2000).



a) three different versions of ZORN LWDs along with the corresponding data loggers



b) field transportation trolley

Figure 3.2 Zorn equipment.

Table 3.1 Zorn LWDs configurations.

Version	Plate style	Plate diameter (in)	Falling height (in)	Falling weight mass (lbm)	Plate mass (lbm)	Applied force (kip)
ZORN 2000-300mm	Solid	12	28.35	22.05	33.07	1.59
ZORN 2000-200mm		8	22.05	22.05	33.07	1.24
ZORN Lab-3.0		6	14.76	11.02	33.07	0.80

3.1.2 Ohaus MB120

The ability to measure the soil gravimetric water content accurately and quickly in the field is essential for compaction QA. Schwartz et al. (2017) found the Ohaus MB45 moisture analyzer is a robust device but less suitable for larger aggregates due to its low capacity (1.59 oz, 45 g). Therefore, a newer model of Ohaus moisture analyzer – MB120, shown in Figure 3.3, with a higher capacity (4.23 oz, 120 g), was used in this research.

**Figure 3.3 Ohaus MB120.**

The Ohaus MB120 was evaluated in the laboratory against oven-drying measurements for four kinds of soils — gravel, sand, silt, and clay (AASHTO T 265, 2015). For each soil, 30 to 35 tests at various moisture contents were performed. Results from the evaluation can be compared by R-squared (R^2), which is a statistical measure that represents the proportion of the variation in the dependent variable that is predictable from the independent variable, it can be determined by built-in function (RSQ) in the Excel. An R^2 equals 0.99 showed a very high correlation, as shown in Figure 3.4. Equations shown in Figure 3.4 showed relation of moisture contents between Ohaus MB120 (X) and Oven (Y). The moisture content measured by Ohaus MB120 was

generally slightly lower (by a factor of approximately 0.84) than the moisture measured using the standard oven drying technique. It is likely attributed to the shorter drying period in Ohaus MB120. Results showed that the differences increased as the sample's moisture content increased, because more time was needed to dry the sample with more fines. A default factor of 1.20 can be applied to correct the underestimation of moisture content by the Ohaus MB120, but a soil-specific calibration is recommended.

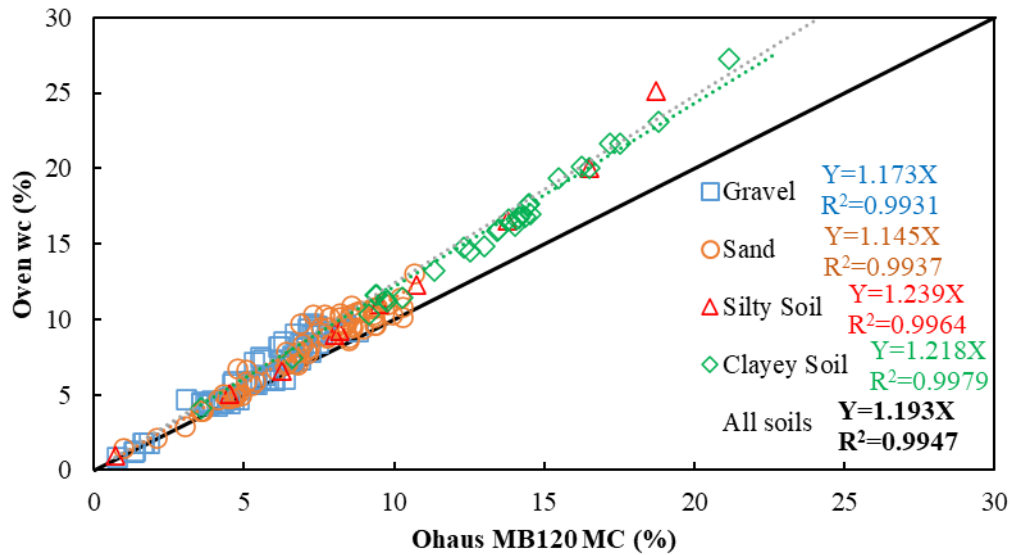


Figure 3.4 Comparison of moisture content measurements by the Ohaus MB120 and oven for different soils.

3.1.3 Aggrameter

The other moisture content measurement device used in this study is the Aggrameter (Figure 3.5), the newer version of the Trident moisture meter was recommended by some researchers (Bryson et al., 2012; Nazzal, 2014). The test is fast and easy to operate, has good data storage capability, and its measurements strongly correlate with those obtained using the traditional oven-dry method (Bryson et al., 2012). The device uses dielectric permittivity to determine the moisture content of unbound materials with its five-pronged sensor. Dielectric permittivity can be described as the ability of a substance to hold an electrical charge. Among all commercially available electronic soil sensors, measurement involving the complex dielectric permittivity remains the most practical way to determine soil moisture content from an in-situ sensor or portable device. Electromagnetic soil sensors use an oscillating radio frequency. As the radio wave propagates and reflects through the soil, the properties and moisture content of the soil will influence the wave. The moisture content, and to a lesser extent, the soil properties will alter and modulate electromagnetic radio signals as they travel through the soil by changing the frequency, amplitude, impedance, and time of travel. Thus, subsequent calibrations are needed to correlate the raw sensor response to a specific soil moisture estimation. The range of the Aggrameter readings starts from 27.9 in the air to 409.5 when submerged in water.

The effect of layer thickness and compaction level on the device readings were evaluated using coarse sandy soil. Five layers of sand were compacted in an acrylic box to assess the impact of layer thickness. Figure 3.6 shows the Aggrameter and the acrylic test box. The first layer's thickness equals the probe length (3.54 in, 90 mm). Then another four layers of 0.98 in (25 mm) thickness were compacted on top of the first layer. The device readings were taken from five different points in the box for each layer. Figure 3.7 shows the Aggrameter readings in millivolts versus the total soil thickness for two different moisture contents. The layer thickness does not impact the device reading, provided all the device probes are embedded within the soil. The sand was compacted in the same acrylic box to a height of 4 in (100 mm) to evaluate the effect of compaction level on Aggrameter readings. However, the soil was compacted using a different number of lifts ranging from 2 to 5. The compaction energy was then estimated using the equation provided in ASTM D1557-12 (2012). Figure 3.8 shows the Aggrameter readings versus compaction energy. The device readings increased with the compaction level until reaching a constant reading. This increase can be attributed to better contact between the soil and the Aggrameter probes.



Figure 3.5 Aggrameter from the James Instruments.



Figure 3.6 Aggrameter and acrylic test box.

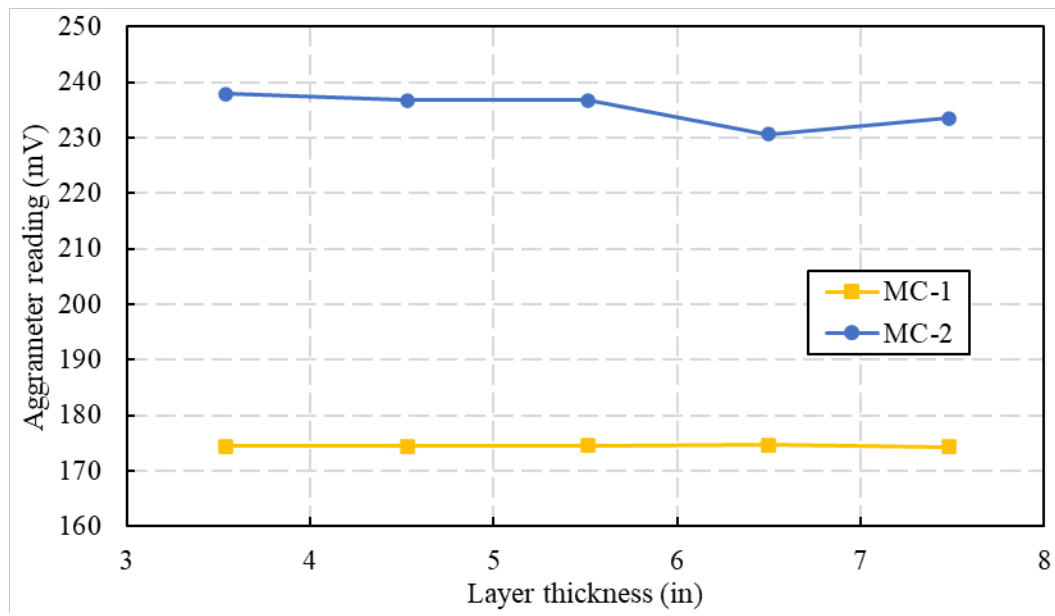


Figure 3.7 Aggrameter readings versus layer thickness.

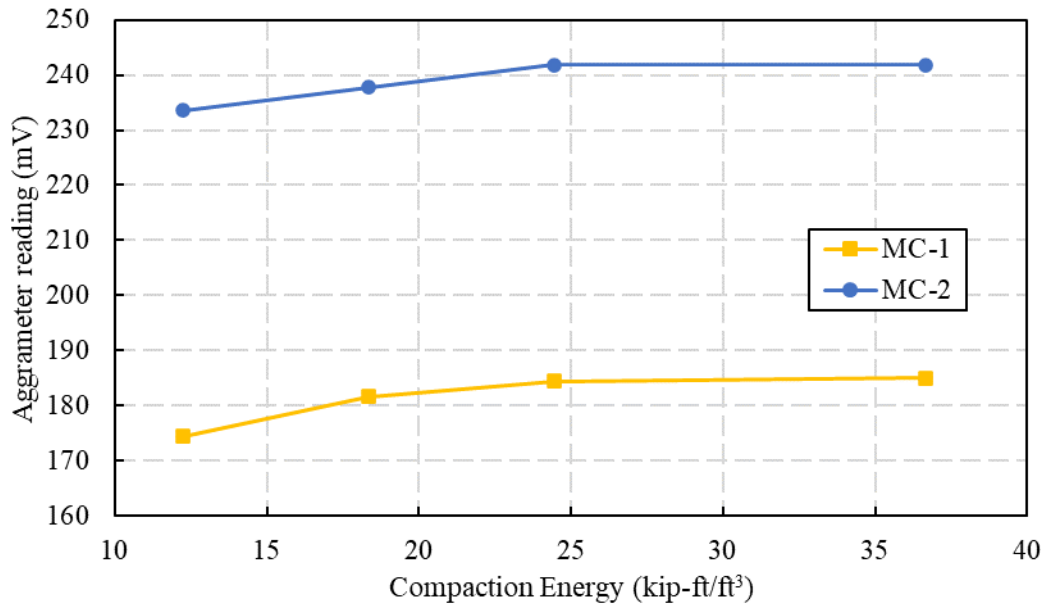


Figure 3.8 Aggrameter readings versus compaction energy.

3.2 Laboratory Testing for Collected Materials

In this section, the laboratory test results for four types of soils were discussed including (1) a lean clay commonly used as subbase, subgrade, and embankment fill material in the state of Missouri, (2) a well graded sand that is commonly used as backfill for retaining structures (e.g., MSE walls), and subbase layers for bridge approaches, (3) an aggregate used as a base course material, and (4) a silty clay collected from bridge pile foundation. These soils were collected from four construction sites of two projects, I-270 North and Buck O'Neil bridge projects, and transported to Missouri S&T geotechnical laboratory for testing.

3.2.1 Material Characterization

Figure 3.9 presents the gradation curves of the four soils according to ASTM D422 (2016). The percent passing of sieve #200 for the well graded sand and the base course was less than 5%. Therefore, there is no need to run hydrometer analysis and Atterberg limits for the two soils. The particle-size distribution for the lean and silty clays less than No. 200 sieve (0.075 mm) was determined using hydrometer tests. For the two clays, the Atterberg limits (i.e., liquid limit, LL, plastic limit, PL, and plasticity index, PI) were evaluated for passing sieve # 40 according to ASTM D4318 (2017). The specific gravities, G_s , were evaluated according to ASTM D854 (2016). Based on Atterberg limits and sieve analysis results, the collected materials were classified according to the Unified and AASHTO Soil Classification Systems (AASHTO M 145, 1991; ASTM D2487, 2020). A summary of the soil classification results is presented in Table 3.2. The lean clay contained 85% fines and was classified as Lean Clay, CL, as per USCS. The well graded sand comprised 96% sand and was classified as well-graded-sand, SW. The base aggregate material consists of 50% sand and 50% gravel, and it was classified as well-

graded sand with gravel, SW. And the silty clay had 80% fine and was classified as Lean Clay, CL, according to USCS.

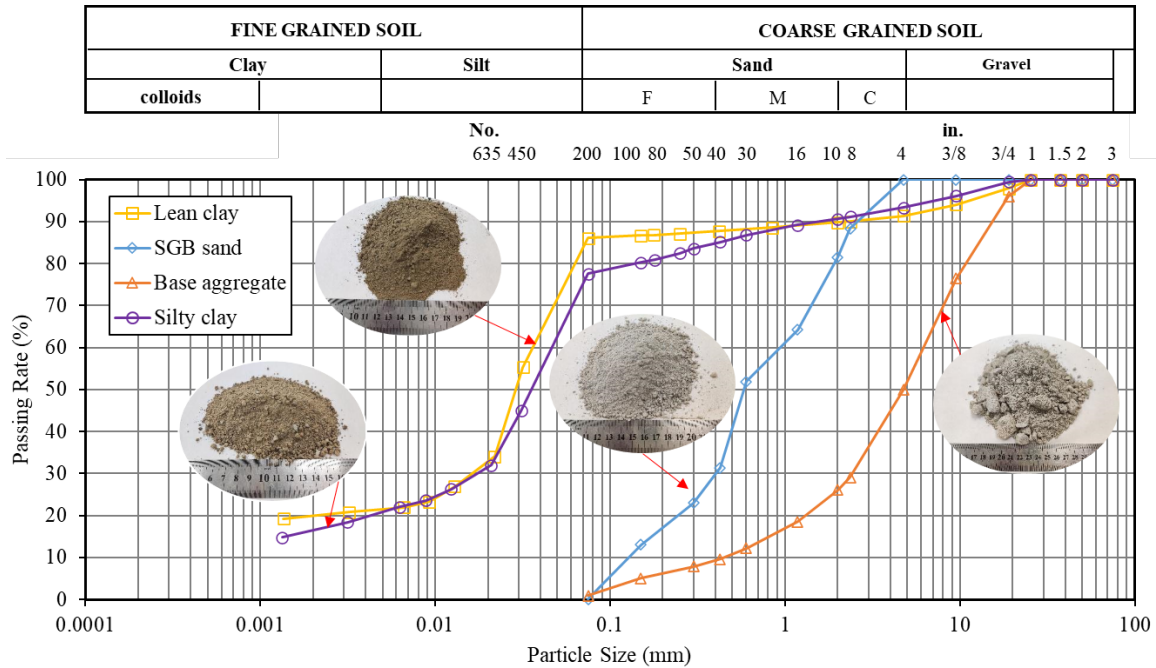


Figure 3.9 Gradations of the four soils.

Table 3.2 Material description.

Material	Cu ¹	Cc ²	LL	PL	PI	P ₂₀₀ ³	G _s	Classification	
								AASHTO	USCS
-	-	-	%	%	%	%	-	-	-
Lean clay	76	17	32.2	23.1	9	86	2.7	A-4	CL
SW	6	1	--	--	--	4	2.65	A-1-b	SW
Base agg.	18.3	2.4	--	--	--	0.7	2.78	A-1-a	SW
Silty clay	50	10.9	30.7	21.0	9.7	78	2.61	A-4	CL

1. C_u is the coefficient of uniformity = D_{60}/D_{10} .

2. C_c is the coefficient of curvature = $D_{30}^2/(D_{10} \cdot D_{60})$.

3. P₂₀₀ is percent passing sieve # 200.

The Soil Water Characteristic Curve (SWCC), or water retention curve, is typically used to describe the ability of soils to hold water under unsaturated conditions. The SWCC is also sensitive to materials' properties, such as pore size distribution and structure, density, and chemical components of the material (Bouazza et al., 2006). Two laboratory tests were performed to determine the SWCC of the collected materials, including pressure plate and salt concentration tests. The pressure plate, PP, test was used to determine the SWCC for suction range from 0 to 217.56 psi (0 to 1500 kPa), while the salt concentration test, SC, was used for higher suction ranges from 87.02 to 4641.21 psi (600 to 32000 kPa).

For the PP test, soils were first compacted in the compaction mold at the OMC, they were then cut into consolidation rings to reduce disturbance and submerged in water for two weeks to saturate. After saturation, samples were transferred onto top of the ceramic plate inside the pressure vessel. Then, designated increments of compressed air pressure were applied. Compressed air forced the excess water within the soil specimen to be expelled out of the soil and flow through the saturated high air entry ceramic disc. The expelled water was collected using a 1.69 oz (50 ml) beaker. An equilibrium condition was considered to be reached when the mass of the beaker plus water was constant for 24 hours. Once at the equilibrium condition, the soil specimen was taken out, and moisture content was determined using the oven drying method. The test was repeated, and the applied air pressure was sequentially increased. The suction values (applied air pressures) and the corresponding moisture contents are plotted to form the SWCC curves for the soils.

The SC test is a thermodynamic-based technique used to determine the SWCC at high suction ranges (>217.56 psi, 1500 kPa). A controlled relative humidity glass jar was used to establish a constant total suction environment. The soils were saturated, cut into small pieces, and put into the controlled suction jar. The saturated specimens were placed in a tinfoil holder with punched holes at the bottom to shorten the time required to reach equilibrium. The excess pore water within the soil specimen evaporates into water vapor and reaches equilibrium with the surrounding relative humidity. The relative humidity was well controlled within the jar by a specific salt concentration of the $MgCl_2$ solute. The corresponding relationships between suction and concentration of $MgCl_2$ solute are listed in Table 3.3, according to Fredlund and Rahardjo (1993). Eight glass jars were prepared with different levels of salt concentrations, and the corresponding suctions ranged from 93.26 to 4753.76 psi (643 to 32776 kPa). Each test lasted 30 days to ensure an equilibrium condition was achieved, and the moisture contents of the samples were determined after each test. From the suction values and the corresponding moisture contents, the SWCC under the high suction range was determined.

Table 3.3 Salt concentrations and corresponding suction.

Mg Cl₂ (oz/gal)	Suction (psi)
1.21	93.3
2.54	189.0
5.09	397.3
6.36	511.0
8.90	760.6
12.72	1196.4
19.08	2110.9
38.72	4753.8

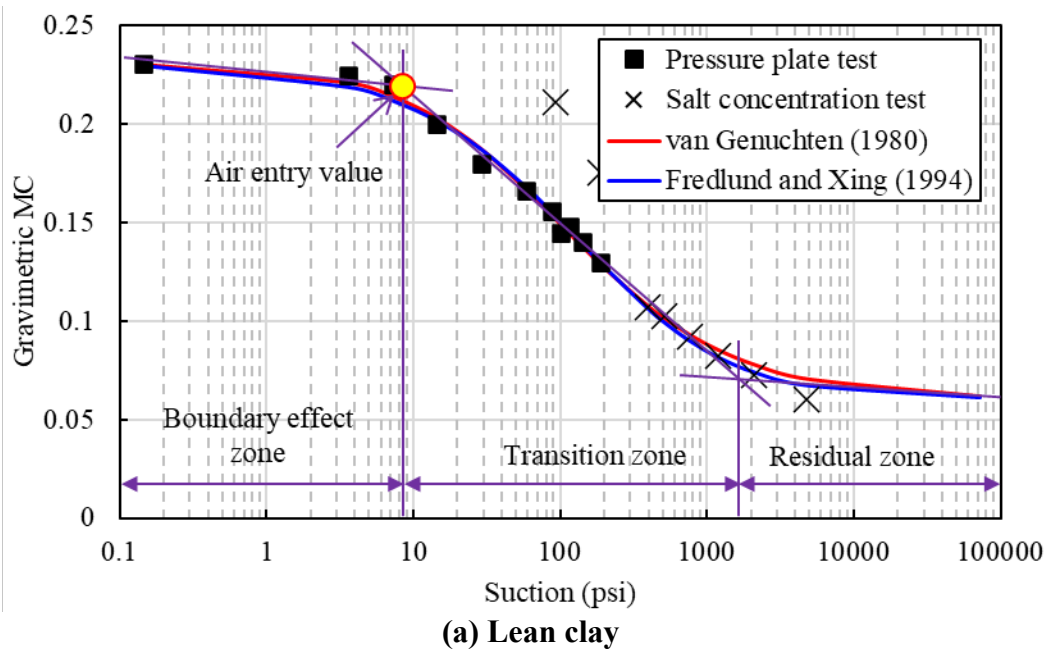
Figure 3.10 shows the SWCCs of the four collected materials based on the results of the two laboratory tests. Results indicate that the lean and silty clay have much higher moisture contents at the same suction values compared with the well graded sand and base aggregate. For the SWCC, the first zone, known as the boundary effect zone, the suction is low, and the soil is in an entirely saturated condition. A decrement in moisture content does not generate a substantial increase in suction. This situation continues until some air bubbles start to appear in the soil skeleton. The suction corresponding to this point is known as the air entry value, and it was equal to 8.50 psi, 0.46 psi, 0.65 psi, and 11.4 psi for the lean clay, well graded sand, base aggregate, and silty clay, respectively. The second part of the SWCC is known as the transition zone. It starts with the air-entry value. With any decrement of moisture content, the suction of the soil considerably increases. In the third part, the residual zone, a significant reduction in moisture content is required for any further suction increase.

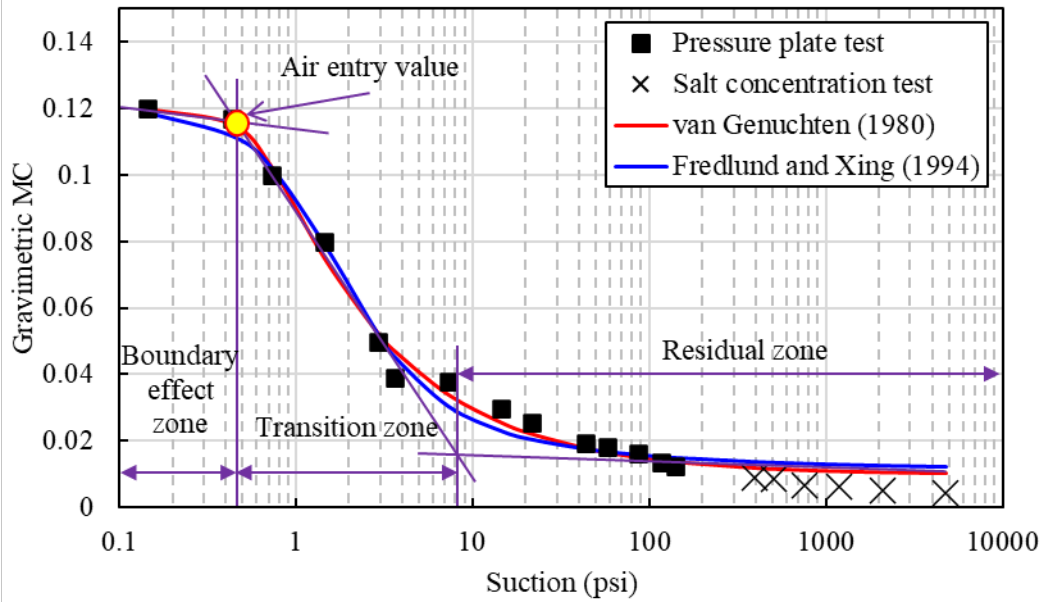
The SWCC is commonly formulated as a nonlinear sigmoid function using the four-parameter equations proposed by van Genuchten (1980) and Fredlund and Xing (1994), as follows:

$$\text{van Genuchten (1980):} \quad w_w = w_r + \frac{w_s - w_r}{[1 + (\alpha\psi)^n]^m} \quad (1)$$

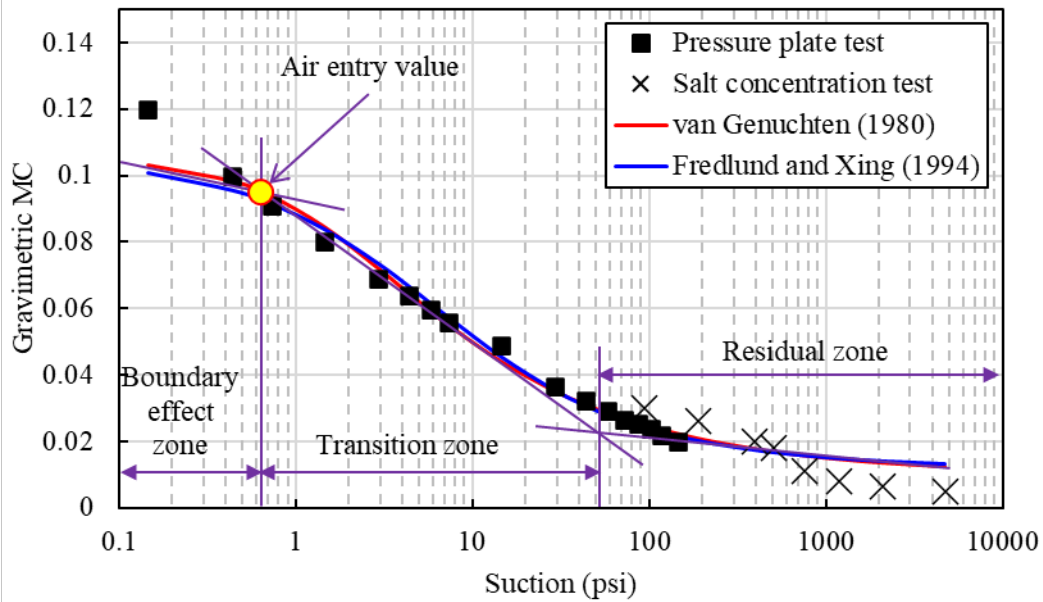
$$\text{Fredlund and Xing (1994):} \quad w_w = w_r + \frac{w_s - w_r}{\left\{ \ln \left[e + \left(\frac{\psi}{a} \right)^n \right] \right\}^m} \quad (2)$$

where w_w is the gravimetric moisture content, w_r is the residual gravimetric moisture content, w_s is the saturation gravimetric moisture content, ψ is the suction, and α , n , m are fitting parameters. Table 3.4 shows the calibrated fitting parameters for each of the soils. Both used models could accurately match the experimental results, as shown in Figure 3.10.

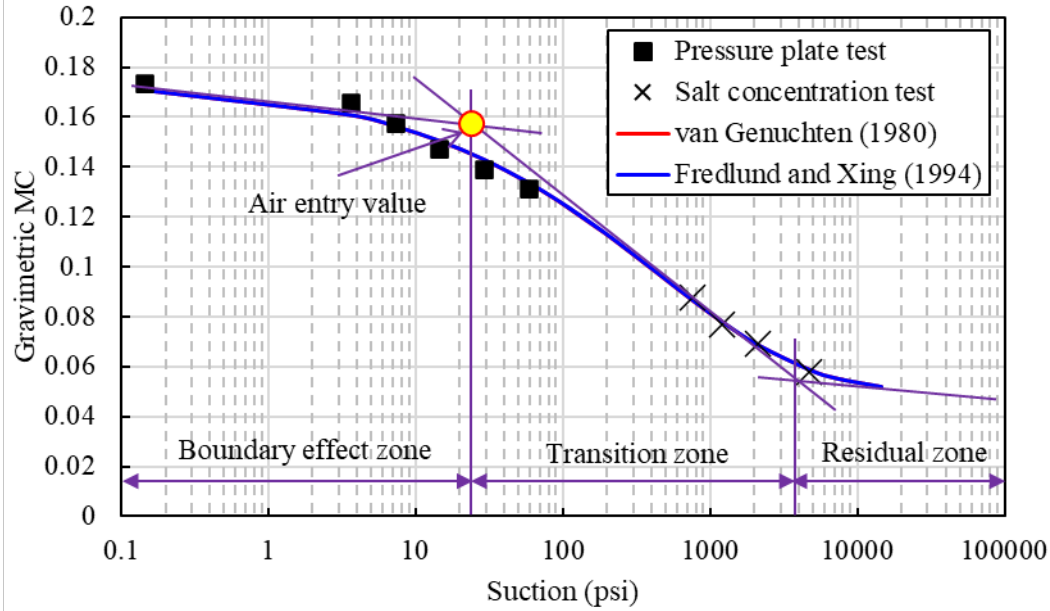




(b) Well graded sand



(c) Base aggregate



(d) Silty clay

Figure 3.10 SWCCs for the four collected geomaterials.

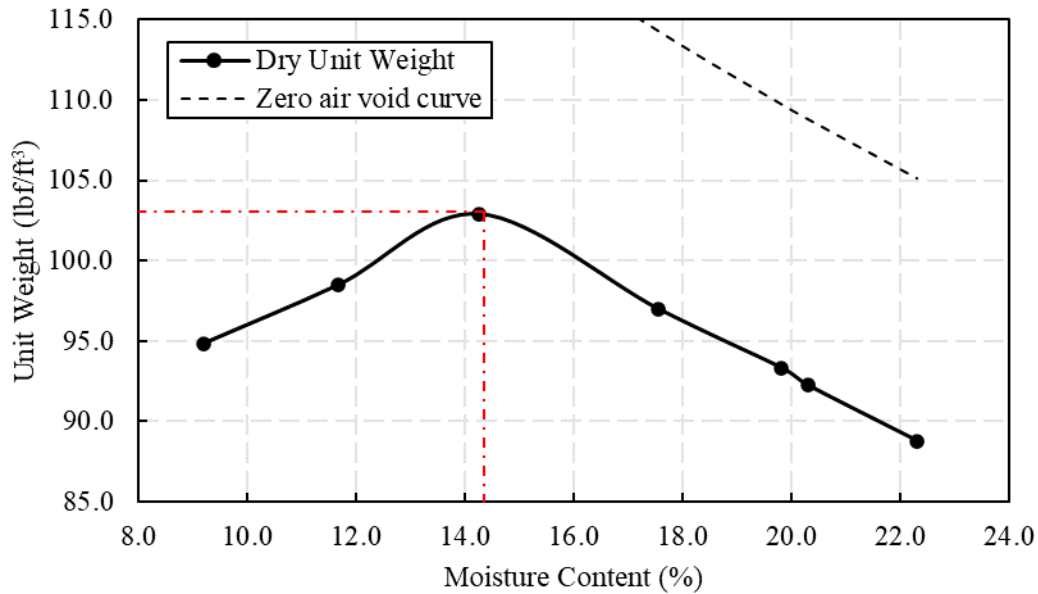
Table 3.4 Calibrated fitting parameters and R^2 for each collected unbound material.

Models	Para.	Lean clay	SW	Base agg.	Silty clay
van Genuchten (1980)	w_s	0.231	0.120	0.105	0.174
	w_r	0.060	0.010	0.010	0.050
	m	0.800	0.179	0.381	12.288
	n	0.834	3.470	1.184	0.455
	α	0.013	1.586	0.631	0.000
	R^2	0.892	0.991	0.978	0.995
Fredlund and Xing (1994)	w_s	0.231	0.120	0.105	0.174
	w_r	0.060	0.010	0.010	0.050
	m	3.539	1.495	2.011	30.820
	n	0.696	1.725	0.790	0.452
	α	214.205	1.301	4.790	96316.066
	R^2	0.900	0.986	0.973	0.995

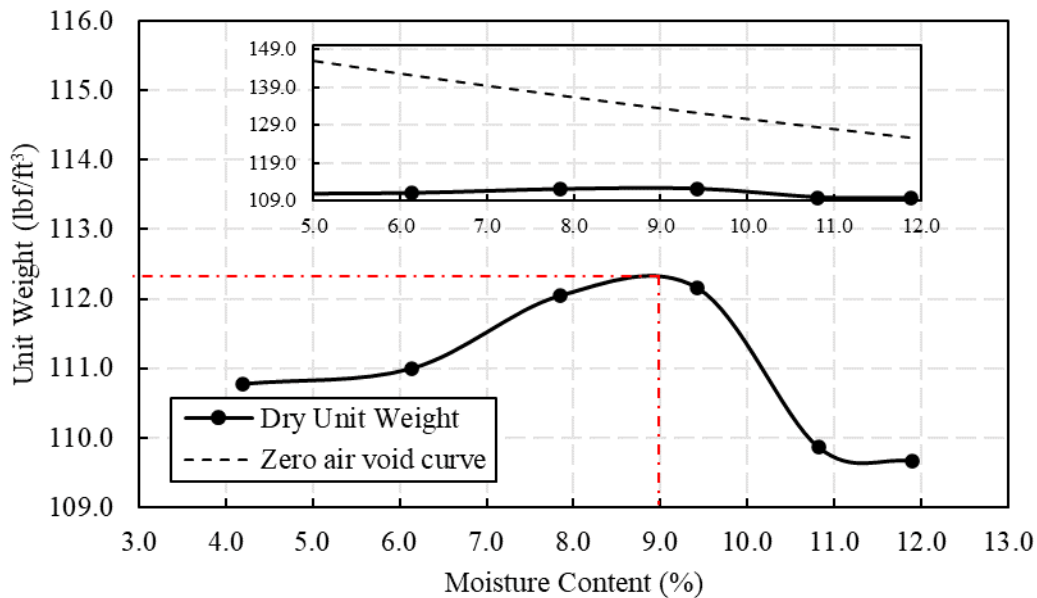
3.2.2 Compaction Test Results

Compaction tests were conducted according to ASTM D1557 (2012) to determine the OMC and MDD of the collected materials. The lean clay and well graded sand were compacted using method A, in which the specimens were compacted in 4 in (100 mm) mold in 5 layers, and each layer was subjected to 25 blows with a 10-lbm (4.5-kg) hammer drop at 18 in (457 mm). While the base aggregate and silty clay were compacted following method C. The specimens were compacted in 6 in mold in 5 layers, and each

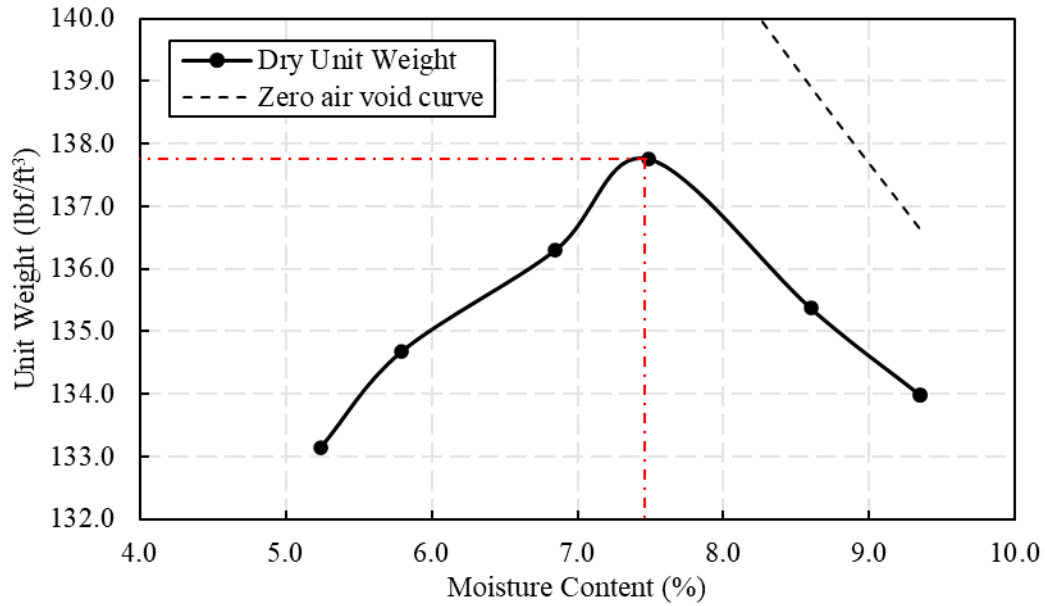
layer was subjected to 56 blows with a 10-lbm (4.5g) hammer drop at 18 in (457 mm). Figure 3.11 presents the moisture-density curves, and Table 3.5 lists the OMCs and MDDs of the four test soils. Results show that the lean clay, well graded sand, base aggregate, and silty clay had OMCs of 14.2%, 9%, 7.5%, and 12.5%, respectively. It can be also noticed that the MDD decreased, and the OMC increased with decreasing of nominal grain size.



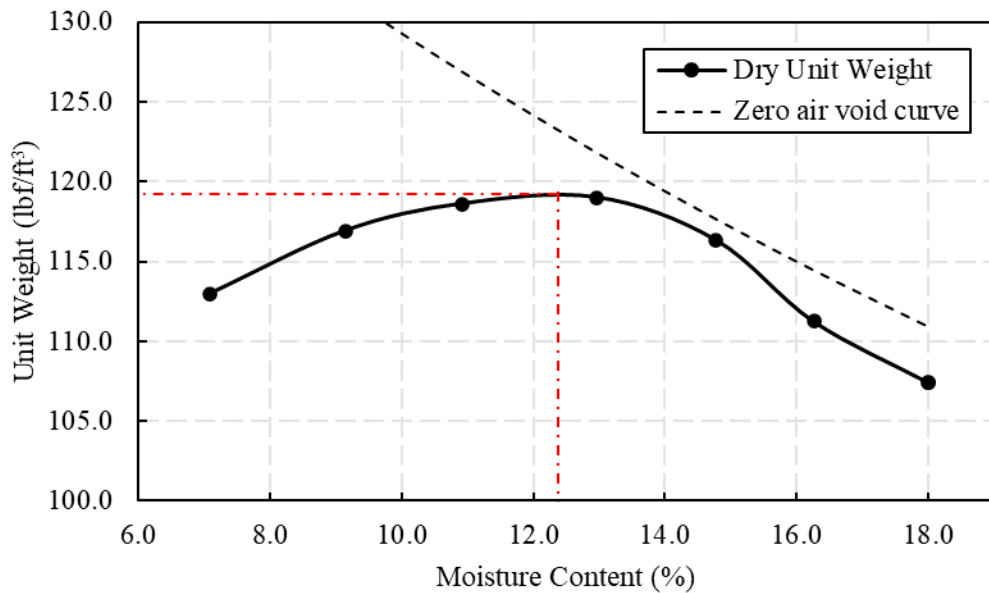
(a) Lean clay



(b) Well graded sand



(c) Base aggregate



(d) Silty clay

Figure 3.11 Moisture-density relationships of the four soils.

Table 3.5 OMCs and MDDs for the four collected soils.

Soil types	Method	Mold Diameter	No. of blows	Compaction energy	MDD	OMC
-	-	in	-	-	lb/ft ³	%
Lean clay	A	4	25	Modified	102.9	14.2
SW	A	4	25	Modified	112.3	9.0
Base agg.	C	6	56	Modified	137.8	7.5
Silty clay	C	6	56	Modified	119.0	12.5

3.2.3 LWD Testing on Proctor Mold

The LWD testing directly on the Proctor compaction mold was recommended, as it can serve as a promising testing tool to establish the target modulus values for the field at a given moisture content and stress condition and provide valuable insights into the soil's response to the moisture, density, and stresses that can be used to tailor the compaction criteria in the field. Therefore, under this task, LWD tests were performed directly on top of the Proctor mold on the laboratory's concrete floor, according to the draft *Standard Method of Test for Laboratory Determination of Target Modulus using LWD Drops on Compacted Proctor Mold* developed in Schwartz et al.'s study (Schwartz et al., 2017). The target moisture contents were first identified based on compaction results and the acceptable field ranges. The research team communicated with the MoDOT inspection team in the I-270 North project and checked the Missouri standard specifications for highway construction to determine the acceptable density and moisture content ranges. For structural backfill (i.e., well graded sand) and base course, 95% relative compaction (RC) is required, and the moisture content acceptable range is from OMC-3% to OMC. For embankment construction (lean clay), 90% relative compaction is needed until 18 in below base rock grade is reached. At that point, 95% relative compaction is required. Based on these ranges and the soil-specific compaction test results, target moisture content values were designated and shown in Tables 3.6 through 3.9. Please note that the research team extended the target moisture content range for the two clay soils to accommodate their higher moisture contents (up to 22%) in the fields. The degree of saturation at every targeted moisture content value is also shown to indicate how far the sample is from saturation. Figures 3.12 to 3.15 show the compaction curve along with moisture contents corresponding to common field relative compactions and the designed final target moisture contents for the four collected soils. The targeted values were selected to cover a wide range of moisture contents above and below the OMC.

Table 3.6 Target values for the lean clay.

Targeted MC (%)	OMC -4%	OMC -2%	OMC	OMC +2%	OMC +4%	OMC +6%
	10.2	12.2	14.2	16.2	18.2	20.2
Dry unit weight (lb/ft³)	96.6	99.8	102.9	99.8	95.6	92.2
Wet unit weight (lb/ft³)	106.5	112.0	117.5	116.0	113.0	110.8

Table 3.7 Target values for the well graded sand.

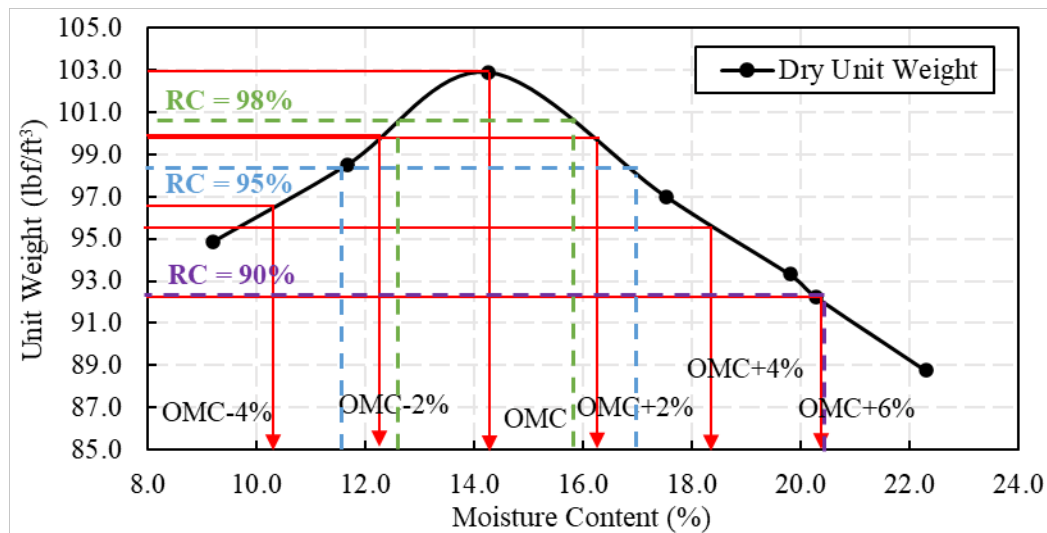
Targeted MC (%)	OMC-4%	OMC-2%	OMC	OMC+1%	OMC+2%
	5.0	7.0	9.0	10.0	11.0
Dry unit weight (lb/ft³)	110.8	111.5	112.3	111.3	109.7
Wet unit weight (lb/ft³)	116.3	119.3	122.4	122.4	121.8

Table 3.8 Target values for the base aggregate.

Targeted MC (%)	OMC-3%	OMC-1.5%	OMC	OMC+1%	OMC+2%
	4.5	6.0	7.5	8.5	9.5
Dry unit weight (lbf/ft ³)	-	135	137.8	135.6	-
Wet unit weight (lbf/ft ³)	-	143.1	148.1	147.1	-

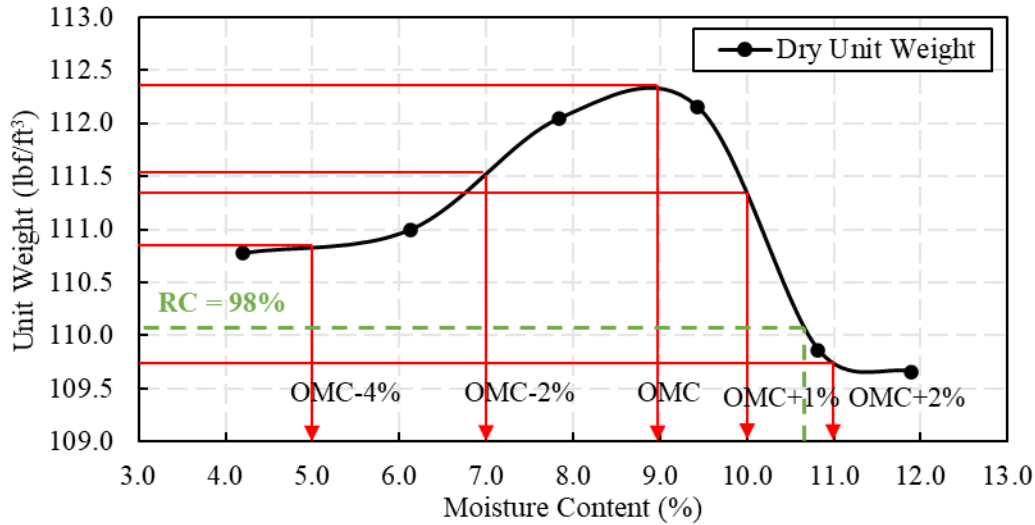
Table 3.9 Target values for the silty clay.

Targeted MC (%)	OMC -4%	OMC -2%	OMC	OMC +2%	OMC +4%	OMC +6%	OMC +8%
	8.5	10.5	12.5	14.5	16.8	18.5	20.5
Dry unit weight (lbf/ft ³)	116.0	118.5	119.0	117.0	110.5	-	-
Wet unit weight (lbf/ft ³)	125.9	130.9	133.9	134.0	129.1	-	-



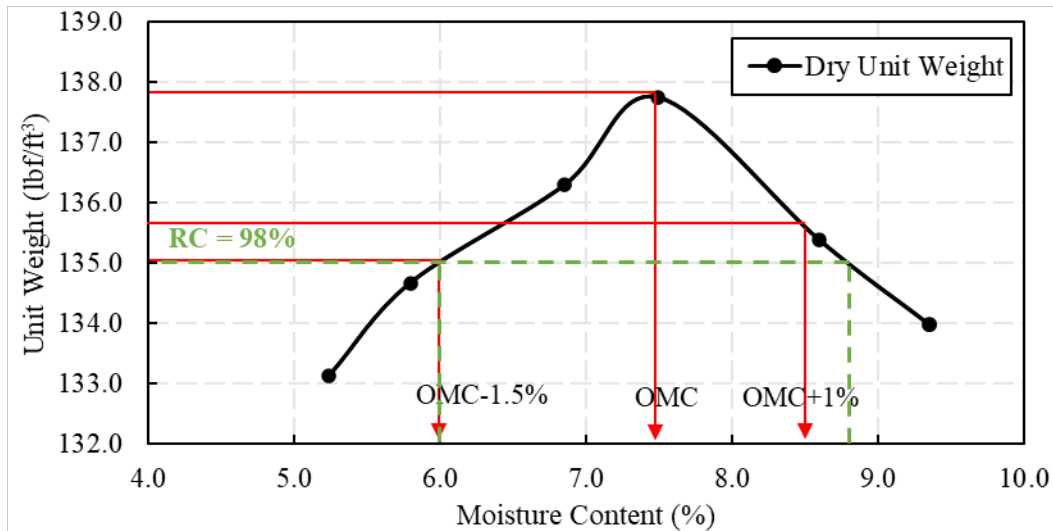
Relative compaction (RC)	98%		95%		90%	
Dry unit weight (lbf/ft ³)	100.8		97.8		92.6	
Moisture contents (%)	12.8	15.9	11.6	17.0	Out of range	20.1
Wet unit weight (lbf/ft ³)	113.7	116.9	109.1	114.4	NA	111.2

Figure 3.12 Moisture content-density relationships for the lean clay along with the corresponding MCs for common relative compaction values (98%, 95%, and 90%).



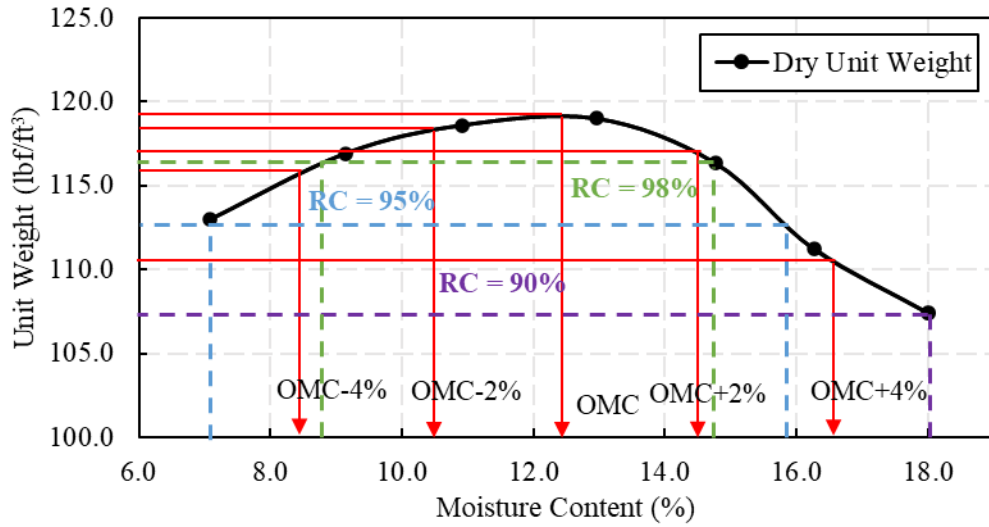
Relative compaction (RC)	98%		95%		90%	
Dry unit weight (lb/ft³)	110.1		106.7		101.1	
Moisture contents (%)	Out of range	15.9	Out of range	Out of range	Out of range	Out of range
Wet unit weight (lb/ft³)	NA	127.6	NA	NA	NA	NA

Figure 3.13 Moisture-density relationships for the well graded sand along with the corresponding MCs for common relative compaction values (98%, 95%, and 90%).



Relative compaction (RC)	98%		95%		90%	
Dry unit weight (lb/ft³)	135.0		130.9		124.0	
Moisture contents (%)	6.0	8.8	Out of range	Out of range	Out of range	Out of range
Wet unit weight (lb/ft³)	143.1	146.9	NA	NA	NA	NA

Figure 3.14 Moisture-density relationships for the base aggregate along with the corresponding MCs for common relative compaction values (98%, 95%, and 90%).



Relative compaction (RC)	98%		95%		90%	
Dry unit weight (lb/ft³)	116.6		113.1		107.1	
Moisture contents (%)	8.8	16.5	7.0	15.8	Out of range	18.0
Wet unit weight (lb/ft³)	126.9	135.9	121.0	130.9	NA	126.4

Figure 3.15 Moisture-density relationships for the silty clay and the corresponding MCs for common relative compaction values (98%, 95%, and 90%).

As indicated by Schwartz et al. (2017), samples were tested at different drop heights to investigate the stress dependency of material and permit interpolation/extrapolation of modulus at various stresses. As previously mentioned, the Zorn LWD does not have a load cell and assumes a constant applied load of 795.82 lbf (3.54 kN) for the lab version when dropped from a total height of 14.80 in (37.50 cm). The applied loads at different heights can be calculated using the single degree of freedom (DOF) mechanical model assumed by the manufacturers of the Zorn LWD. Figure 3.16 shows a schematic plot for the LWD-soil motion as a single DOF system. Then, upon releasing the falling weight, the gravitational potential energy (E) transforms into elastic potential energy, as follows:

$$E = m \cdot g \cdot h = \frac{1}{2} k \cdot \Delta x^2 \quad (3)$$

The force applied to the spring to deform Δx is:

$$F = k \cdot \Delta x \quad (4)$$

Therefore,

$$F = \sqrt{2 \cdot m \cdot g \cdot k} \cdot \sqrt{h} = C \cdot \sqrt{h} \quad (5)$$

where m is the falling weight (lbm), g is gravity (32.2 ft/s²), h is falling height (in), k is the spring stiffness (lb/in), and C is a constant for each Zorn LWD version ($= \sqrt{2 \cdot m \cdot g \cdot k}$) that can be back calculated from the full height generated force relationship. For the Zorn LAB version, this constant was back-calculated as 0.58. From this linear relationship between the falling height and applied force, the applied force at any reduced height can be calculated, as shown in Table 3.10. Heights in integer such as 2, 4, 6, 8, and 10 in were already permanently marked on Lab LWD's rod by the manufacturer.

Therefore, the target heights were determined by referring to a ruler and the permanent height scales, then the hold-and-release handle was moved to these heights and fixed there to ensure accuracy of drop heights. The last drop height 25.82 in (65.59 cm) was beyond the capacity of the Lab LWD version. Therefore, the falling weight of the field version was used on top of the Lab version loading plate to reach the designated force 1052.1 lbf (4.68 kN) and stress 38.4 psi (265 kPa). The falling height of the field version LWD was determined using the ruler only as no height scale was engraved on their guide rods.

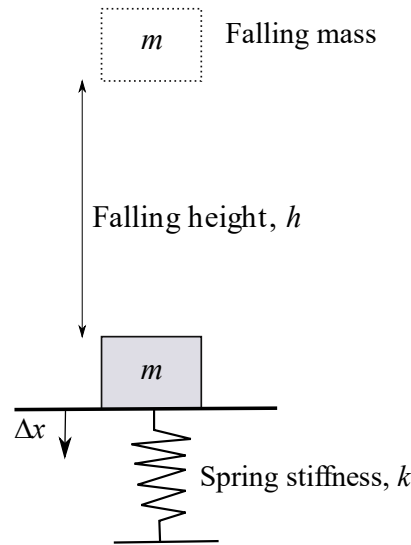


Figure 3.16 Schematic plot for the single degree of freedom mechanism for the LWD-soil motion.

Table 3.10 Reduced LWD drop heights and the corresponding applied forces.

h (cm)	h (in)	F (kN)	F(lbf)	Stress (kPa)	Stress (psi)
5.25	2.07	1.32	296.75	75	10.9
10.50	4.13	1.87	420.39	106	15.4
15.74	6.20	2.29	514.81	130	18.9
20.99	8.26	2.65	595.74	150	21.8
26.24	10.33	2.96	665.43	168	24.4
37.58	14.80	3.54	795.82	200	29.0
65.59	25.82	4.68	1052.11	265	38.4

Soils were mixed with the targeted moisture contents and saved in plastic bags for at least 72 hours to ensure consistency. The soil was then compacted in a 6-inch (DIA) by 6.1-inch (H) mold, then the collar was removed, and the soil was trimmed to a dimension of 6 inches in diameter and 4.6 inches in height with a leveled surface. Zhao et al. (2018) indicated that the interface condition between the aggregate material and the inner wall of the mold would affect the deflection measurements, depending on the aggregate size and moisture content. Therefore, lubricant oil was used on the mold wall for each test on

every collected material to minimize this effect. The collar was reattached to help keep the LWD loading plate in place and minimize any lateral movement of the LWD plate with successive drops. After that, the mold was rested on a stable, concrete floor in the geotechnical lab. The 6 in (150 mm) loading plate was carefully placed on top of the mold and rotated 45° back and forth to seat the plate. Figure 3.17 shows the trimmed mold and LWD test on top of the compaction mold with the collar attached.



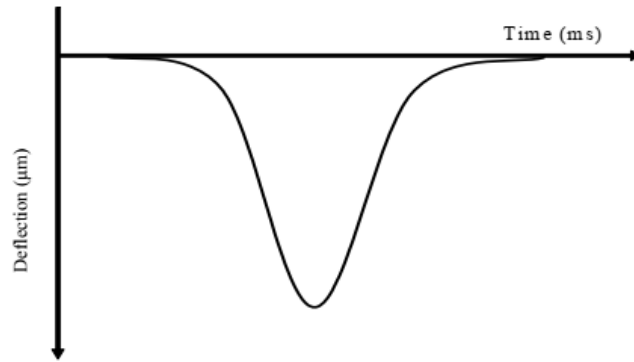
Compacted sample in the Proctor mold



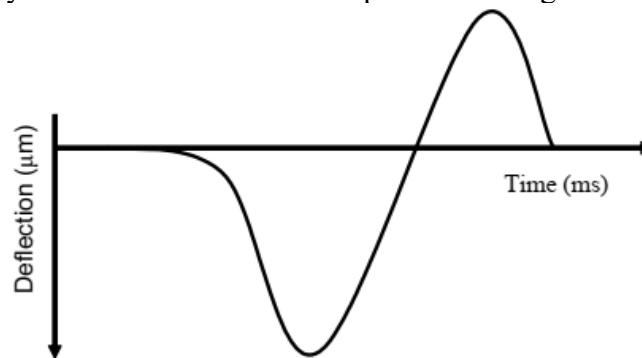
LWD test on Proctor mold

Figure 3.17 LWD test on Proctor mold.

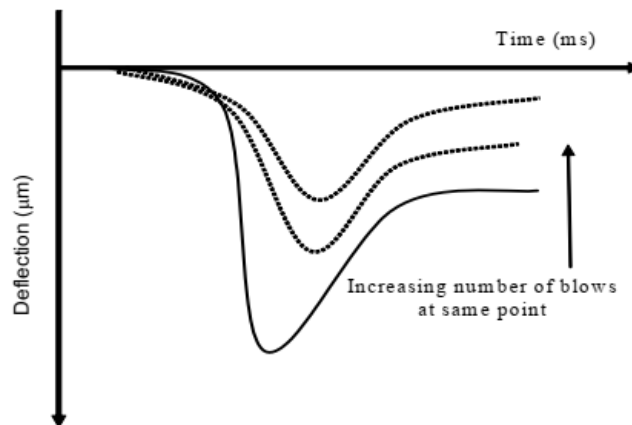
For the LWD testing, the rod was held vertically. Then six drops were applied — three seating drops followed by three measurement drops by raising the falling weight to the designated LWD heights (Table 3.10), allowing the weight to fall freely without lateral movement. The LWD testing was conducted following the ASTM E2835 (2015). The deflections for the six drops and the modulus calculated by the device were recorded. Figure 3.18 shows the different expected shapes of time-deflection curves for high- and low-quality tests on soft and hard materials (Fleming et al., 2009). Other studies (INDOT and MnDOT specifications) recommended that the coefficient of variation (COV) for the three measurement drops shall not exceed 10%. Figure 3.19 shows time-deflection curves from the well graded sand and lean clay tests for seating and measurement drops. The quality of signals improved significantly after the seating drops. As shown in Figure 3.20, two tests on the well graded sand and lean clay showed a high coefficient of variation of 12.50%. According to the curve shape criterion recommended by (Fleming et al., 2009) and the COV criterion specified in INDOT and MnDOT specifications, these tests were excluded.



(a) High-quality tests with deflection-time pulse returning to zero (soft material)



(b) High-quality tests on hard material (response may be due to hard material causing the plate to lift off the ground or the presence of excess water, characterized by the high 'rebound' of the deflection to a positive (upward) value).



(c) Low-quality test (reduced deflection with number of blows and a 'permanent' element of the deflection – time pulse)

Figure 3.18 Common time-deflection curves from LWD test (Fleming et al., 2009).

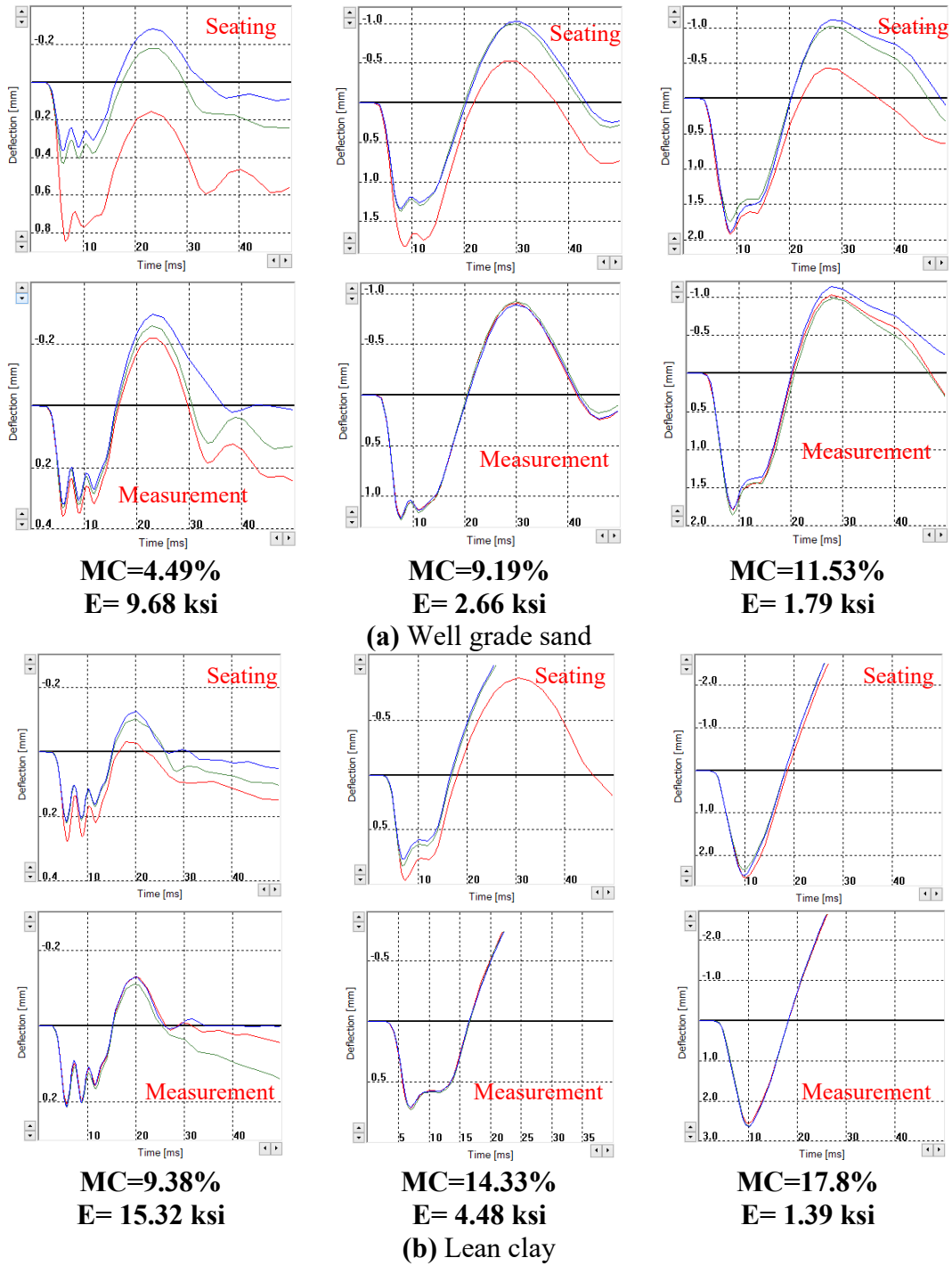
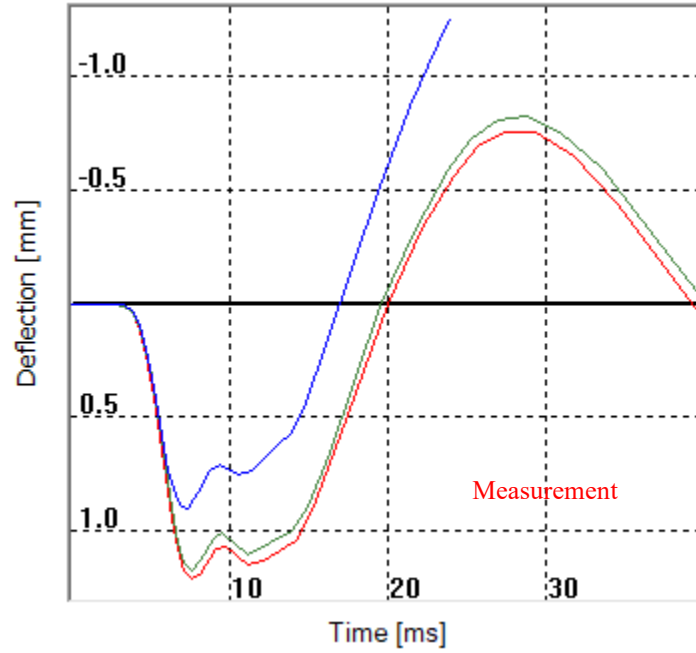
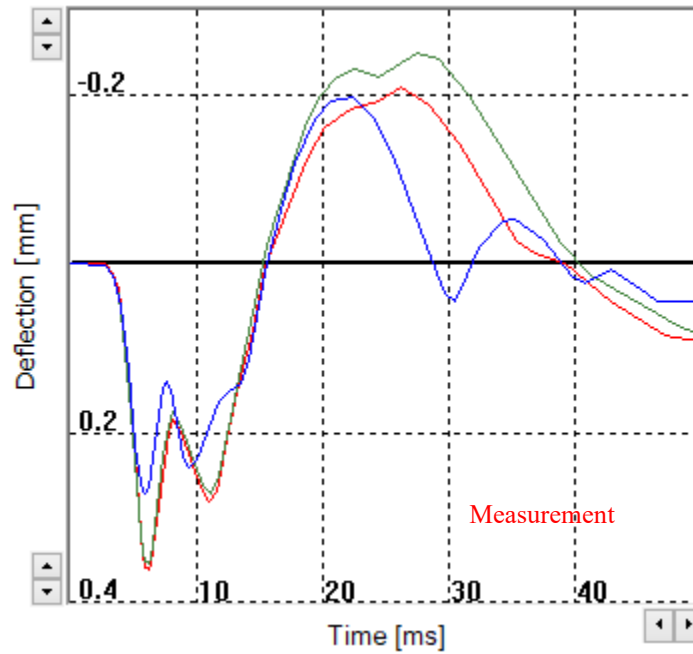


Figure 3.19 Time-deflection curves from LWD testing on the well graded sand and the lean clay for seating and measurement drops.



(a) Three measurement drops for the well graded sand.



(b) Three measurement drops for the lean clay.

Figure 3.20 Time-deflection curves for low-quality tests.

The LWD device calculates the LWD modulus using Equation (6), assuming the test media is a linearly elastic, isotropic, and homogeneous semi-infinite continuum.

$$E_{LWD} = \frac{2k(1 - \nu^2)}{Ar_0} \quad (6)$$

where E_{LWD} is LWD modulus (MPa) determined by the LWD test on the Proctor mold test, k is soil stiffness $= F_{peak}/\delta_{peak}$ as measured by the LWD during the three measurement drops, in which F is applied load (kN) and δ is average maximum deflection (mm) for the three measurement drops, A is a stress distribution factor and depends on the soil type and stress distribution shape, ν is Poisson's ratio, and r_0 is the plate radius (m).

However, calculating the LWD modulus using Equation (6) is not accurate for the LWD test on compaction mold. Zorn LWDs assume Poisson's ratio of 0.50 to calculate the soil modulus. Therefore, Equation (7) derived in a previous study (Schwartz et al., 2017) was used, assuming a constrained cylinder of elastic material. Poisson's ratios were extracted from the typical values provided by the Mechanistic-Empirical Pavement Design Guide (MEPDG), shown in Table 3.11. Values of 0.20, 0.15, 0.35, 0.20 were selected for the lean clay, well graded sand, base aggregate, and silty clay, respectively.

$$E_{LWD} = \left(1 - \frac{2\nu^2}{1 - \nu}\right) \frac{4H}{\pi D^2} k \quad (7)$$

where H is mold height (m) and D is mold diameter (m).

Table 3.11 Typical Poisson's ratio values for different geomaterials from MEPDG.

Material	Range of values	Typical value
Untreated granular materials	0.30-0.40	0.35
Cement-treated granular materials	0.10-0.20	0.15
Cement-treated fine-grained soils	0.15-0.35	0.25
Lime-stabilized materials	0.10-0.25	0.20
Loose sand or silty sand	0.20-0.40	0.30
Dense sand	0.30-0.45	0.35
Saturated soft clays	0.40-0.50	0.45
Silt	0.30-0.35	0.32
Clay (unsaturated)	0.10-0.30	0.20
Sandy clay	0.20-0.30	0.25
Coarse-grained sand	0.15	0.15
Fine-grained sand	0.25	0.25

The maximum deformation (δ_{peak}) was averaged from the last three drops (measurement drops), and the moduli were then calculated using Equation (7) for each drop height. Three independent replications were conducted at each targeted moisture content and drop height, and the LWD moduli, deflection, moisture content, and density were collected at each point. Results from three replications were then analyzed and used for further analysis.

Figure 3.21 shows the lean clay's LWD test results versus moisture contents at each applied stress, as well as the dry density changes with moisture contents. Figure 3.21a shows that deflection increased exponentially with increasing moisture content and deflection generally increased with the applied LWD stress. Rather than the increasing

trend shown in Figure 3.21a, Figure 3.21b shows a decreasing trend that the LWD modulus (calculated using Equation (7)) decreased with an increase of the moisture content. The modulus became almost constant and equivalent under different applied stresses when the soil approaches saturation with a moisture content greater than 21%.

Figure 3.22 shows the LWD test results versus moisture content at each applied stress for the well graded sand. It also shows the dry density changed with moisture content. Figure 3.22a shows that deflection increased with increasing moisture content. Besides, it indicates that deflection generally increased with the applied LWD stresses. Unlike the deflection, Figure 3.22b shows that the modulus (calculated using Equation (7)) decreased with increasing the moisture content. Both the deflection and soil modulus increased with the applied stress. However, as indicated in Figure 3.22, the modulus became almost constant and equivalent under different applied stresses when the soil approached saturation with a moisture content greater than 10%.

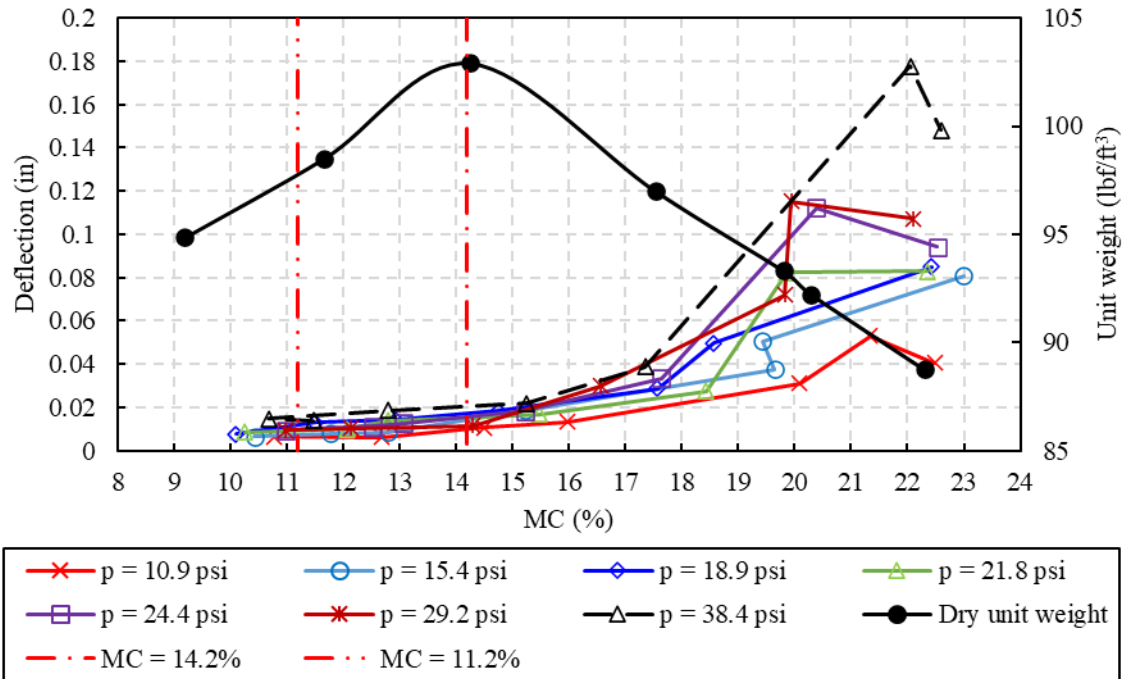
Figure 3.23 depicts the LWD test results and moisture content at each applied stress for the base aggregate and the dry density changes with moisture content. Figure 3.23a shows that deflection increased with increasing moisture content. It also indicates that deflection generally increased with the applied LWD stress. Unlike deflection, Figure 3.23b shows that modulus (calculated using Equation (7)) decreased with increasing the moisture content. Both deflection and soil modulus increased with the applied stress. As indicated in Figure 3.23, the modulus became almost constant at around 8.5% when the soil state approaches saturation due to excess pore water pressure.

Figure 3.24 shows the LWD test results versus moisture content at each applied stress for the silty clay, where the compaction characteristics curve is also shown. It is noticed that deflection increased with increasing moisture content as well as applied LWD stress in Figure 3.24a. On the other hand, contrary to deflection, Figure 3.24b indicates that the LWD modulus decreased with increasing the moisture content and kept constant when moisture content exceeds 18% due to excess pore water pressure.

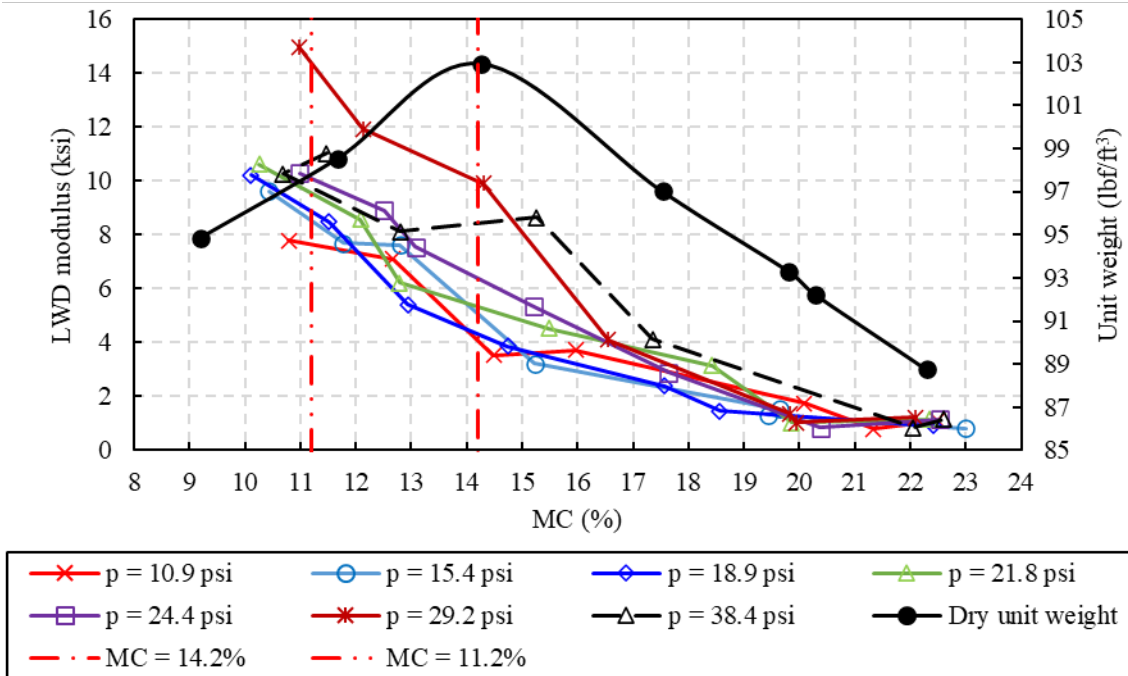
These results indicate that the LWD test on the compaction mold is capable to capture the stress and moisture dependency trends for different types of soils. All four soils generally showed increasing modulus with increasing the applied stress. Generally, for the lean clay (fine-grained soil), the modulus showed a stronger function in moisture content with a clear trend of modulus increasing and moisture content decreasing. Unlike the density-moisture content relationship, there was no turning point (peak value) in modulus that can be used as a target value for future field testing. A previous study also reached similar findings (Schwartz et al., 2017).

Moreover, it can also be observed that the four soils had different deflection levels. Clay soils deflected up to 0.22 in (5.5 mm), where the silty clay deflected more than the lean clay. The largest deflection for well graded sand was 0.09 in (2.3 mm), while base aggregate had a maximum displacement of 0.045 in (1.1 mm). In addition, LWD modulus had the same trend: the silty clay had the highest stiffness of 18 ksi (124 MPa),

the lean clay 15 ksi (103 MPa), the well graded sand 10.5 ksi (72 MPa), and the base aggregate 10 ksi (69 MPa).

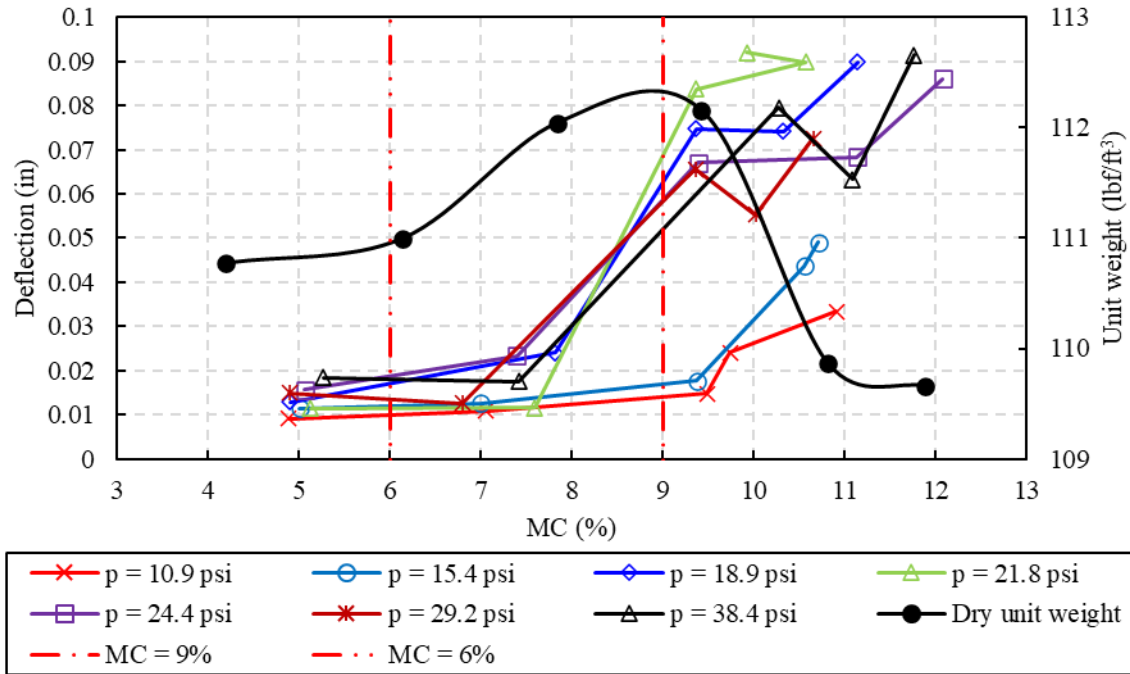


(a) Deflection versus moisture content

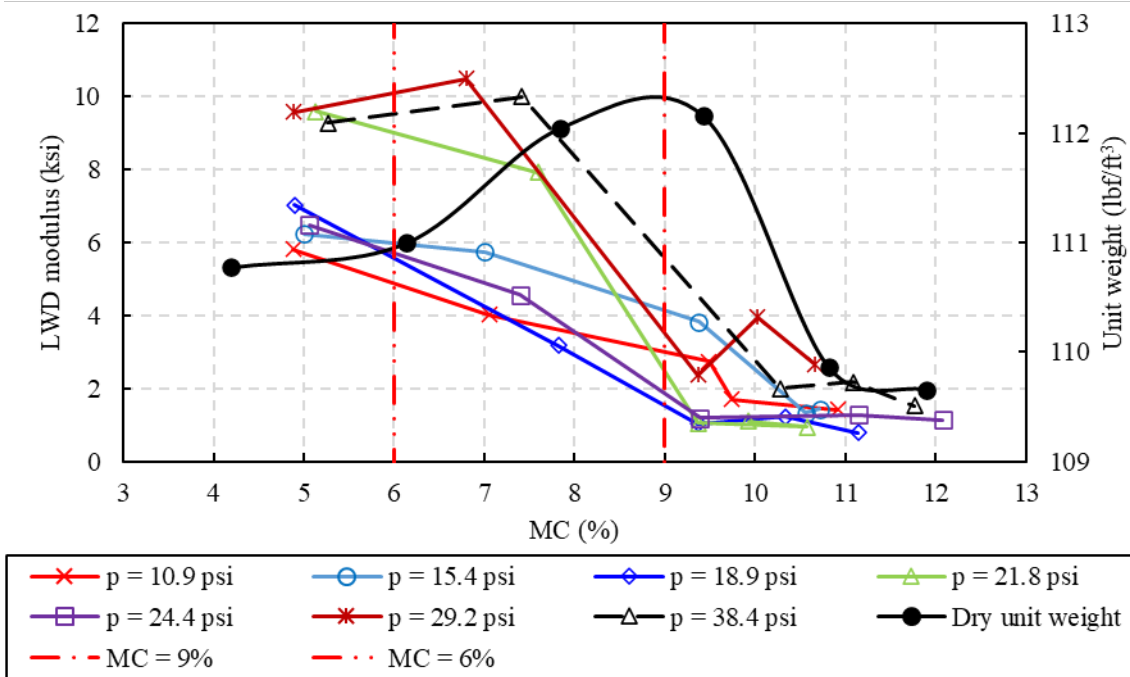


(b) Modulus versus moisture content

Figure 3.21 LWD testing on Proctor mold results for the lean clay.

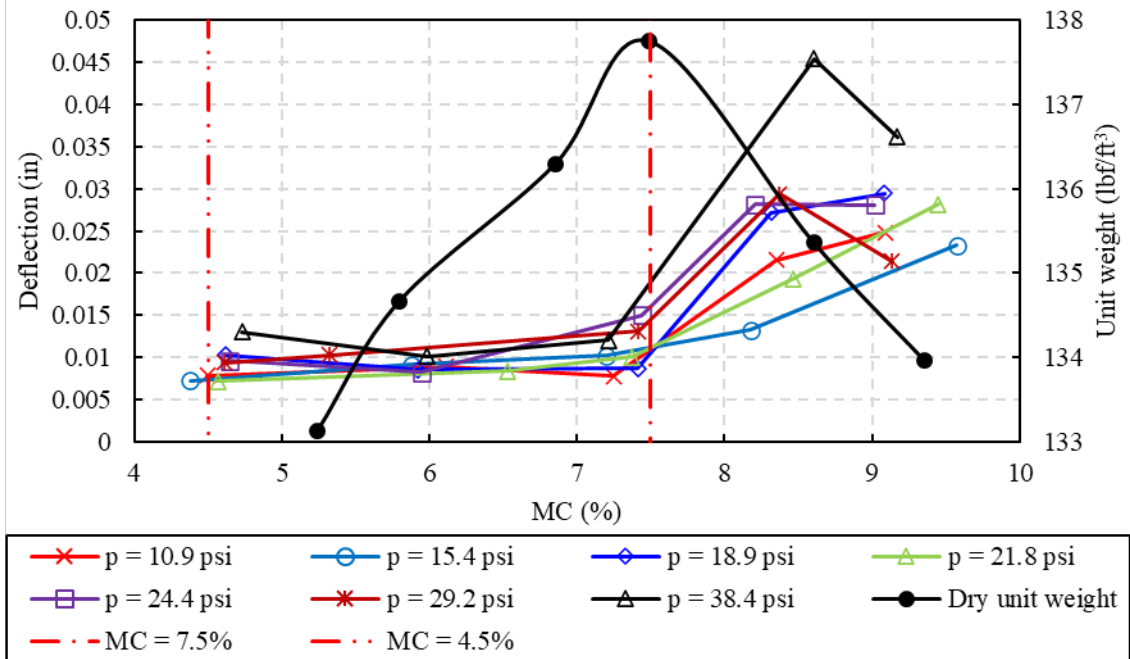


(a) Deflection versus moisture content

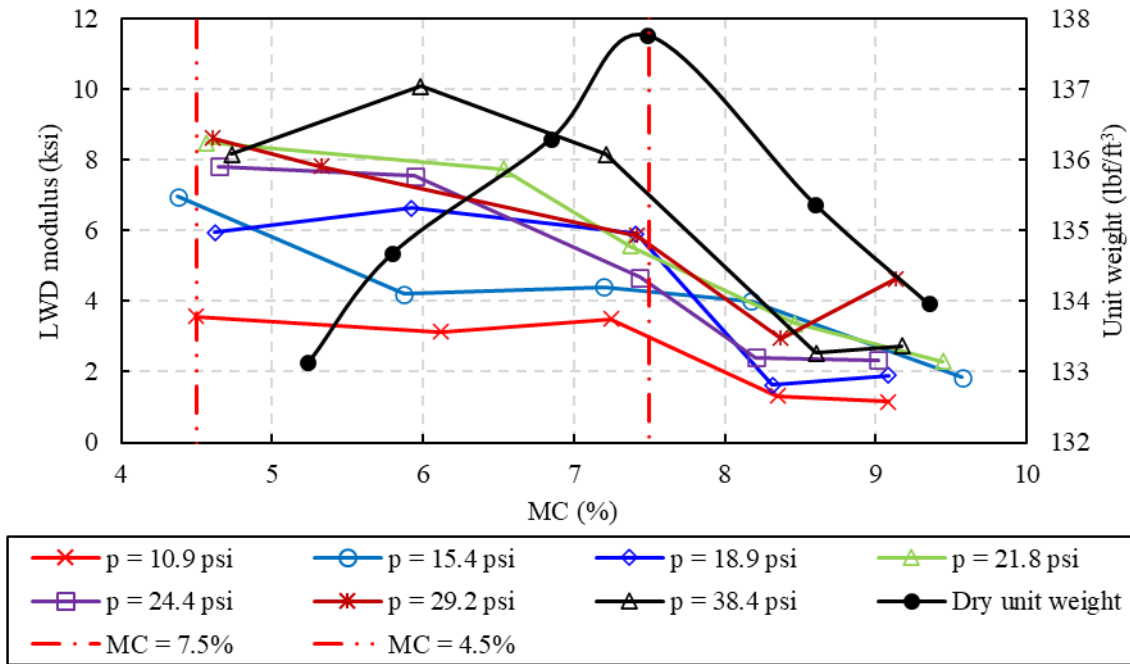


(b) Modulus versus moisture content

Figure 3.22 LWD testing on Proctor mold results for the well graded sand.

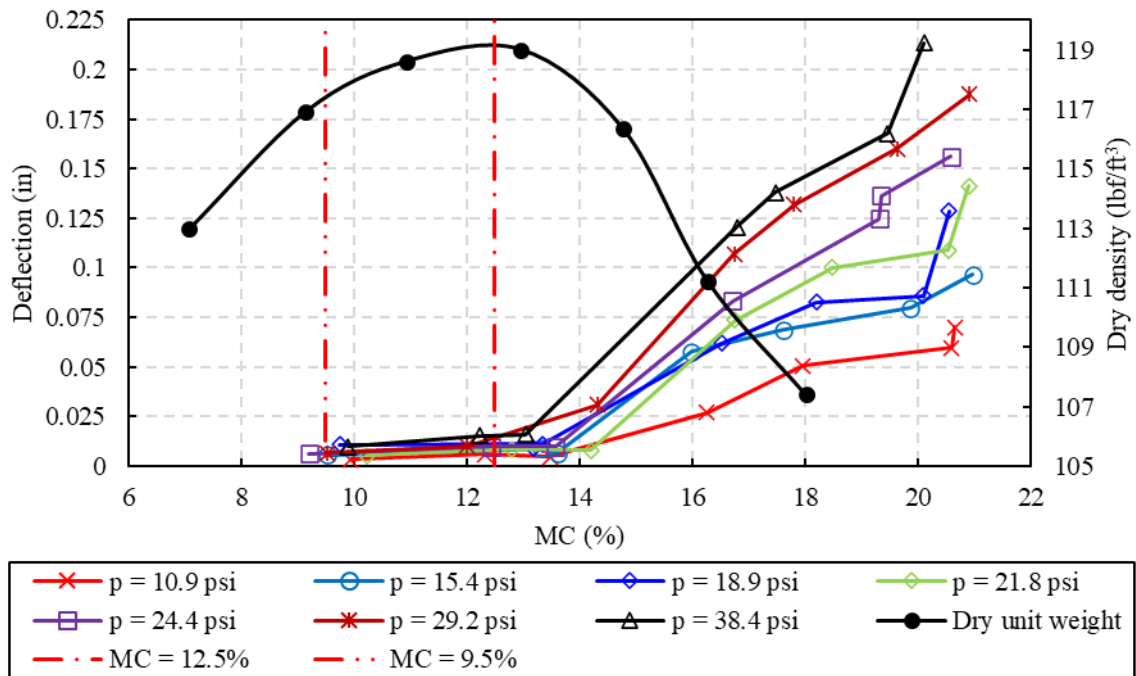


(a) Deflection versus moisture content

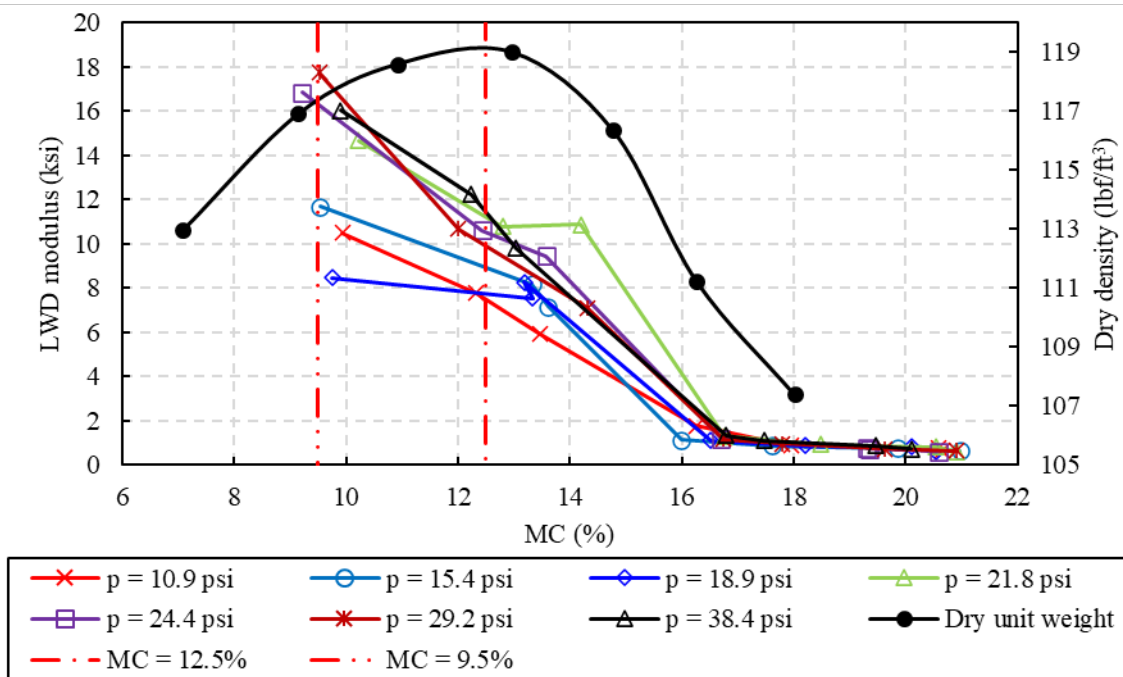


(b) Modulus versus moisture content

Figure 3.23 LWD testing on Proctor mold results for the base aggregate.



(a) Deflection versus moisture content



(b) Modulus versus moisture content

Figure 3.24 LWD testing on Proctor mold results for the silty clay.

3.2.4 Determination of Regression Coefficients

LWD lab tests were also used to obtain regression coefficients for a two-variable quadratic equation (Equation (8)) besides investigating the dependency of mechanical response on soil properties. Field LWD modulus was predicted by Equation (9) with the input of field applied stress and moisture content, as indicated by Schwartz et al. (2017). In this subsection, those regression coefficients are determined.

$$E_{lab} = a_0 + a_1 \times MC_{lab} + a_2 \times MC_{lab}^2 + a_3 \times P_{lab} + a_4 \times P_{lab}^2 \quad (8)$$

$$E_{target} = a_0 + a_1 \times MC_{field} + a_2 \times MC_{field}^2 + a_3 \times P_{field} + a_4 \times P_{field}^2 \quad (9)$$

where

E_{lab} = LWD modulus determined by LWD test on Proctor mold (LWD lab test), (psi),

a_0, \dots, a_4 = regression coefficients,

MC_{lab} = moisture content of the sample in LWD lab test, (%),

P_{lab} = applied stress in LWD lab test, (psi),

E_{target} = target LWD modulus in the field, (psi),

MC_{field} = moisture content of the sample in the field, (%), and

P_{field} = applied stress in LWD lab test (psi).

As discussed in section 3.2.3, the acceptable moisture content range is from OMC-3% to OMC in subgrade and base/subbase construction. Therefore, regression coefficients of the Equations (8) and (9) were determined based on the acceptable moisture content range for each soil. For example, a test conducted around the moisture content range of 11.2% to 14.2% was considered for the lean clay and the moisture content span of 6% to 9% for the well graded sand. Table 3.12 shows regression coefficients of E_{target} prediction model for the lean clay, well graded sand, base aggregate, and silty clay, as well as their R^2 . It can be seen from Table 3.12, the well graded sand had the best regression result ($R^2 = 0.94$), while the rest three soils had good ones, and lowest R^2 of 0.80 occurred in the regression of the base aggregate.

Table 3.12 Regression coefficients in the prediction model for four soils.

Soils	a_0	a_1	a_2	a_3	a_4	R^2
Lean clay	18.72	-1.42	0.01	334.67	-3740.31	0.88
SW	-3.66	3.70	-0.34	-19.26	3290.33	0.94
Base aggregate	-0.98	1.39	-0.18	383.08	-5160.05	0.80
Silty clay	53.32	-7.33	0.26	498.70	-6483.68	0.89

3.3 Lab Moisture Content Measurements Using Field Moisture Content Devices

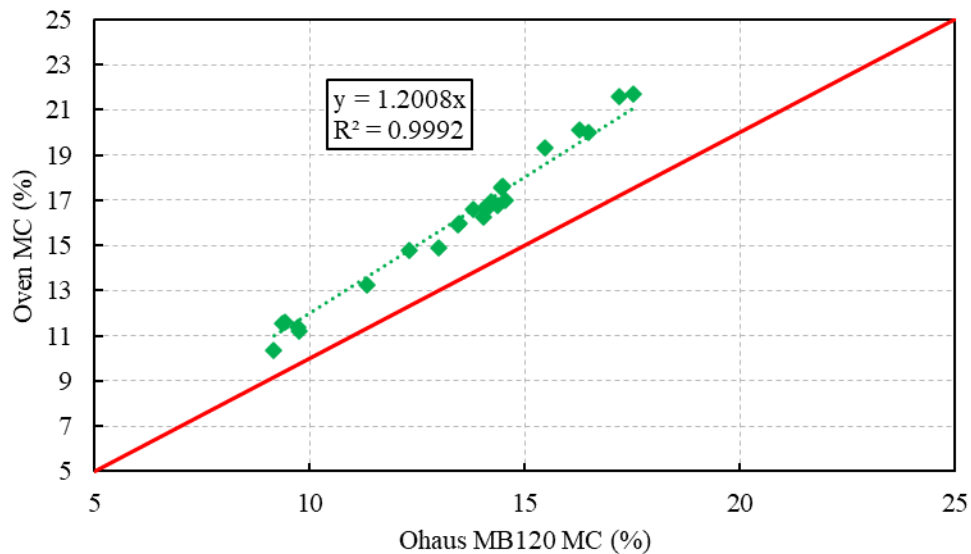
3.3.1 Field Moisture Content Devices Soil-Specific Calibration

Based upon previous research (Nazarian et al., 2015; Nazzal, 2014; Schwartz et al., 2017) and the general calibration done at the beginning of this study, it is recommended that soil-specific calibration should be performed for the field moisture content devices. In

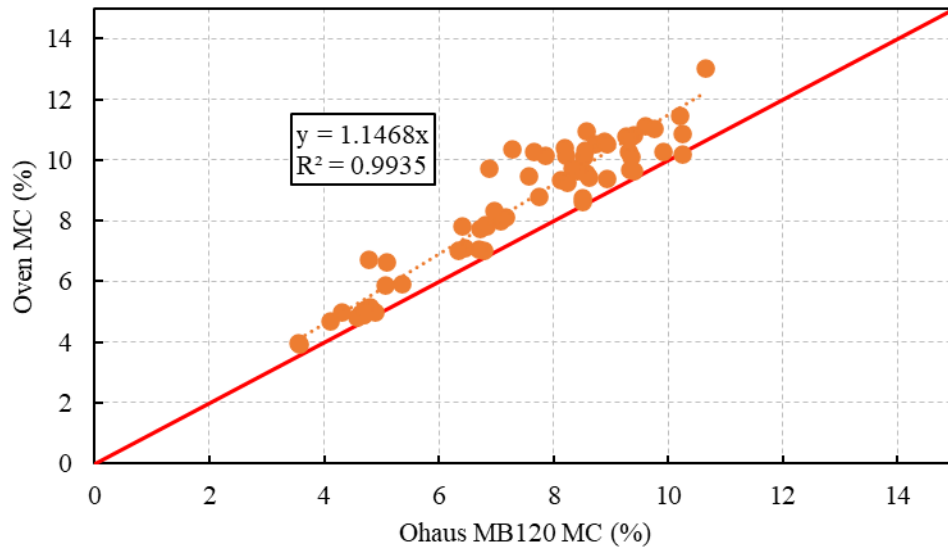
this study, the Aggrameter and Ohaus MB120 are calibrated for the lean clay, well graded sand, base aggregate, and silty clay. At least 20 samples were prepared at different moisture contents (more samples near the OMC) and tested using both devices and the conventional oven drying method. It is worth noting that the Aggrameter was calibrated on compacted soil samples. It was difficult to insert the Aggrameter probes into the base aggregate materials. Even with the help of a driller, it was difficult to drill through the aggregate particles and drill proper holes that have correct angles and distribution for the Aggrameter. At the same time, Aggrameter probes are fragile and easy to be damaged. As a result, no calibration was performed for the base aggregate and silty clay since the Aggrameter is not applicable for these soils. Table 3.13 presents the calibration parameters for the collected materials. Figures 3.25 and 3.26 show these materials' Ohaus and Aggrameter calibration results. A spot check was done, in which Aggrameter was used to determine the moisture content for the well graded sand, and the whole sample was then dried in the oven for moisture content determination. Figure 3.26b shows the spot check results, indicating that the calibration was also valid for the whole sample.

Table 3.13 Ohaus MB120 and Aggrameter calibration results.

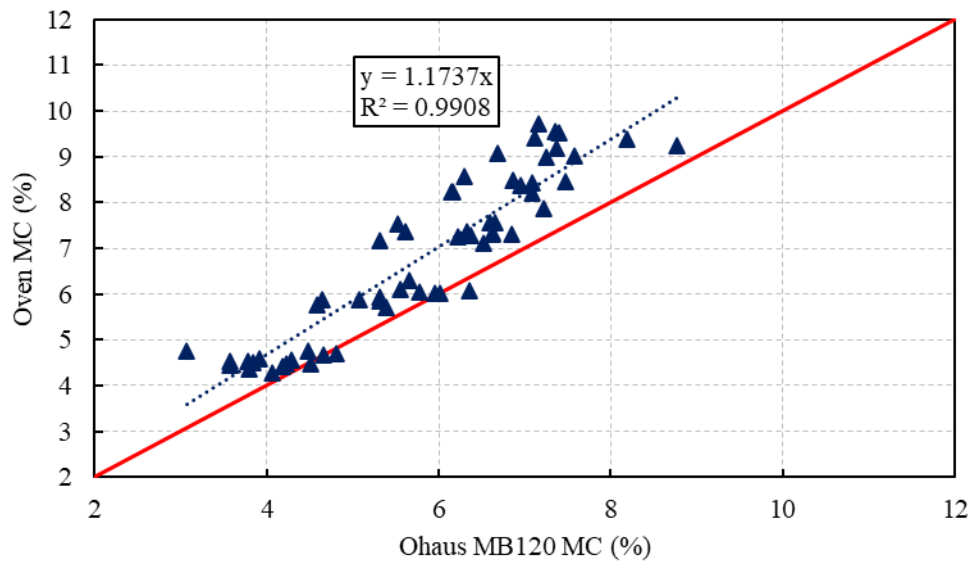
Material	Ohaus MB120		Aggrameter	
	Offset	Gain	Offset	Gain
Lean clay	-	1.20	-13.98	0.09
Well grade sand	-	1.15	-5.70	0.04
Base aggregates	-	1.17	NA	NA
Silty clay	-	1.26	NA	NA



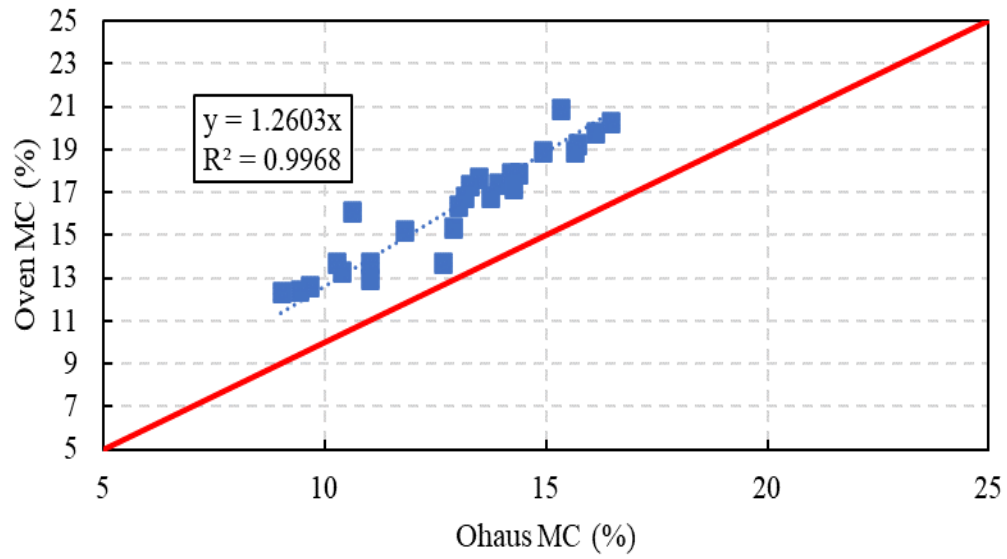
(a) Lean clay



(b) Well graded sand

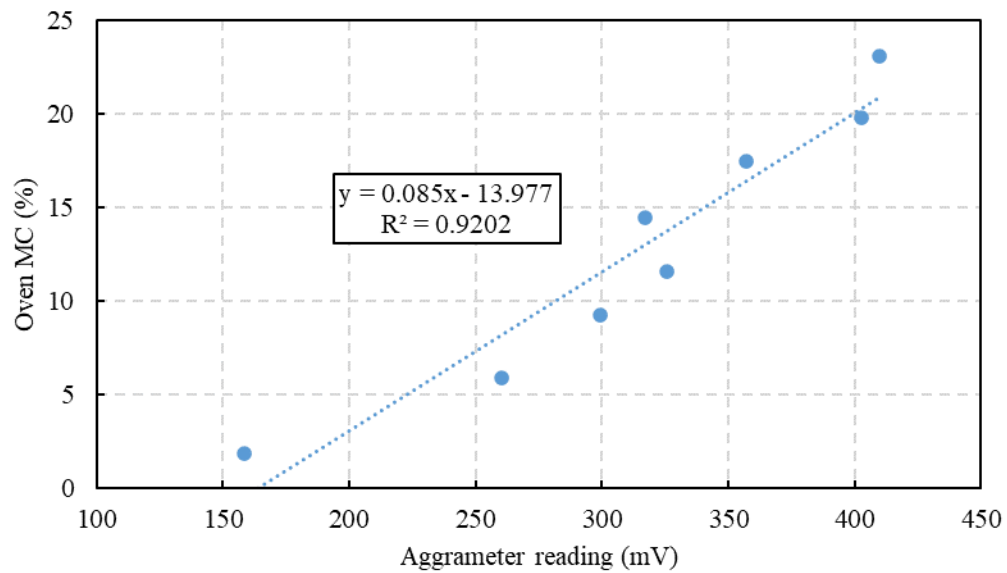


(c) Base aggregate

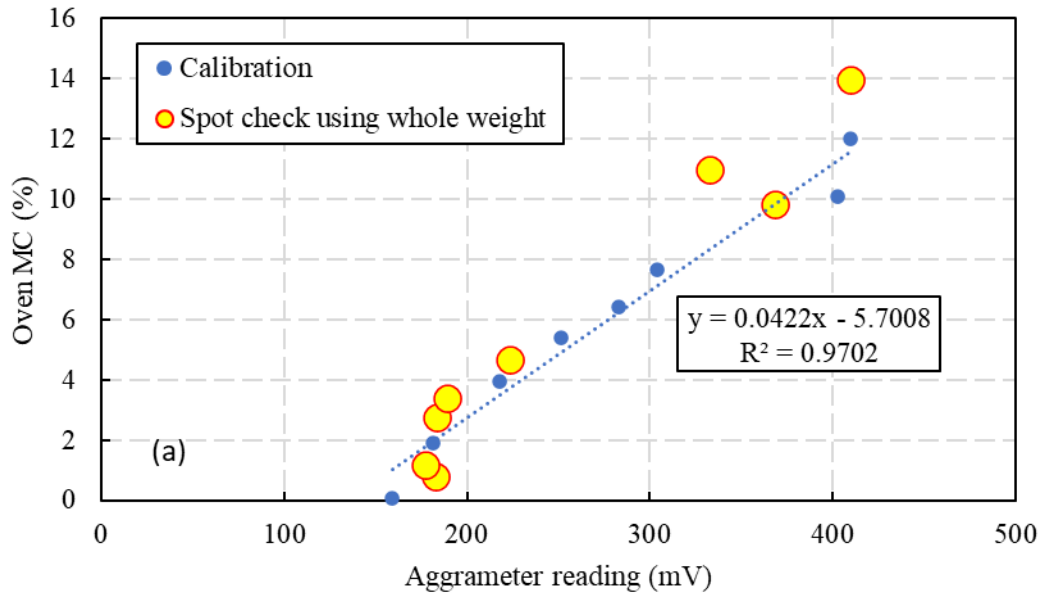


(d) Silty clay

Figure 3.25 Ohaus MB120 calibration for the four soils.



(a) Lean clay



(b) Well graded sand
Figure 3.26 Aggrameter calibration for the lean clay and well graded sand.

3.3.2 Validation with the LWD Test on Proctor Mold Test

As previously mentioned, samples were collected for the moisture content measurement after every LWD test on Proctor mold. The Aggrameter and Ohaus MB120 were then used to detect the moisture content and compare it with the values determined utilizing oven drying. Due to soil hardness, it was difficult to insert the Aggrameter probes into the compacted lean clay sample, especially under low moisture content conditions. To overcome this limitation, a drill was used to pre-drill holes with a diameter equal to the Aggrameter rod. Since the Aggrameter readings can be significantly affected by the presence of any metal containers, the soil samples were extruded from the compaction mold before testing. Several trials were conducted to pre-drill through the compacted samples for Aggrameter testing for base aggregate. However, all these trials were unsuccessful. Figure 3.27 shows the testing procedures for a lean clay sample using the Aggrameter. After taking five Aggrameter readings, one sample from the middle is usually taken for Ohaus MB120 testing. Then, three samples from the mold's top, middle, and bottom are taken for oven drying. The Aggrameter readings were then averaged, and soil-specific calibration values corresponding to each device (i.e., Ohaus MB120 and Aggrameter) were applied. Figures 3.28 through 3.31 show the comparison in moisture content results between moisture content measurement devices and oven drying for the lean clay, well graded sand, base aggregate, and silty clay, respectively. If the moisture content measurements from the measurement devices match those obtained from oven drying, the points should lay on the equality line (diagonal).

As can be seen from Figures 3.28 through 3.31, the Ohaus MB120 can reasonably measure the moisture content of all materials, and results from the Aggrameter has a good match with those obtained from the oven-drying method for the well graded sand. However, the Aggrameter cannot correctly predict moisture content for most of the clay

samples, as shown in Figure 3.28, which echoes the conclusion obtained in the previous section. This mismatch can be attributed to the Aggrameter's unsuitability to test clayey materials. The instructions manual for the Aggrameter cautioned that the device should not be used for any soils that are produced by chemical weathering, such as all clay types. Hence, the Aggrameter should only be used on the sand.



a) drilling holes



b) sample extrusion



c) Aggrameter testing

Figure 3.27 Steps for Aggrameter testing on a lean clay sample.

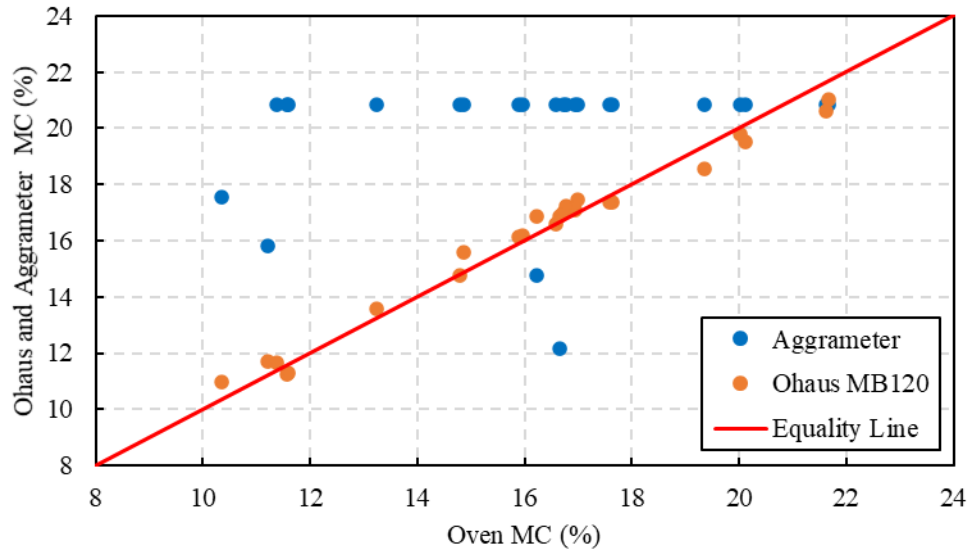


Figure 3.28 Ohaus MB120 and Aggrameter moisture content versus oven moisture content for the lean clay.

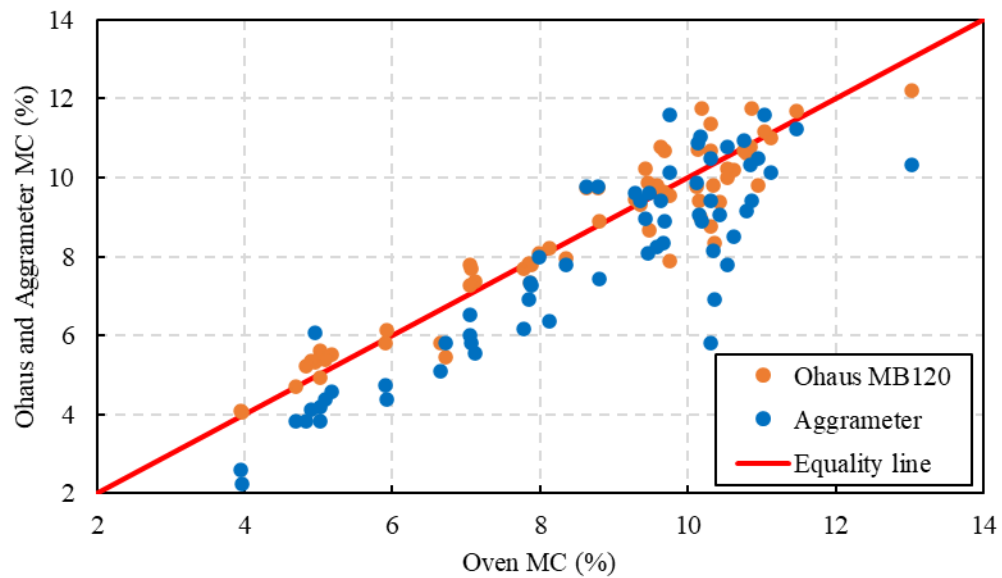


Figure 3.29 Ohaus MB120 and Aggrameter moisture content versus oven moisture content for the well graded sand.

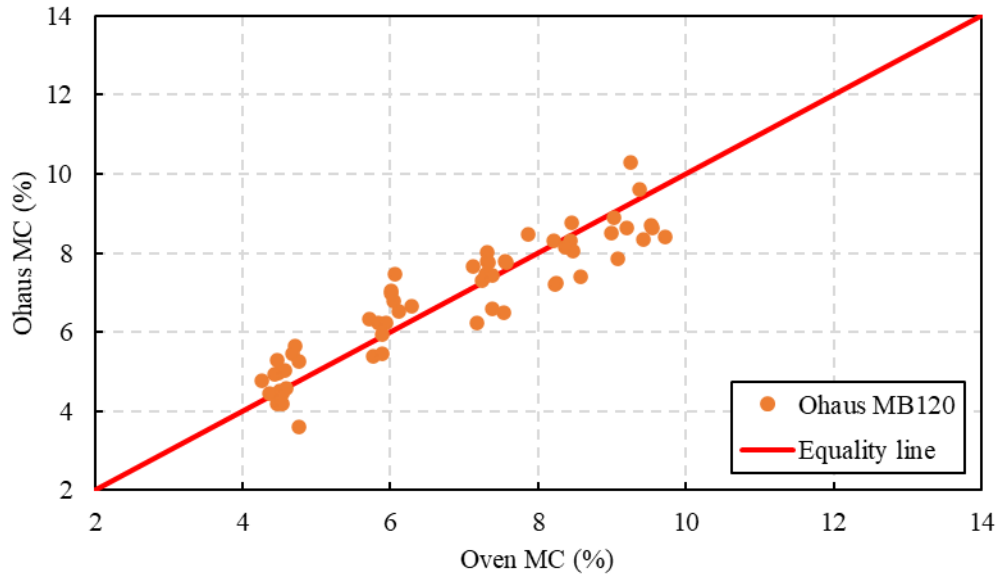


Figure 3.30 Ohaus MB120 moisture content versus oven moisture content for the base aggregate.

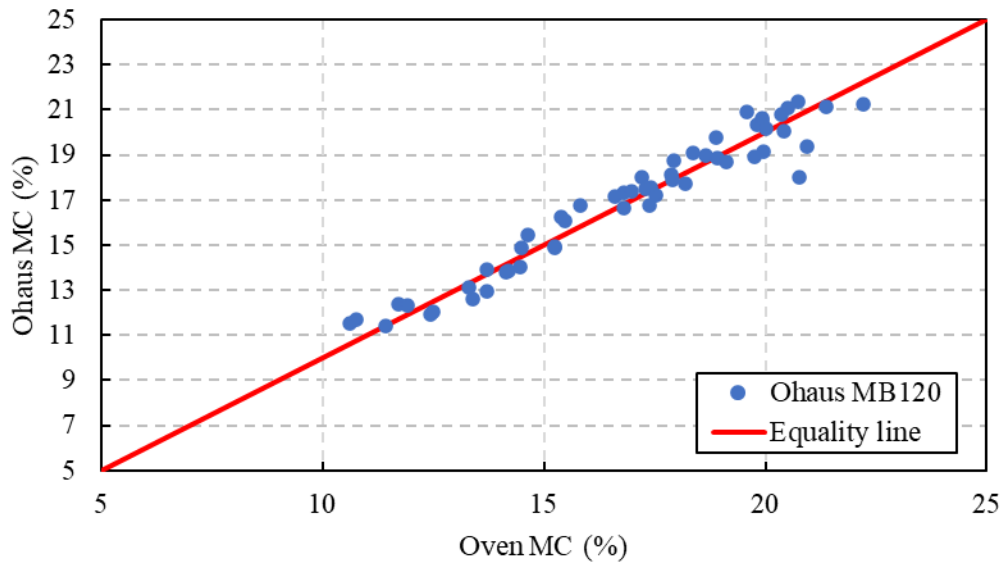
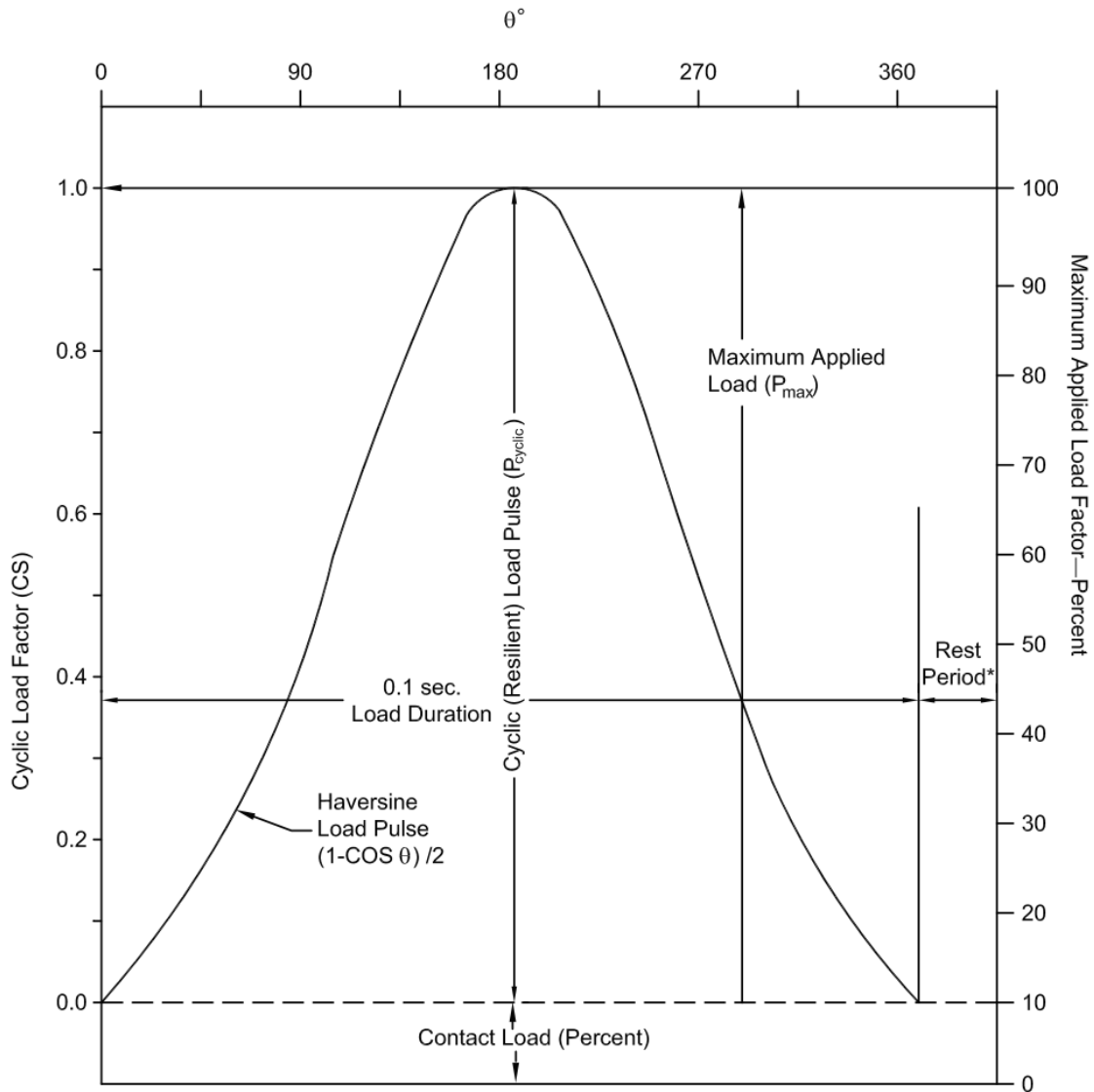


Figure 3.31 Ohaus MB120 moisture content versus oven moisture content for the silty clay.

3.4 Resilient Modulus Testing

Resilient modulus (M_R) is an essential material input for pavement design for subgrade and base soils required by the MEPDG. The M_R for an individual soil can significantly vary with changes in the density, moisture content, gradation, plasticity index, and stress level (Vanapalli et al., 1999). The M_R of unbound materials is determined in the laboratory by the repeated load triaxial test (RLTT) according to the procedure in AASHTO T307 (2006). Typically, 15 combinations of different axial loads and confining

pressures are applied during the test in addition to the preconditioning phase. The combination values change based on the vertical location of the material in the pavement structure (subgrade or base/subbase). Tables 3.14 and 3.15 depict the test loading sequences for subgrade and base/subbase soils, respectively. Figure 3.32 shows the shape of a haversine loading wave and terms of a load pulse in the RLTT. As shown in the Figure 3.32, a loading pattern consists of a 0.1-s haversine loading pulse and a 0.9-s rest period. The RLTT apparatus is a computer-controlled closed-loop hydraulic system with programmed loading sequences and data acquisition rates. Figure 3.33 shows the MTS 858 load frame and 2.8-inch and 4-inch diameter triaxial cells for M_R tests in this project. The specimen diameter was 2.8-inch for the two clay soils and the well graded sand and 4-inch for the base aggregate.



* The rest period will be 0.9 s for hydraulic loading devices and 0.9 to 3.0 s for pneumatic loading devices.

Figure 3.32 RLTT wave shape and terms: contact stress, cyclic axial stress, and maximum applied stress (AASHTO T 307, 1999).

Table 3.14 Testing sequence for subgrade soils (AASHTO T 307, 1999).

Sequence No.	Confining Pressure, σ_3		Max. Axial Stress, σ_{max}		Cyclic Stress, σ_{cyclic}		Constant Stress, $0.1 \sigma_{max}$		No. of Load Applications
	kPa	psi	kPa	psi	kPa	psi	kPa	psi	
-									-
0	41.4	6	27.6	4	24.8	3.6	2.8	0.4	500–1000
1	41.4	6	13.8	2	12.4	1.8	1.4	0.2	100
2	41.4	6	27.6	4	24.8	3.6	2.8	0.4	100
3	41.4	6	41.4	6	37.3	5.4	4.1	0.6	100
4	41.4	6	55.2	8	49.7	7.2	5.5	0.8	100
5	41.4	6	68.9	10	62.0	9.0	6.9	1.0	100
6	27.6	4	13.8	2	12.4	1.8	1.4	0.2	100
7	27.6	4	27.6	4	24.8	3.6	2.8	0.4	100
8	27.6	4	41.4	6	37.3	5.4	4.1	0.6	100
9	27.6	4	55.2	8	49.7	7.2	5.5	0.8	100
10	27.6	4	68.9	10	62.0	9.0	6.9	1.0	100
11	13.8	2	13.8	2	12.4	1.8	1.4	0.2	100
12	13.8	2	27.6	4	24.8	3.6	2.8	0.4	100
13	13.8	2	41.4	6	37.3	5.4	4.1	0.6	100
14	13.8	2	55.2	8	49.7	7.2	5.5	0.8	100
15	13.8	2	68.9	10	62.0	9.0	6.9	1.0	100

Table 3.15 Testing sequence for base/subbase soils (AASHTO T 307, 1999).

Sequence No.	Confining Pressure, σ_3		Max. Axial Stress, σ_{max}		Cyclic Stress, σ_{cyclic}		Constant Stress, $0.1 \sigma_{max}$		No. of Load Applications
	kPa	psi	kPa	psi	kPa	psi	kPa	psi	
-									-
0	103.4	15	103.4	15	93.1	13.5	10.3	1.5	500–1000
1	20.7	3	20.7	3	18.6	2.7	2.1	0.3	100
2	20.7	3	41.4	6	37.3	5.4	4.1	0.6	100
3	20.7	3	62.1	9	55.9	8.1	6.2	0.9	100
4	34.5	5	34.5	5	31.0	4.5	3.5	0.5	100
5	34.5	5	68.9	10	62.0	9.0	6.9	1.0	100
6	34.5	5	103.4	15	93.1	13.5	10.3	1.5	100
7	68.9	10	68.9	10	62.0	9.0	6.9	1.0	100
8	68.9	10	137.9	20	124.1	18.0	13.8	2.0	100
9	68.9	10	206.8	30	186.1	27.0	20.7	3.0	100
10	103.4	15	68.9	10	62.0	9.0	6.9	1.0	100
11	103.4	15	103.4	15	93.1	13.5	10.3	1.5	100
12	103.4	15	206.8	30	186.1	27.0	20.7	3.0	100
13	137.9	20	103.4	15	93.1	13.5	10.3	1.5	100
14	137.9	20	137.9	20	124.1	18.0	13.8	2.0	100
15	137.9	20	275.8	40	248.2	36.0	27.6	4.0	100



MTS 858 load frame



2.8-inch load cell



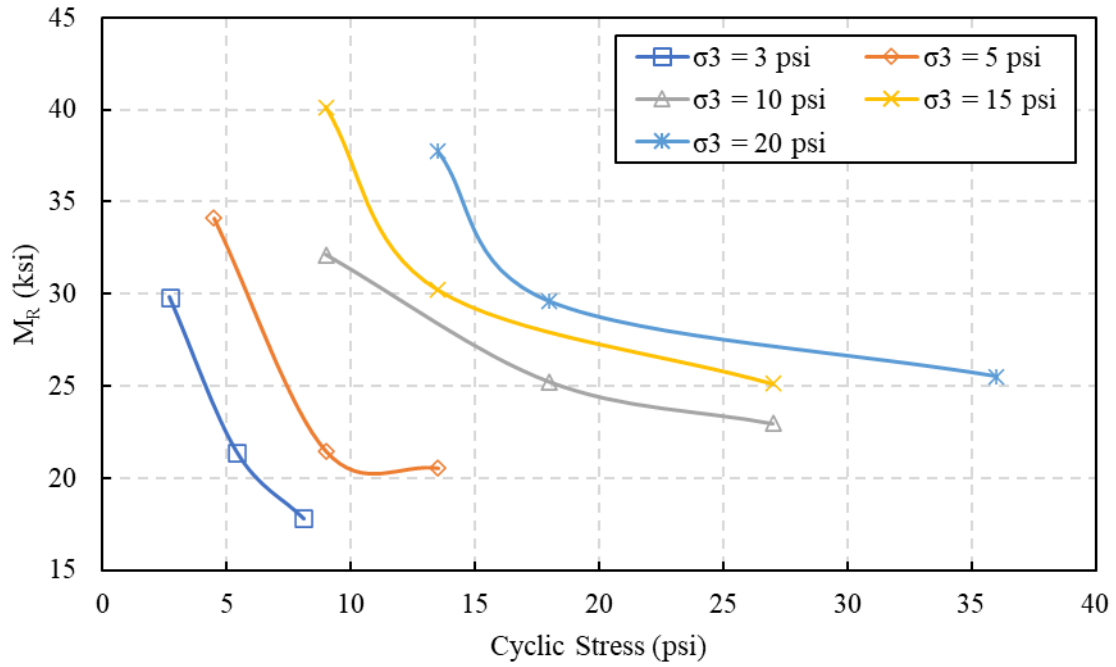
4-inch load cell

Figure 3.33 MTS 858 load frame and used cells for M_R tests.

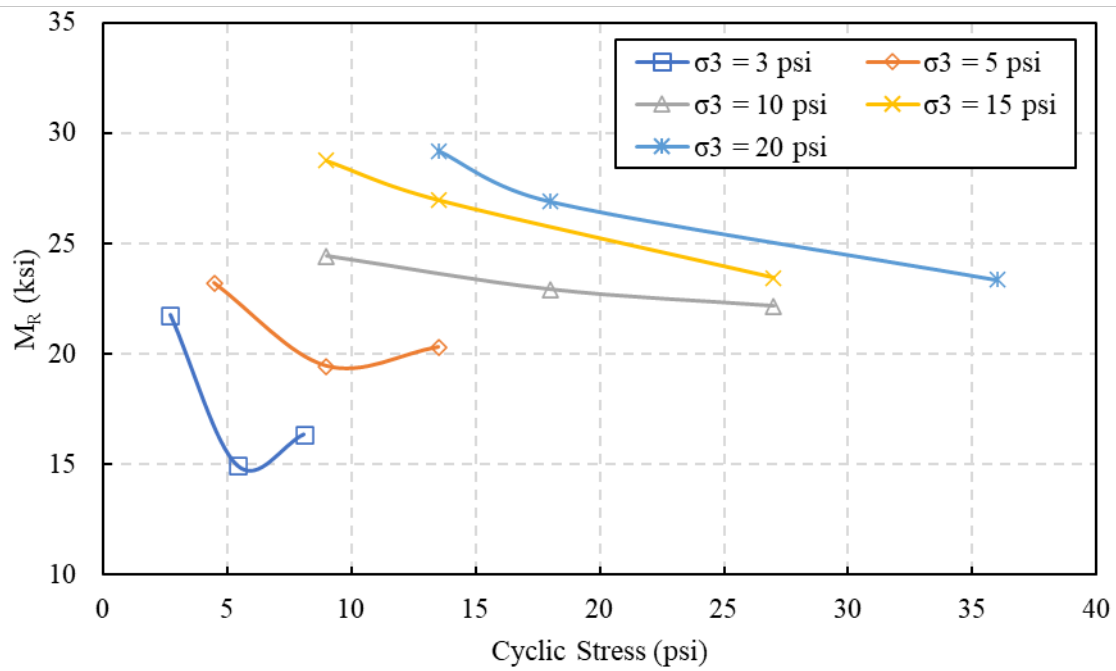
The RLTTs were performed at targeted moisture contents similar to those used in the LWD tests on Proctor mold, as shown in Tables 3.6 through 3.9. However, the two clay soils at high moisture content were relatively unstable and failed at certain loading sequences during the testing. For example, the lean clay failed at moisture content of 18.2%, and the silty clay failed at 18.5% moisture content. RLTT samples were prepared in molds with a height to diameter ratio of two using the Proctor hammer. The number of layers and drops per layer were adjusted for the RLTT mold to achieve densities similar to that of the Proctor test, as shown in Tables 3.6 through 3.9.

Since the well graded sand and the base aggregate required the testing sequence shown in Table 3.15 with higher confining pressures and stresses, it was decided to apply the same sequence to the two clays for the purpose of a level comparison of all four materials. The M_R versus applied cyclic stresses at different confining pressures and moisture contents for all soils are shown in Figures 3.34 through 3.37, the five levels of confining pressures were plotted into five series in each figure, such that relationship between the M_R , cyclic stress, and confining pressure are presented comprehensively.

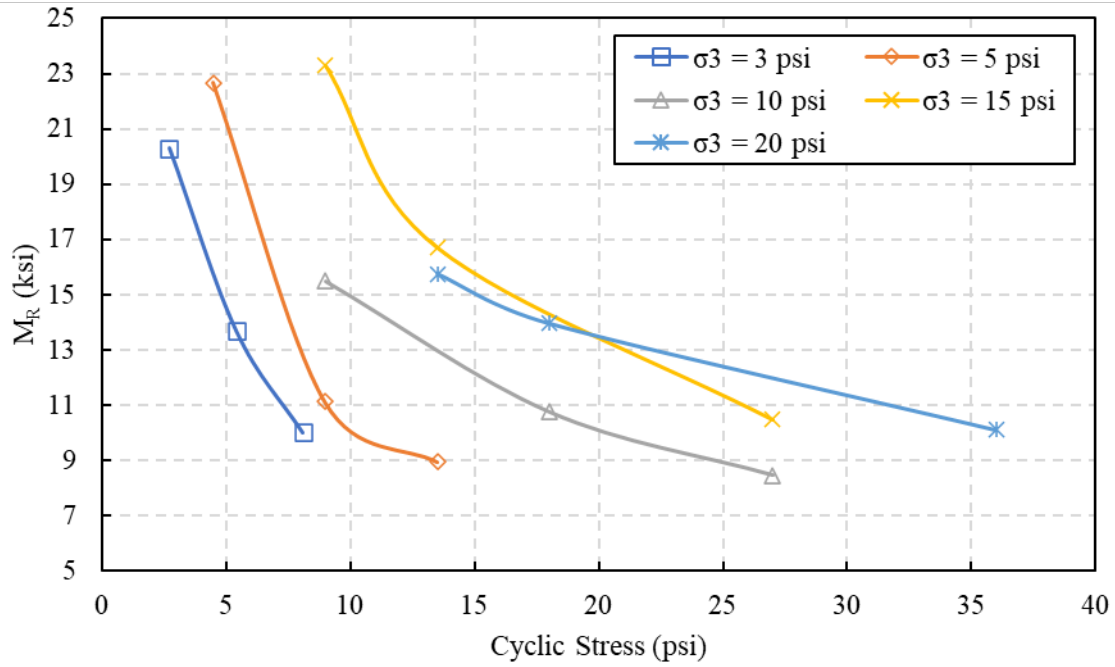
For the lean clay, it is obvious in Figure 3.34 that the M_R decreased with increasing the deviatoric stresses at each confining pressure. Another variable that affects the M_R value is the confining pressure, the M_R generally increased as increasing the confining pressures, the only exception is the testing at confining pressure of 20 psi (137.9 kPa) in Figure 3.34c.



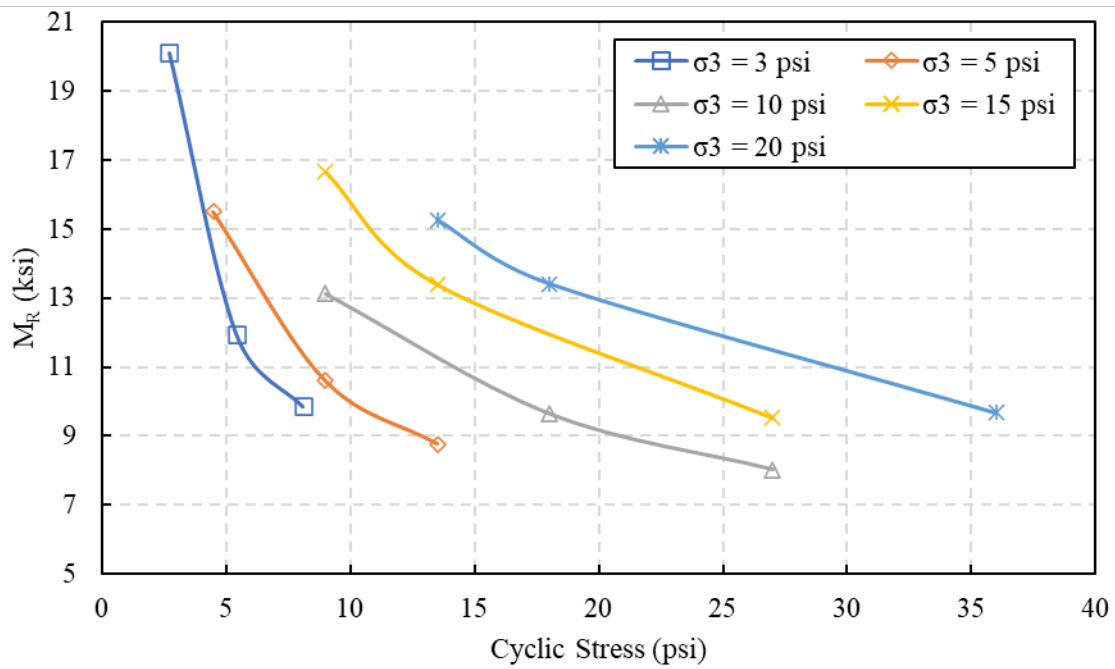
(a) Moisture content = 10.2%



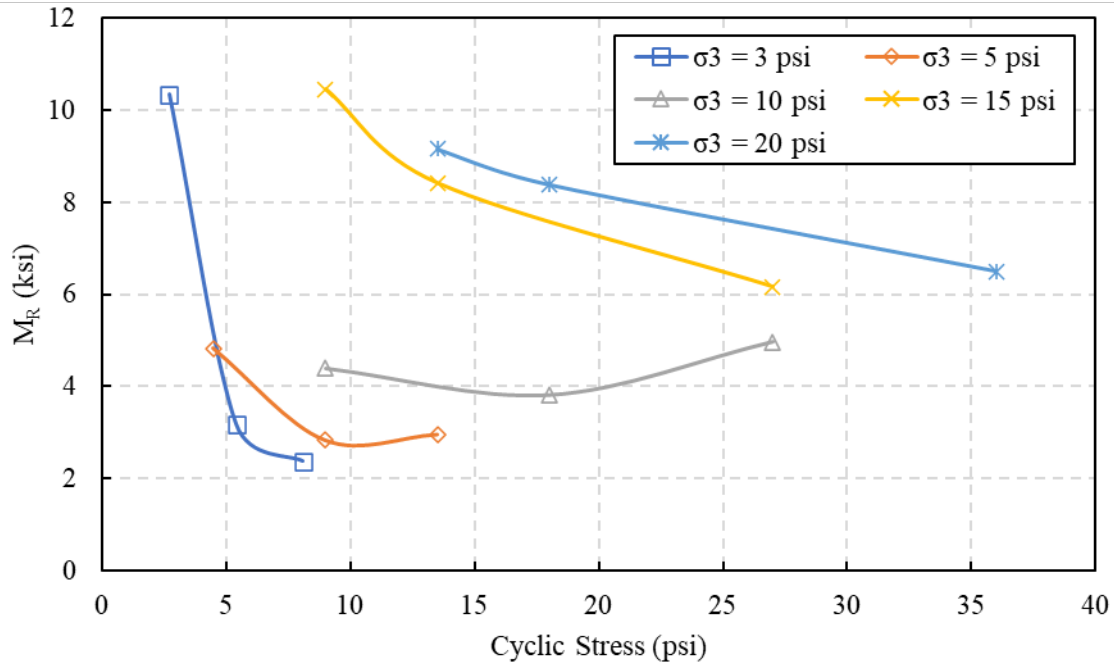
(b) Moisture content = 12.2%



(c) Moisture content = 14.2%



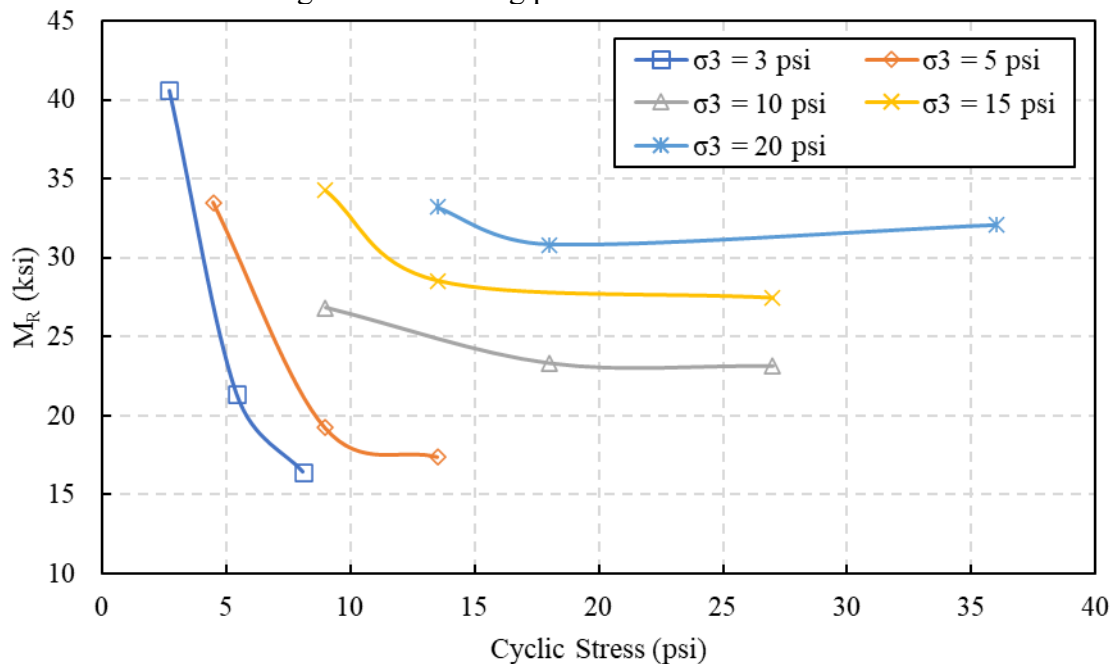
(d) Moisture content = 16.2%



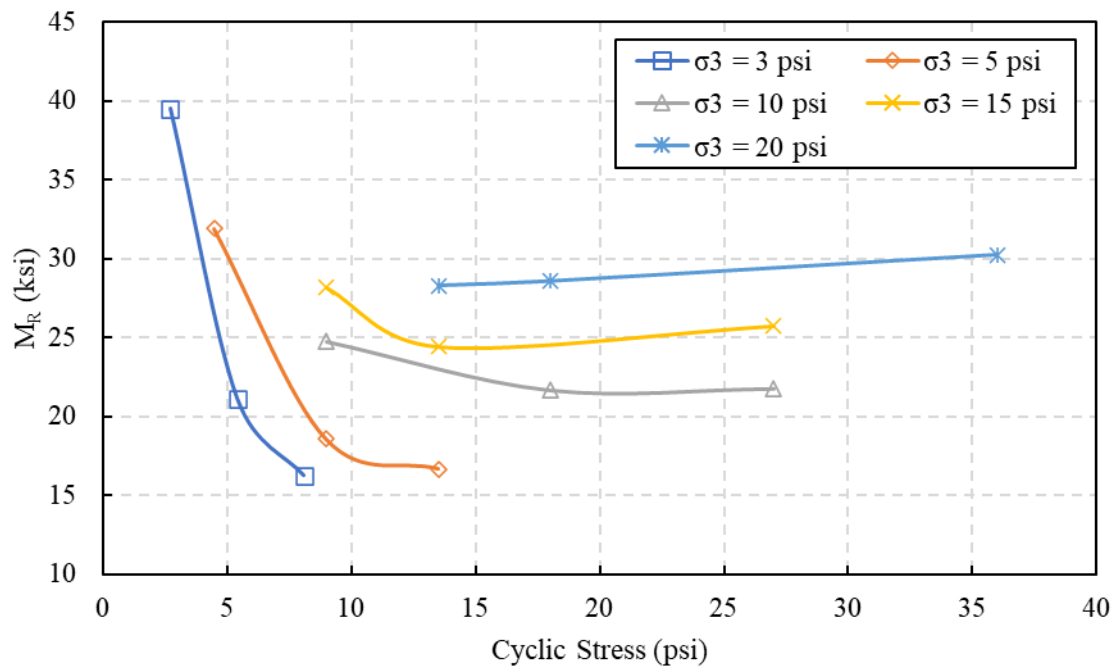
(e) Moisture content = 18.2%

Figure 3.34 M_R test results at different confining pressures and different moisture contents for the lean clay.

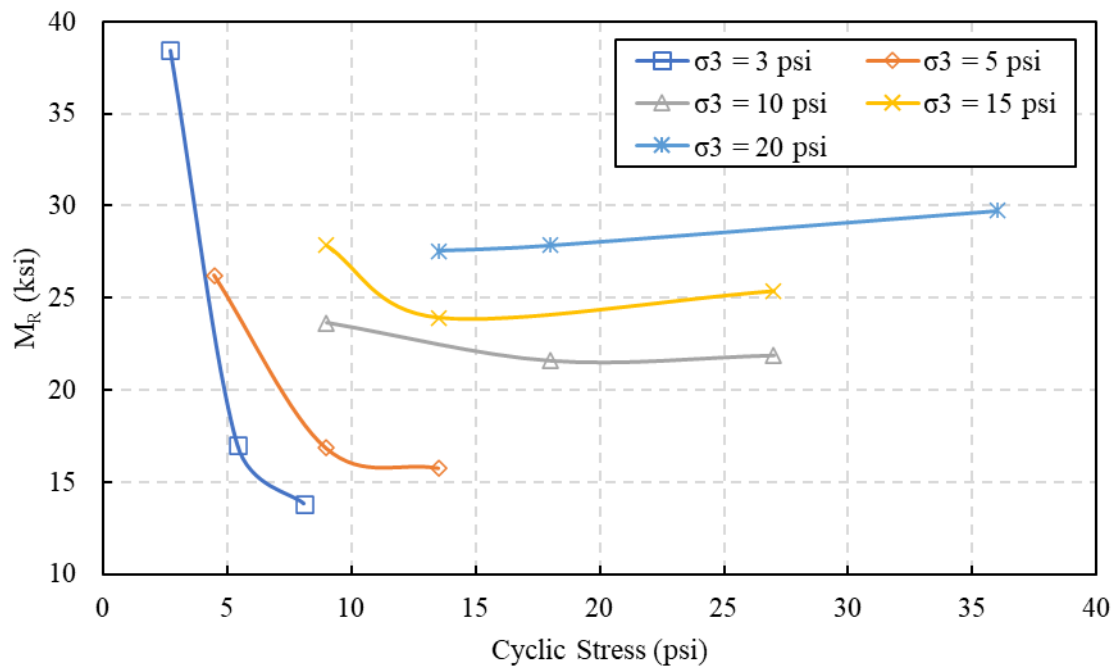
For the well graded sand, Figures 3.35a to 3.35e show that the M_R decreased as the cyclic stresses increased at confining pressures of 3 psi (20.7 kPa), 5 psi (34.5 kPa), and 10 psi (68.9 kPa) but increased at 15-psi (103.4 kPa) and 20-psi (137.9 kPa) confining pressures. Regarding to the confining pressures, the M_R of the well graded sand also increased with increasing of the confining pressures.



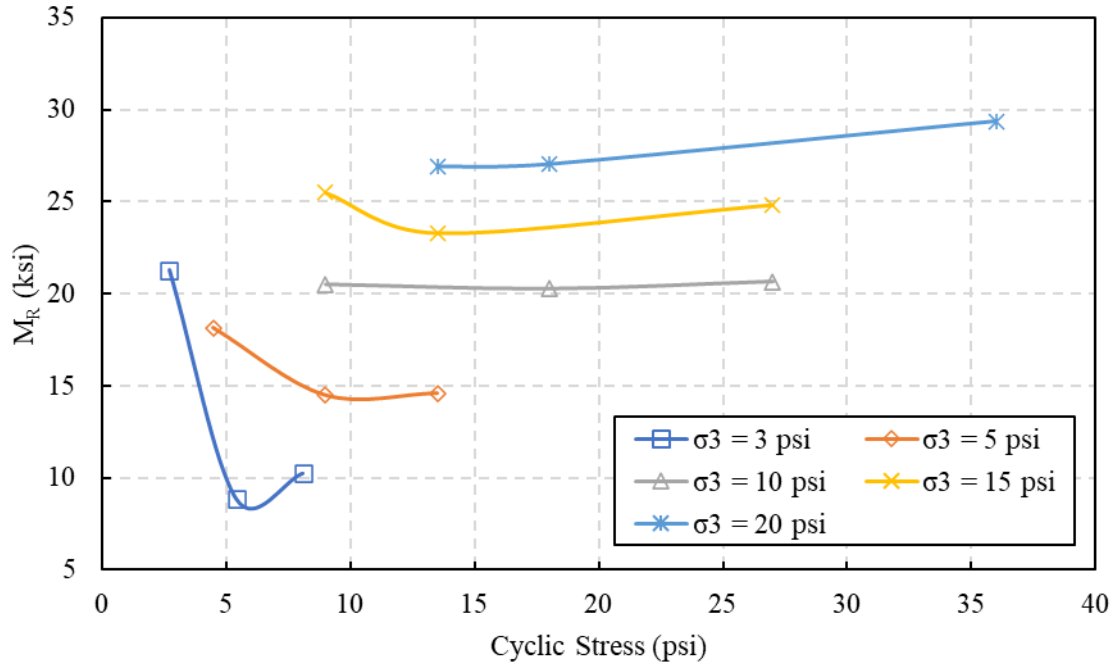
(a) Moisture content = 5%



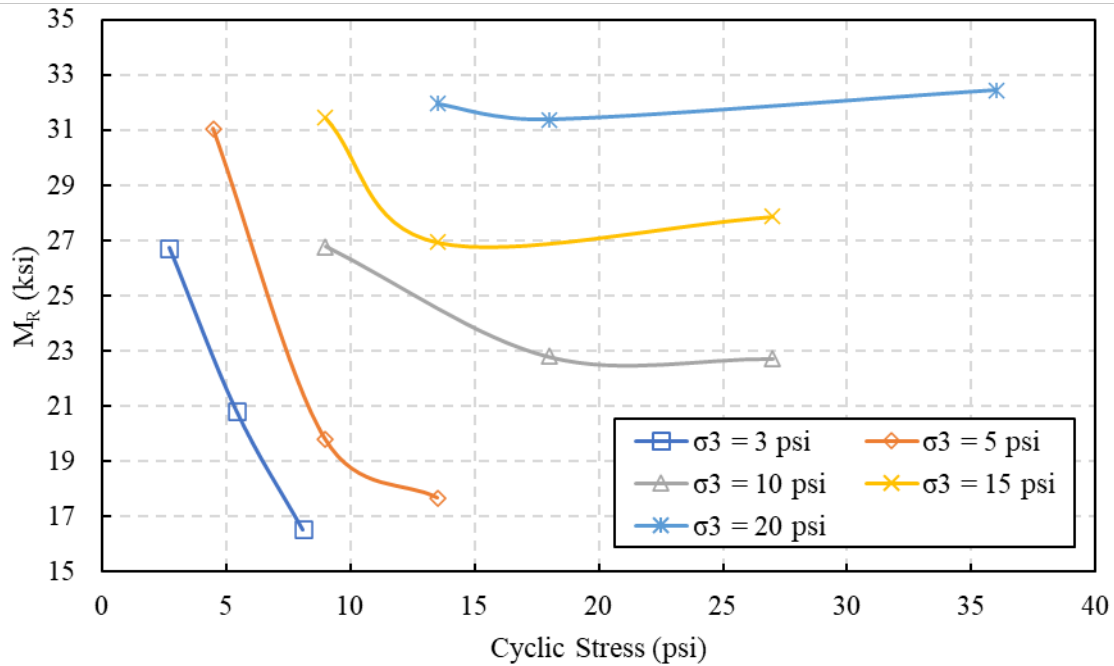
(b) Moisture content = 7%



(c) Moisture content = 9%



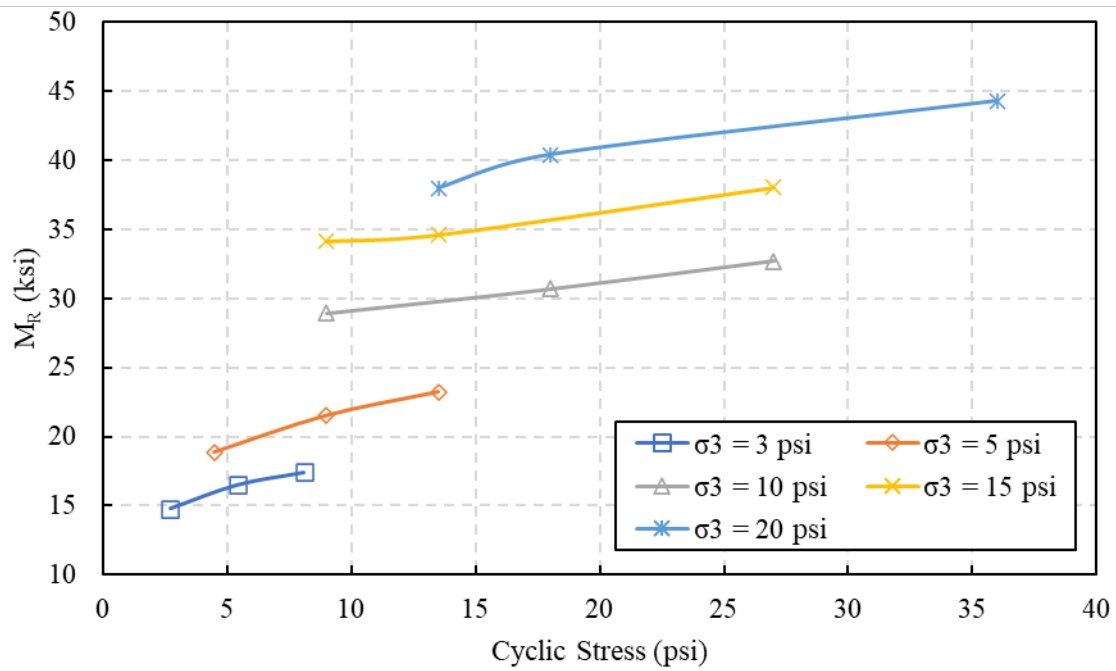
(d) Moisture content = 10%



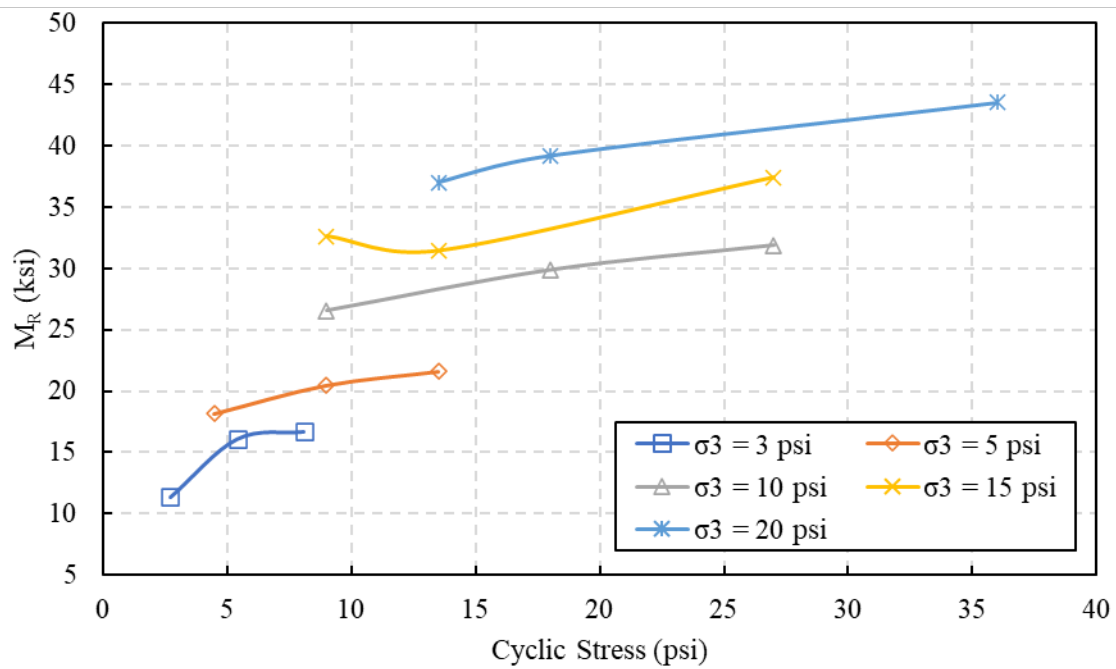
(e) Moisture content = 11%

Figure 3.35 M_R test results at different confining pressures and different moisture contents for the well graded sand.

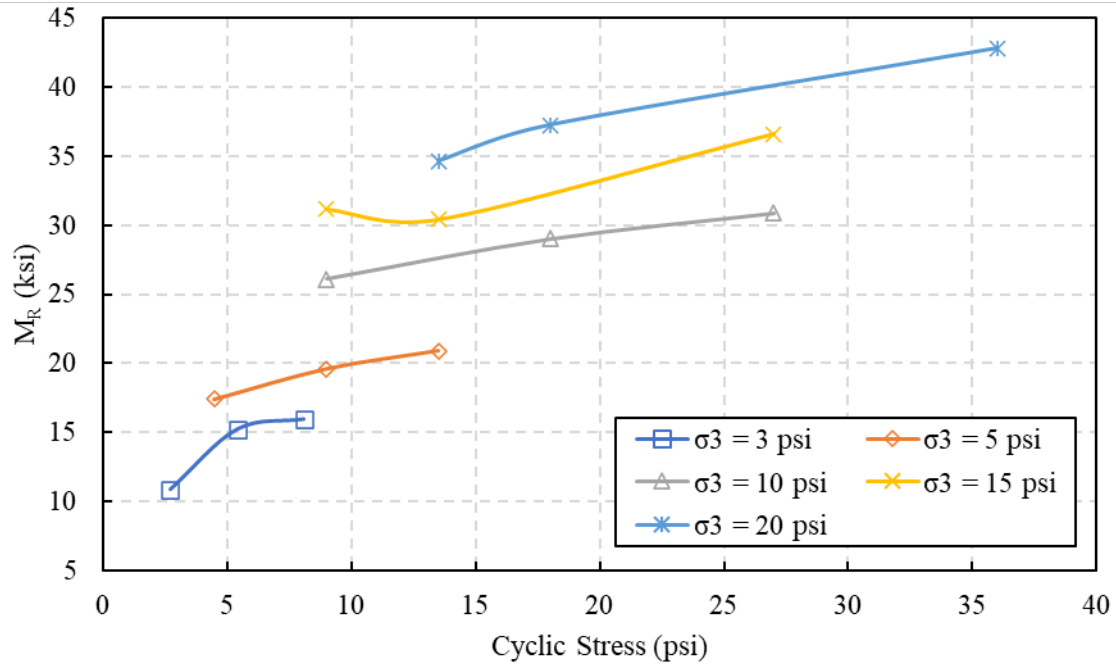
The base aggregate showed different trend compared with the previous two soils. As shown in Figures 3.36a to 3.36e, the M_R consistently increased as the deviatoric stresses increased under every confining pressure and showed definitive increase with the confining pressures increased.



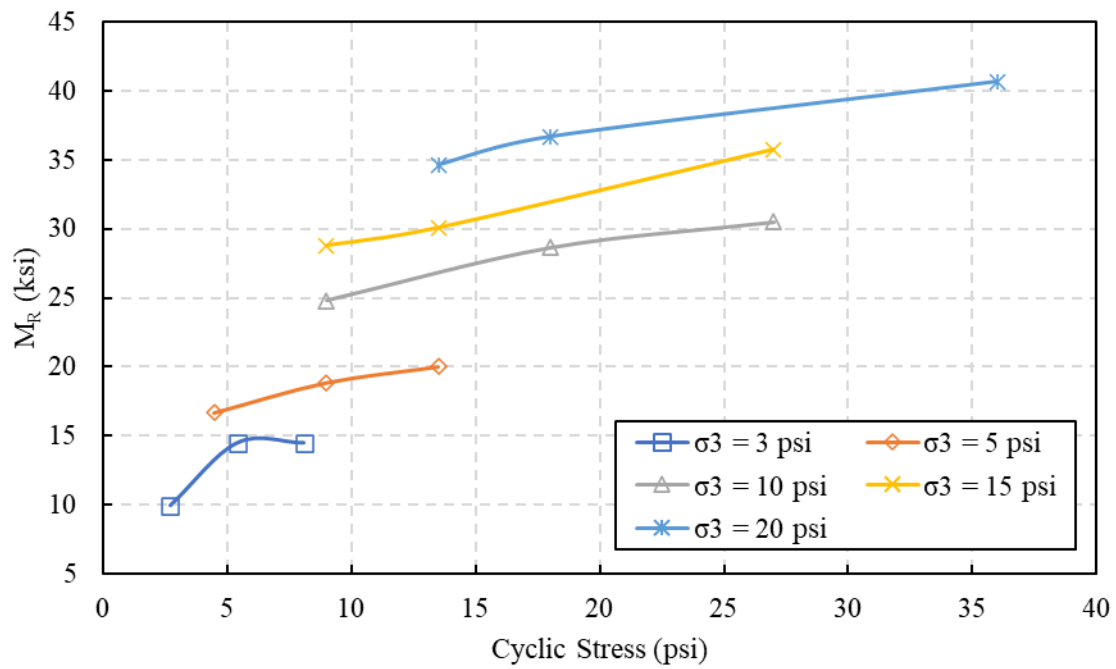
(a) Moisture content = 4.5%



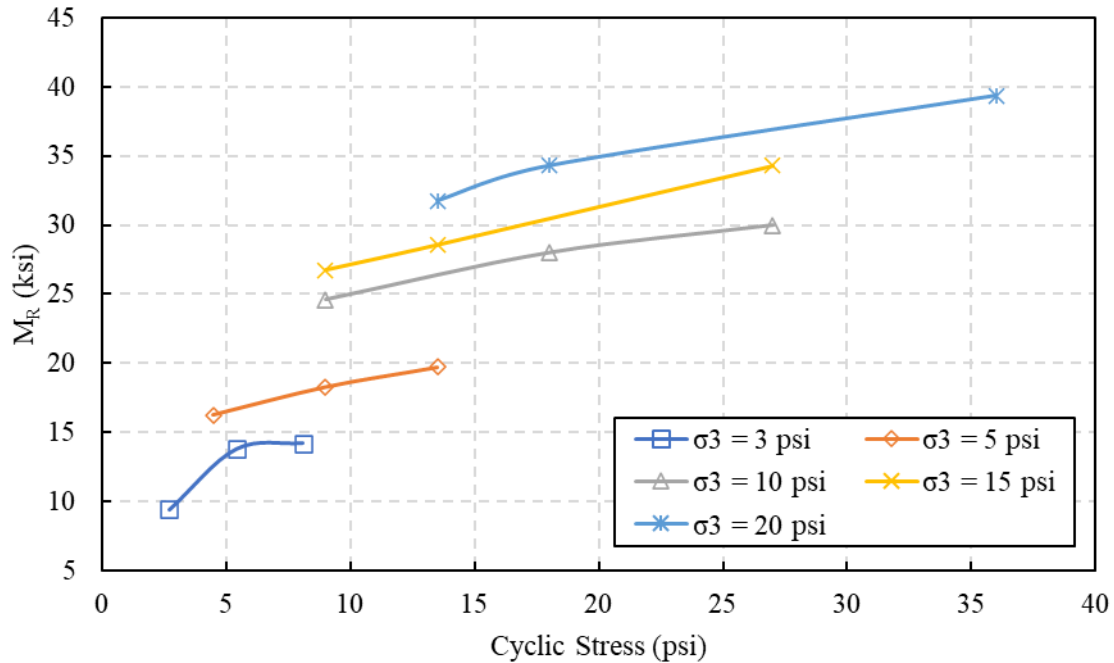
(b) Moisture content = 6%



(c) Moisture content = 7.5%



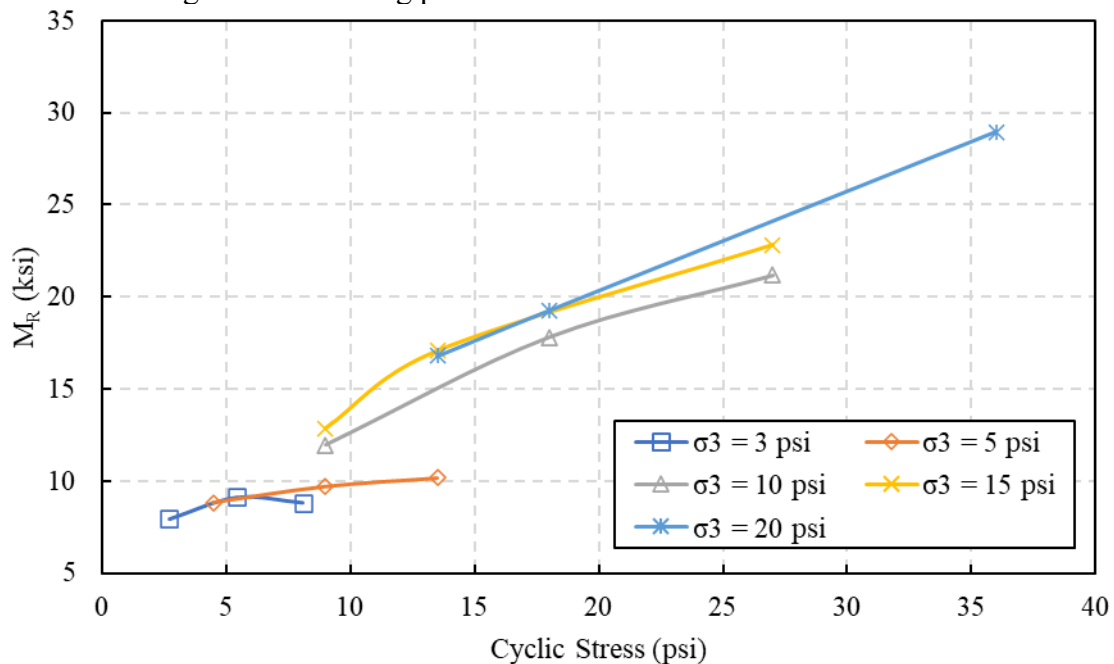
(d) Moisture content = 8.5%



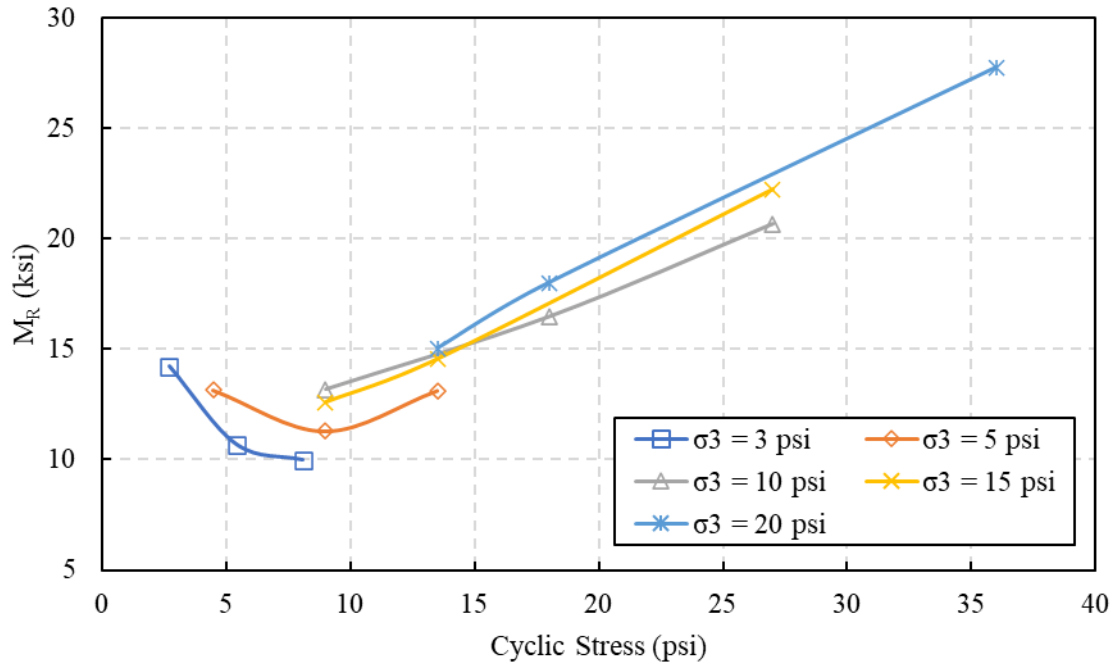
(e) Moisture content = 9.5%

Figure 3.36 MR test results at different confining pressures and different moisture contents for the base aggregate.

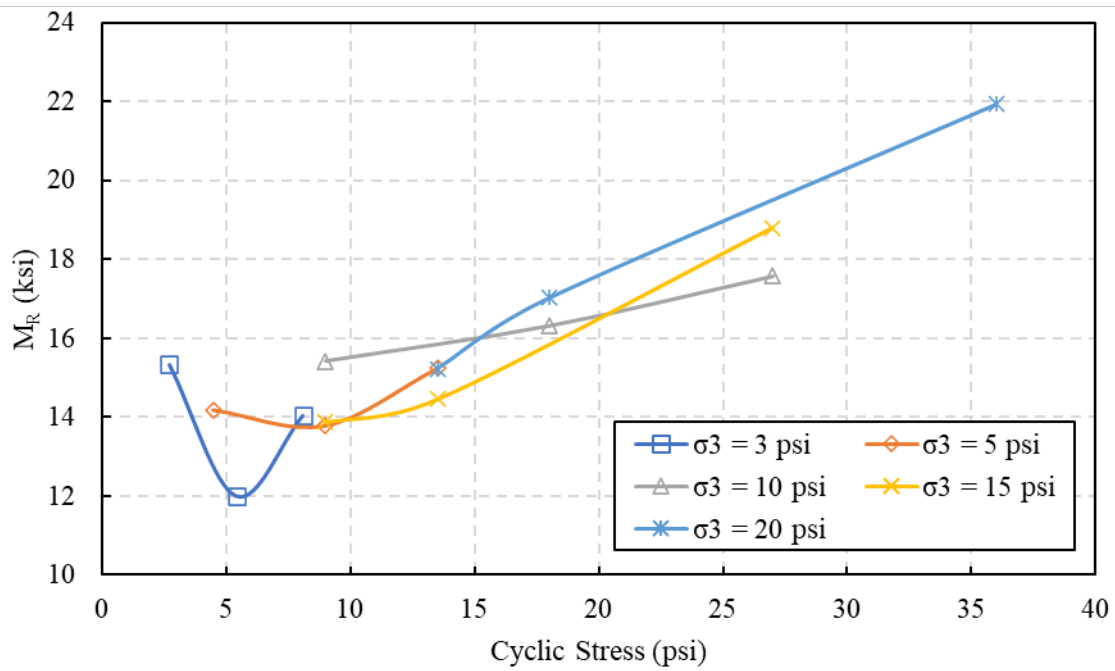
For the silty clay, Figures 3.37a to 3.37e show that the M_R generally increased with cyclic stresses increased except for some results obtained in first sequence at each confining pressure, where the highest M_R was measured compared with the other two sequences at the same confining pressure. Besides, the M_R also showed a general increase responding to the increasing of the confining pressures.



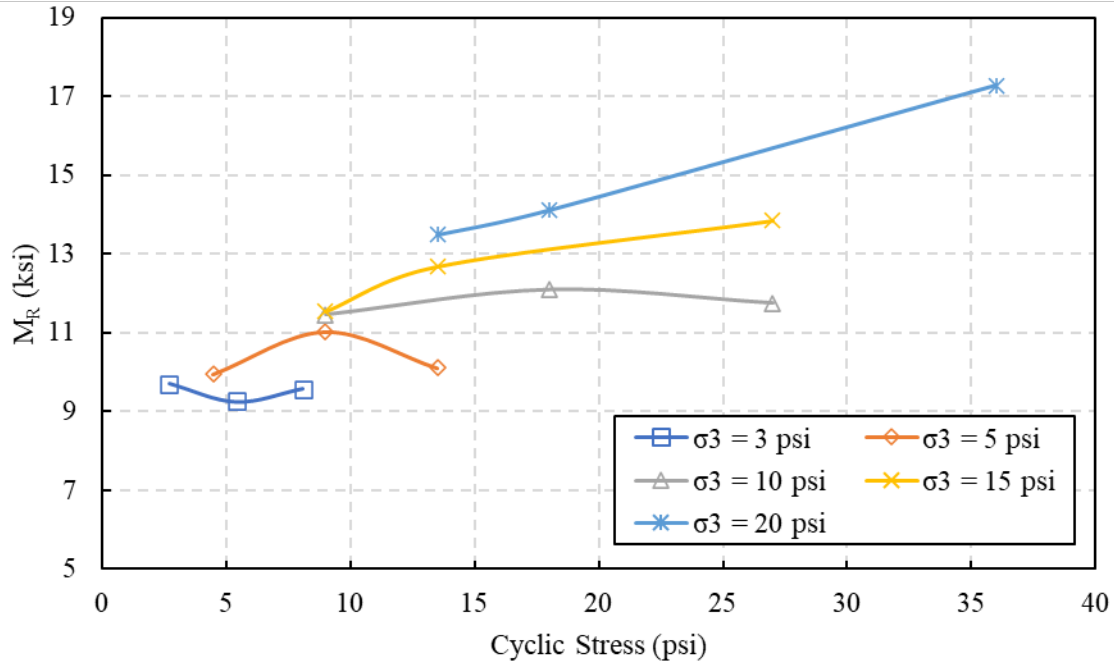
(a) Moisture content = 8.5%



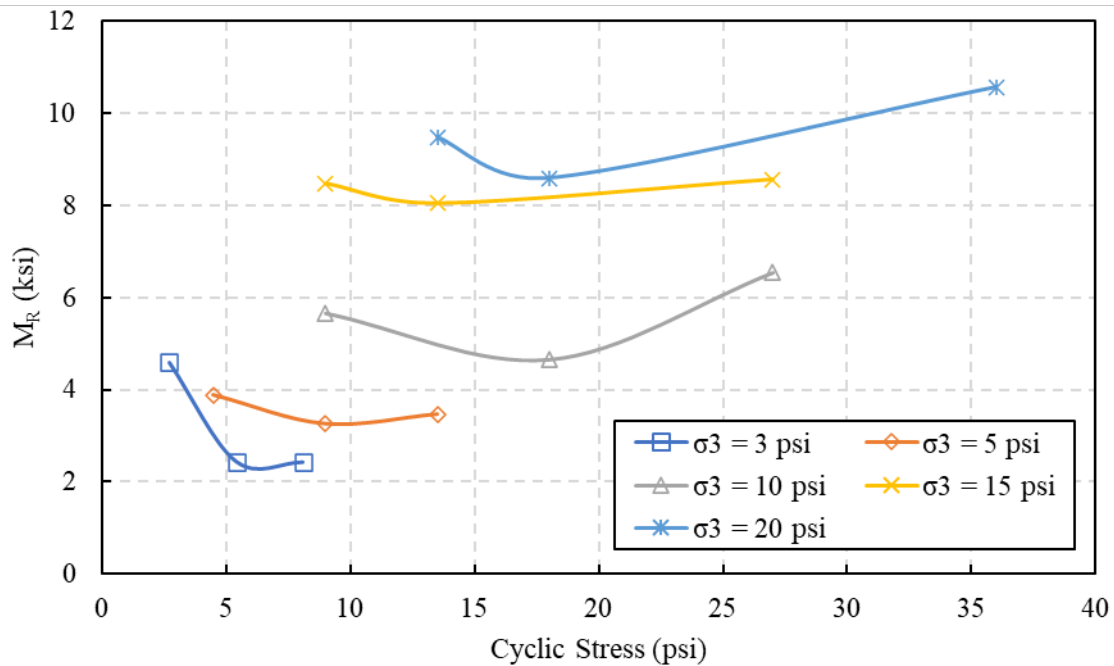
(b) Moisture content = 10.5%



(c) Moisture content = 12.5%



(d) Moisture content = 14.5%



(e) Moisture content = 16.5%

Figure 3.37 M_R test results at different confining pressures and different moisture contents for the silty clay.

According to the analysis of the four tested geomaterials including the lean and silty clays, well graded sand, and base aggregate, the base aggregate showed the most obvious stress dependency property that most unbound geomaterials have as well as the highest M_R , the M_R of the base aggregate increased significantly with increasing of cyclic

stresses and confining pressures, while other three geomaterials showed lower degree of stress dependency. This is because the base aggregate has the largest nominal maximum particle size (NMPS) among the four soils, the effective stress inside the soil was supported mainly by large particles for the base aggregate, which have higher stiffness and stability than smaller particles and fines that bear effective stresses in the rest three soils.

Moreover, the experimental results were reformulated and replotted to present the effect of moisture content under the condition of different bulk stresses. Figure 3.38 shows the M_R changes with bulk stresses at different moisture contents for the lean clay. It indicates that M_R significantly decreased as the moisture content increased at the same bulk stresses. Similar trends were also noticed for the well graded sand and base aggregate materials, as shown in Figures 3.39 and 3.40, respectively. However, a jump in the M_R value was noticed in the well graded sand for specimens at moisture content of 11%, and M_R of silty clay began with a low value for samples having moisture content of 8.5% and 10.5% under low bulk stress, as indicated in Figures 3.39 and 3.41, respectively. This jump can be attributed to the excess pore water pressure generated due to fast loading for a near saturation sample ($S_r=89\%$). The reason why the silty clay started from low M_R values could be insufficient percent compaction due to poor soil lubrication at low moisture content.

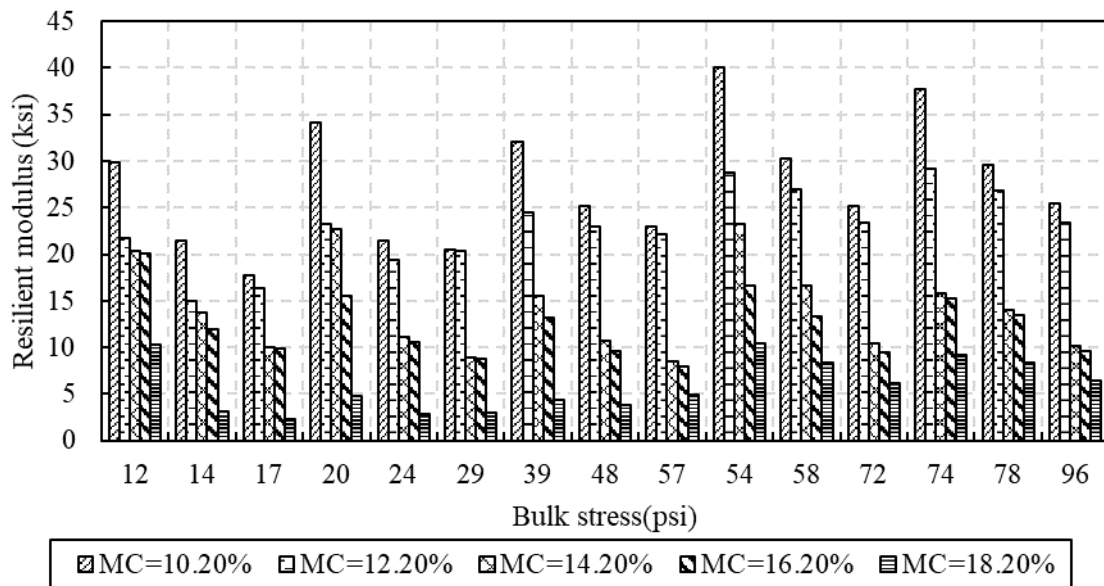


Figure 3.38 M_R changes with moisture content and bulk stress for the lean clay.

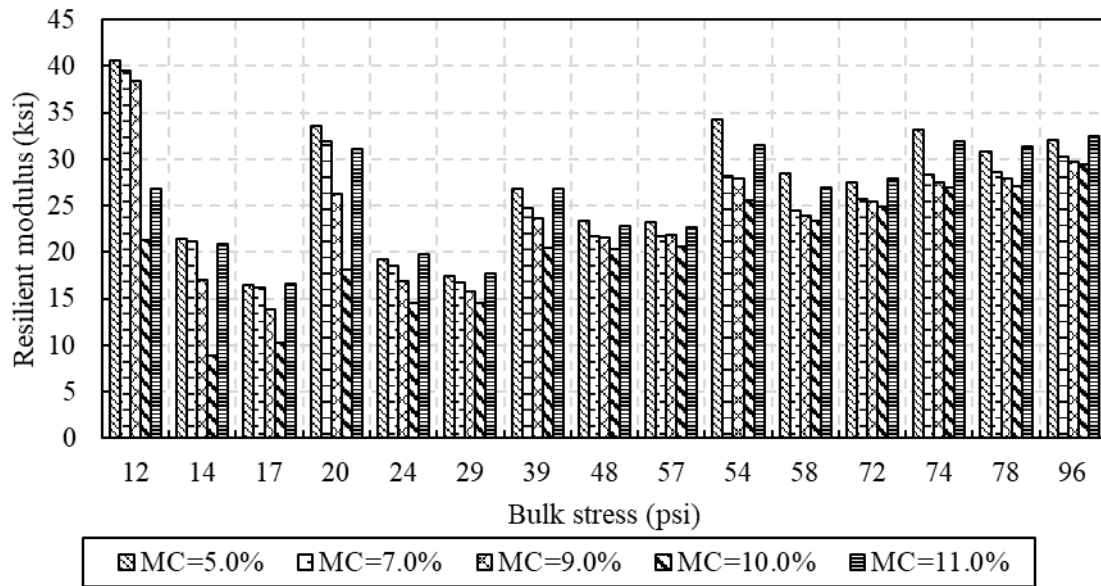


Figure 3.39 M_R changes with moisture content and bulk stress for the well graded sand.

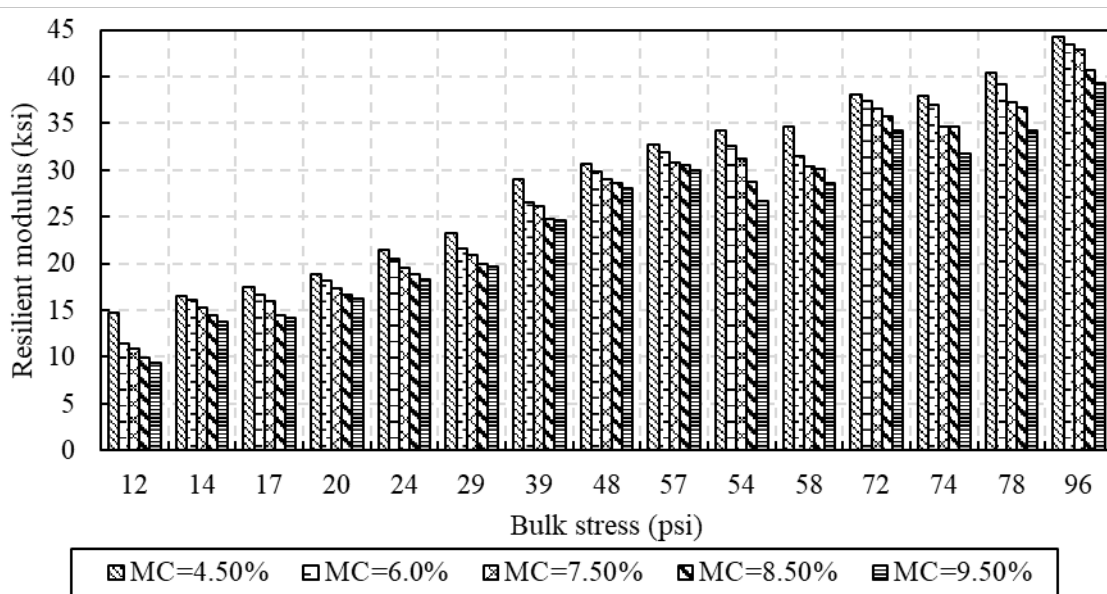


Figure 3.40 M_R changes with moisture content and bulk stress for the base aggregate.

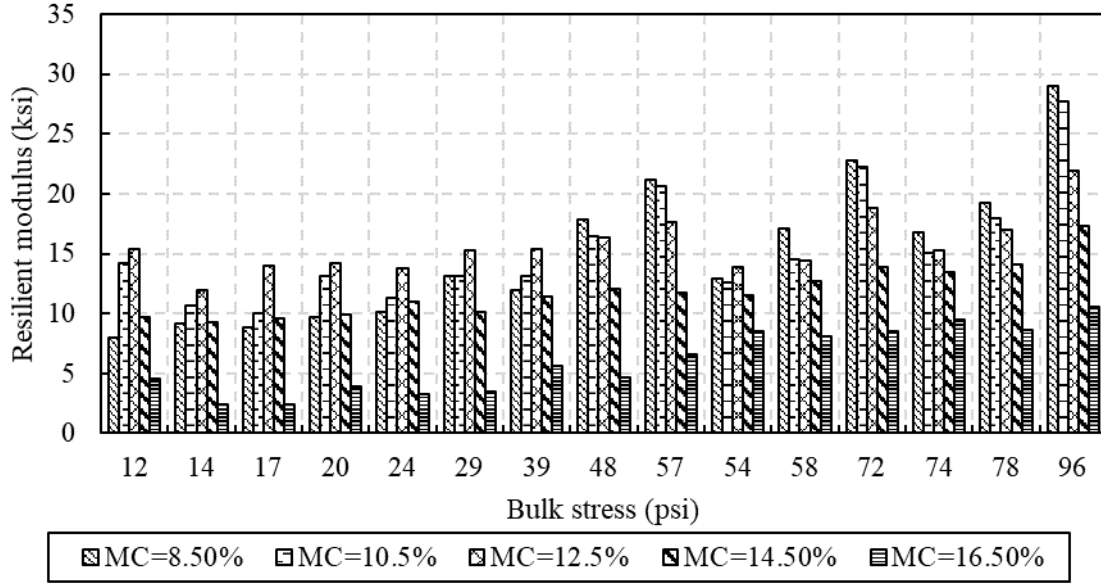


Figure 3.41 M_R changes with moisture content and bulk stress for the silty clay.

Regression analyses were then performed to best fit the MEPDG universal constitutive model using the experimental results. It is worth noting that the MEPDG model considers the effect of applied mechanical stresses only as follows:

$$M_R = k_1 p_a \left(\frac{\theta}{p_a} \right)^{k_2} \left(\frac{\tau_{oct}}{p_a} + 1 \right)^{k_3} \quad (10)$$

where:

M_R = resilient modulus, (ksi),

$\theta = \sigma_1 + \sigma_2 + \sigma_3 = \sigma_1 + 2\sigma_3$ = bulk stress, (psi),

$\tau_{oct} = \frac{1}{3} \sqrt{(\sigma_1 - \sigma_2)^2 + (\sigma_1 - \sigma_3)^2 + (\sigma_2 - \sigma_3)^2} = \frac{\sqrt{2}}{3} (\sigma_1 - \sigma_2)$ = octahedral shear stress, (psi),

p_a = atmospheric pressure used to normalize the equation, 15.0 psi (101.3 kPa), and

k_1, k_2, k_3 = regression constants calibrated from experimental results.

The regression coefficient k_1 in the MEPDG model is a positive number directly proportional to the modulus. The coefficient k_2 is a positive value known as the stress hardening term, this is most significant in granular materials. The coefficient k_3 is a negative value, known as the stress softening term. The k_3 coefficient is more significant in clay, showing a modulus reduction with increased octahedral shear stress.

Tables 3.16 through 3.19 summarize the average test results and coefficients of the M_R universal model for the lean clay, well graded sand, base aggregate, and silty clay. As mentioned earlier, the model neglects the effect of moisture content on M_R results. Therefore, independent sets of regression parameters were calibrated for each moisture content. Some statistical characteristics are provided in these tables, such as the summation of square errors (SSE) and the R^2 between model predictions and experimental results. For the lean clay, the softening parameter k_3 were negative values and less than other materials due to the M_R decrease with increasing the deviatoric

stresses while negative k_3 appeared only at last high moisture content for silty clay. This parameter, however, had positive values for the base aggregate and four moisture contents of silty clay. The hardening parameter k_2 were positive values for all soils due to the M_R increase with increased bulk stresses.

Table 3.16 Regression parameters of the MEPDG model for the lean clay.

Sample ID	#	1	2	3	4	5
MC	%	10.2	12.2	14.2	16.2	18.2
γ_d	lb/ft ³	110.8	116.5	120.3	116.5	112.0
p_a	psi	15.0	15.0	15.0	15.0	15.0
k_1	-	1633.13	1405.54	1231.07	1715.76	267.72
k_2	-	0.78	0.46	0.52	0.21	1.25
k_3	-	-2.07	-0.98	-2.65	-2.41	-2.95
SSE	ksi ²	137.34	29.21	92.85	114.09	81.89
Sqrt(SSE)	ksi	11.72	5.40	9.64	10.68	9.05
R ²	%	87.4	90.9	64.4	68.8	45.1

Table 3.17 Regression parameters of the MEPDG model for the well graded sand.

Sample ID	#	1	2	3	4	5
MC	%	5.0	7.0	9.0	10.0	11.0
γ_d	lb/ft ³	129.4	130.3	131.1	130.0	128.3
p_a	psi	15.0	15.0	15.0	15.0	15.0
k_1	-	937.91	1147.10	1332.36	1004.04	851.94
k_2	-	0.66	0.42	0.32	0.47	0.59
k_3	-	-0.66	-0.47	-0.41	-0.52	-0.46
SSE	ksi ²	49.62	111.89	269.16	107.65	10.49
Sqrt(SSE)	ksi	7.04	10.58	16.41	10.38	3.24
R ²	%	93.0	70.8	38.4	73.0	98.0

Table 3.18 Regression parameters of the MEPDG model for the base aggregate.

Sample ID	#	1	2	3	4	5
MC	%	4.5	6.0	7.5	8.5	9.5
γ_d	lb/ft ³	133.0	136.9	139.4	138.8	136.9
p_a	psi	15.0	15.0	15.0	15.0	15.0
k_1	-	1162.32	981.00	714.41	959.13	998.79
k_2	-	0.44	0.55	0.44	0.48	0.44
k_3	-	0.03	0.04	0.51	0.26	0.14
SSE	ksi ²	12.48	33.57	17.45	56.41	16.12
Sqrt(SSE)	ksi	3.53	5.79	4.18	7.51	4.01
R ²	%	98.6	97.4	97.8	95.3	98.0

Table 3.19 Regression parameters of the MEPDG model for the silty clay.

Sample ID	#	1	2	3	4	5
MC	%	8.5	10.5	12.5	14.5	16.5
γ_d	lb/ft ³	119.7	119.7	120.3	119.0	113.9
p_a	psi	15.0	15.0	15.0	15.0	15.0
k_1	-	493.89	612.38	813.94	594.67	194.06
k_2	-	0.27	0.04	-0.02	0.19	0.85
k_3	-	1.11	1.29	0.74	0.27	-0.48
SSE	ksi ²	4.96	33.37	13.69	9.26	11.79
Sqrt(SSE)	ksi	2.23	5.78	3.70	3.04	3.43
R ²	%	99.0	89.9	83.4	86.0	88.8

3.4.1 Developing a New Resilient Modulus Prediction Model

As previously mentioned, the MEPDG prediction model only considers the mechanical stresses. The M_R , however, is affected by other factors such as material type (clay, sand, gravel), applied stresses, density, and moisture content. Since the LWD modulus is highly sensitive to moisture content, in this section, based on experimental results explained in

the last section, a new M_R prediction model was developed to account for the impact of moisture content. It is worth noticing that previous researchers developed many M_R prediction models that account for the physical properties of base materials (Hick & Monismith, 1971; Kalcheff & Hicks, 1973; Witczak & Uzan, 1988). However, the physical properties correlated to M_R varied between different materials and locations (Dai & Kremer, 2006; Hick & Monismith, 1971; Hopkins et al., 2007; Mohammad et al., 2009).

A modified universal expression for M_R of collected materials was obtained based on the MEPDG model (Equation 10) and considering the interaction of moisture content, as shown in Equation (11).

$$M_R = k_1 p_a \left(\frac{\theta}{p_a} \right)^{k_2} \left(\frac{\tau_{oct}}{p_a} + 1 \right)^{k_3} \quad (11)$$

where

$$k_1 = c_1 + c_2 w,$$

$$k_2 = c_3 + c_4 w,$$

$$k_3 = c_5 + c_6 w,$$

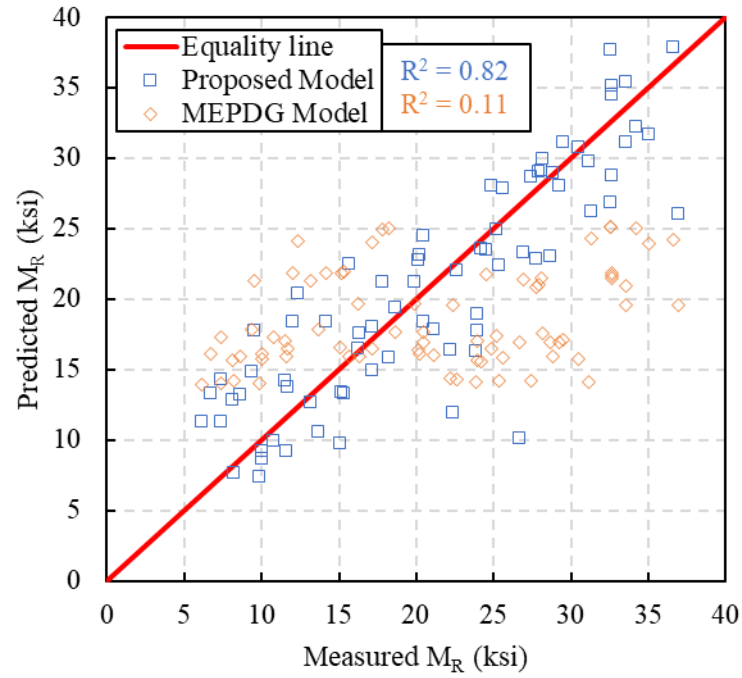
w = moisture content (%), and

c_i = regression constants.

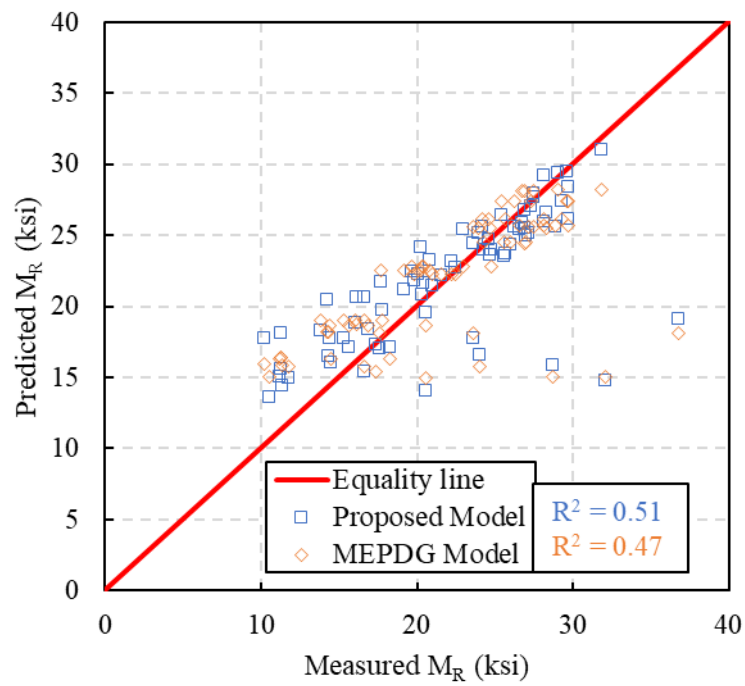
Then, multiple nonlinear regressions were performed to fit the M_R from laboratory testing data and determine regression coefficients for each soil in Equation (11). Table 3.20 lists the calibrated regression parameters. Figure 3.42 compares measured and predicted M_R values from the original and modified MEPDG model and their R^2 values. That modified model always has higher R^2 than the original MEPDG model (e.g., 0.82>0.11, 0.51>0.47, 0.89>0.88, and 0.78>0.37), indicates the effectiveness and robustness of the proposed modified model. The prediction accuracy of new model is higher for the lean clay and the silty clay because they have wider ranges of and higher sensitivity to the moisture content than the other two soils.

Table 3.20 Calibrated parameters for the new model.

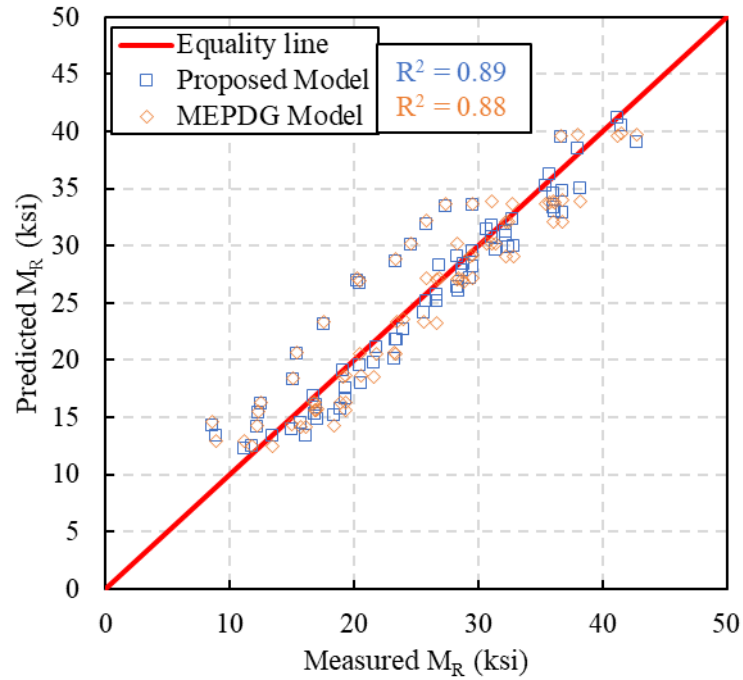
Parameter	Lean clay	SW	Base agg.	Silty clay
c_1	3440.81	1602.21	1183.62	1178.79
c_2	-156.38	-50.24	-29.63	-52.34
c_3	0.03	0.44	0.54	-0.26
c_4	0.03	0.00	-0.01	0.04
c_5	0.52	-0.95	-0.13	1.75
c_6	-0.15	0.06	0.04	-0.08



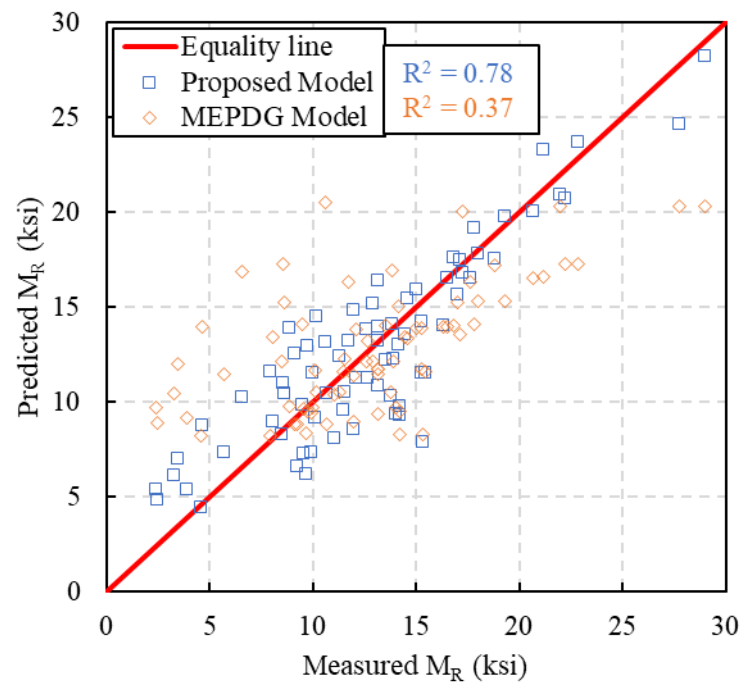
(a) Lean clay



(b) Well grade sand



(c) Base aggregate



(d) Silty clay

Figure 3.42 Comparison between the MEPDG and the proposed prediction model.

CHAPTER 4 FINDINGS FROM FIELD TESTING

4.1 Introduction

In order to evaluate the application of Zorn 2000 LWD, select field moisture content measurement devices for typical Missouri soils in actual construction practices, and correlate the field LWD surface modulus with the laboratory LWD test on Proctor mold results, the research team performed four field-testing campaigns in collaborating with the MoDOT personnel and the contractor.

Each field trip mainly includes the following tasks:

- To collect soil samples for laboratory testing and to check the consistency of soil gradation and compaction results.
- To acquire climatic conditions and soil surface temperature during construction.
- To measure in-situ compaction moisture contents using the Aggrameter and Ohaus MB120.
- To conduct LWD tests according to the testing plan (shown later) and establish the spatial variability of moisture contents and LWD moduli of the subgrade or base soils, as well as to investigate the reproducibility of three Zorn ZFG 2000 LWD devices. The LWD field and moisture content tests were performed immediately and two hours after the compaction to capture the effect of drying after compaction at some testing sites.
- To collect samples for laboratory testing on moisture content using the oven drying method.

4.2 Field Projects and Testing Method

4.2.1 *Introduction to Testing Sites*

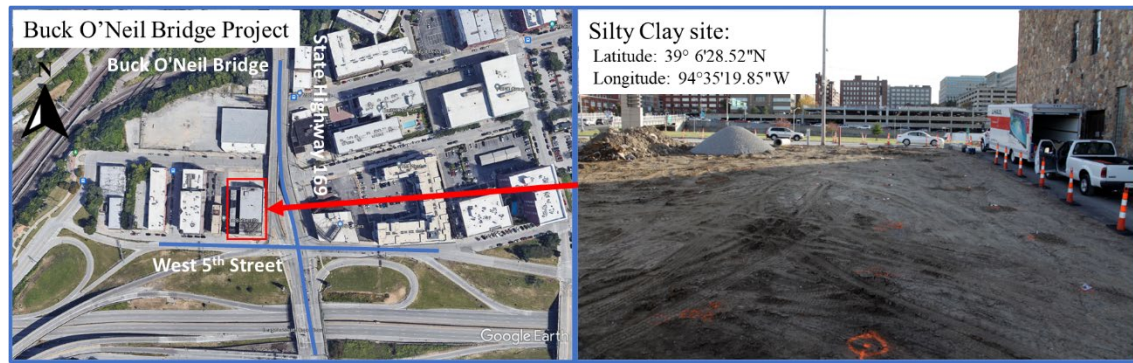
Four construction sites were selected, three of which were from the I-270 North (Figure 4.1a) and one was the Buck O'Neil Bridge projects (Figure 4.1b) provided by MoDOT. Four representative soils at the four construction sites were tested, including lean clay, well graded sand, base aggregate, and silty clay. Besides field views and their geographical coordinates shown in Figure 4.1, information including testing date, soil functions, and soil types are shown in Table 4.1.

The climatic conditions and soil surface temperature during testing for sites are averaged and shown in Table 4.2. As can be seen from Tables 4.1 and 4.2, the average air temperature at each site changed due to change of seasons over time, where the lean clay site tested on September 9th 2021 had the highest air temperature while the silty clay site tested on November 15th 2021 had the lowest one. The soil temperature at sites were generally 44.6 °F (7 °C) to 48.2 °F (9 °C) lower than the air temperature, except for the very close air and soil temperature at the well graded sand site, which may result from the well graded sand having both porous structure and low moisture content was easily heated up by the sunlight. In addition, the base aggregate site had the highest wind speed,

humidity, and humidity ratio, while the silty clay site had the lowest wind speed and humidity ratio, and the lowest humidity occurred at the lean clay site. The station pressures and evaporation rates at four sites were almost the same.



(a) I-270 North project



(b) Buck O'Neil Bridge project

Figure 4.1 Location and field view of four tested sites.

Table 4.1 Filed visit date and construction soils.

Date	Project	Soil type	Classification		Function
			AASHTO	USCS	
Jun./03/2021	I-270 N	Well grade sand	A-1-b	SW	Retaining wall backfill
Sep./09/2021	I-270 N	Lean clay	A-4	CL	Subgrade
Oct./20/2021	I-270 N	Base aggregate	A-1-a	SW	Base course
Nov./15/2021	Buck O'Neil Bridge	Silty clay	A-4	CL	Foundation backfills

Table 4.2 Average of weather conditions and soil temperatures at four sites.

Site	Soil temp. (°F)	Wind speed (mi/h)	Air temp. (°F)	Humidity (%)	Evaporation rate (gr/ft ² /hr)	Humidity ratio (gr/lbm)	Station pressure (psi)
Lean clay	77.68	1.62	90.6	27.78	17.32	59.50	14.48
SW	86.58	1.35	86.6	32.57	14.65	62.79	14.40
Base agg.	67.26	2.09	80.1	48.67	11.99	75.18	14.47
Silty clay	50.22	0.58	67.5	37.81	18.65	38.43	14.27

The lean clay was compacted and used as a subgrade soil near the intersection of the interstate highway 270 and state highway 67 as shown in Figure 4.1a. Thirty test points were selected, which were uniformly distributed in a 78.7 ft (24 m) by 65.6 ft (20 m) area, as shown in Figure 4.2. Row and column spacings were 13.1 ft (4 m), and margins were in 6.6-ft (2-m) width. However, two points at the northwest corner were skipped because they were under field construction and not accessible. In addition, all 28 points were tested with three LWD devices right after compaction, while points 2, 5, 7, 9, 11, 13, 15, 20, 23, 25, and 27 were tested with LWD 3879 two hours after compaction to study how the LWD modulus and moisture content change over time. Soil samples were taken immediately at points where the LWD tests were performed and brought back to the laboratory for moisture content determination using the oven-drying method.

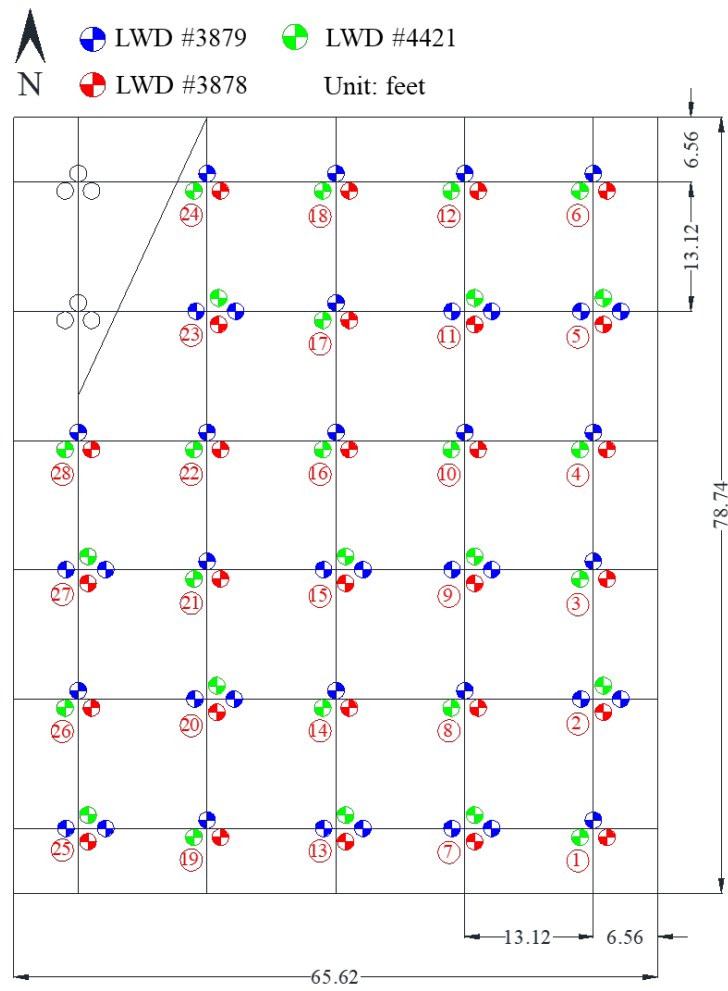


Figure 4.2 Points distribution at the lean clay site.

The well graded sand was used as a backfill material for a MSE wall constructed for the bridge approach near the intersection of the interstate highway 270 and North Florissant Road, as shown in Figure 4.1a. Two continuous test sections were selected, with 10 testing points in section 1 and 30 testing points in section 2. The layout of the two sections and their testing points distribution are shown in Figure 4.3. The distance between any two adjacent points was around 8.2 ft (2.5 m) in section 1, though the row spacing was only 5.5 ft (1.68 m) there. The section 2 had row and column spacing of 8.2 ft (2.5 m) and 6.6 ft (2 m), respectively. In section 1, LWD tests were performed at 10 testing points using all three devices LWD 3879, 3878, and 4421 immediately after the compaction. In addition, LWD tests were performed two hours after the compaction using the LWD 3879 only. In section 2, 30 LWD tests were performed using LWD 3879 only immediately after the compaction. Soil samples were taken immediately at locations where the LWD tests were performed and brought back to the laboratory for moisture content determination using the oven-drying method.

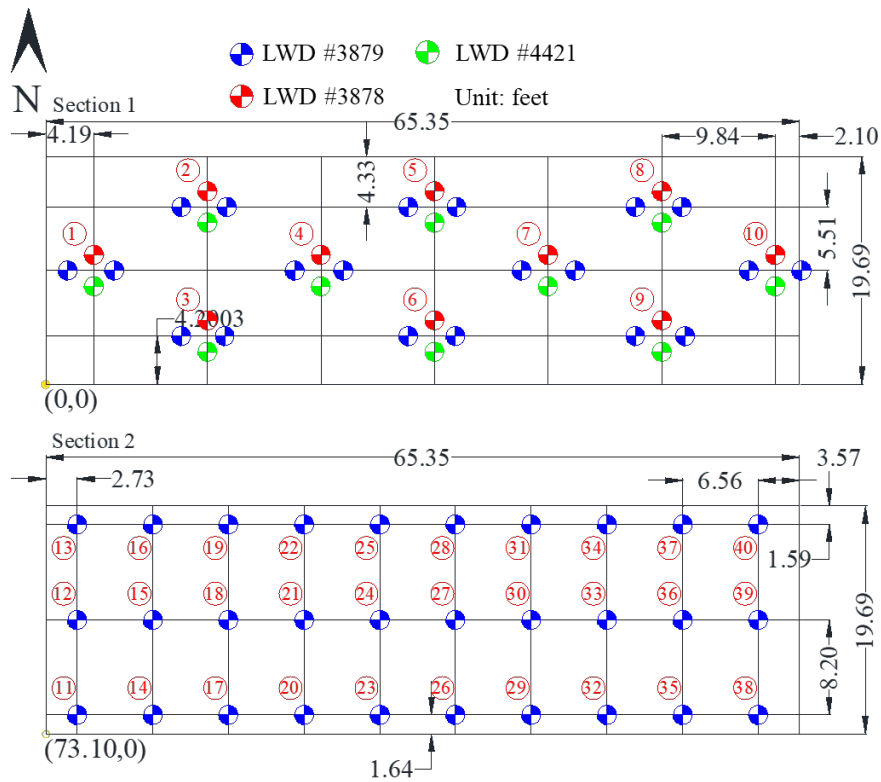


Figure 4.3 Points distribution at the well graded sand site.

The base aggregate was used as a base course material near the intersection of the interstate highway 270 and Halls Ferry Road, as shown in Figure 4.1a. The unbound aggregate base course had a thickness of 4 in (0.1 m) and was built on top of a lean clay subgrade. The research team marked and attempted to test 100 continuous points at the site. However, these points were divided into three adjacent sections due to interruption from the construction process, and a total of 65 testing points were tested with the three LWD devices as shown in Figure 4.4. The section 1 had 21 testing points, among which points 1-10 were tested using all three LWD devices, points 11-12 were tested using two LWD devices (LWD 3878 and 3879), and points 13-20 were tested using the LWD 3879 only due to interruption from construction. The test section 2 included 33 testing points numbered from 43 to 75, which were tested using all three LWD devices. The test section 3 included 12 testing points numbered from 76 to 87, among which points 76 to 83 were tested using all three LWD devices, while points 84 to 87 were tested using LWD 3879 only due to test termination caused by a rainfall event.

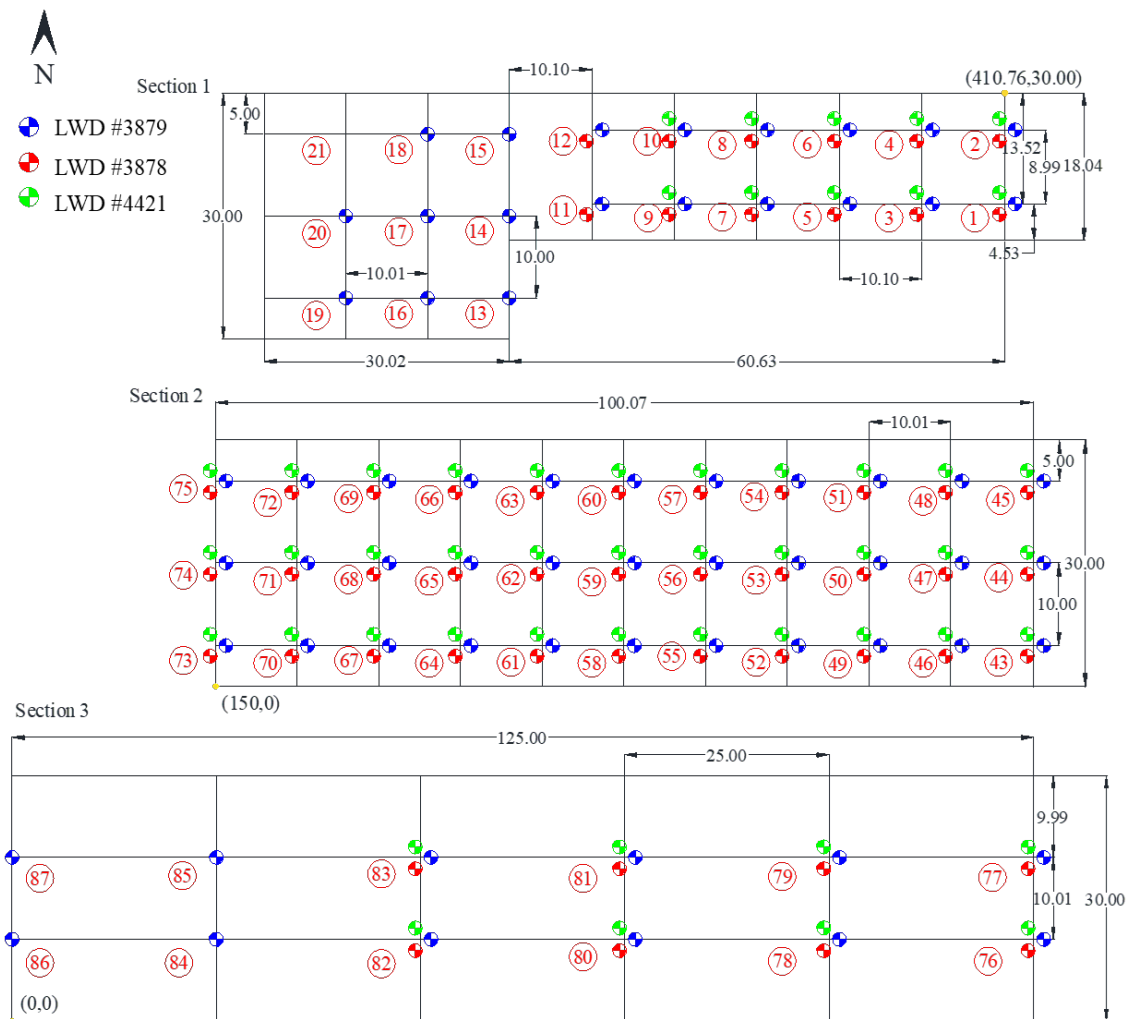


Figure 4.4 Points distribution at the base aggregate site.

The silty clay site of the Buck O'Neil Bridge project in Kansas City had an area of 118.11 ft (36 m) by 98.4 ft (30 m) near the intersection of state highway 169 and West 5th Street, as shown in Figure 4.1b. The silty clay at the site was filled into a basement and compacted as an approach for Buck O'Neil bridge. As shown in Figure 4.5, the site was able to contain 9 rows by 11 columns, a total of 99, testing points with 9.8-ft (3-m) spacing both horizontally and vertically. However, 71 out of 91 were tested with all three LWD devices because of the three shaded areas shown in Figure 4.5, where the shaded region at the south end of the site was under construction and the rest two shaded regions were two piles of waste soil from construction.

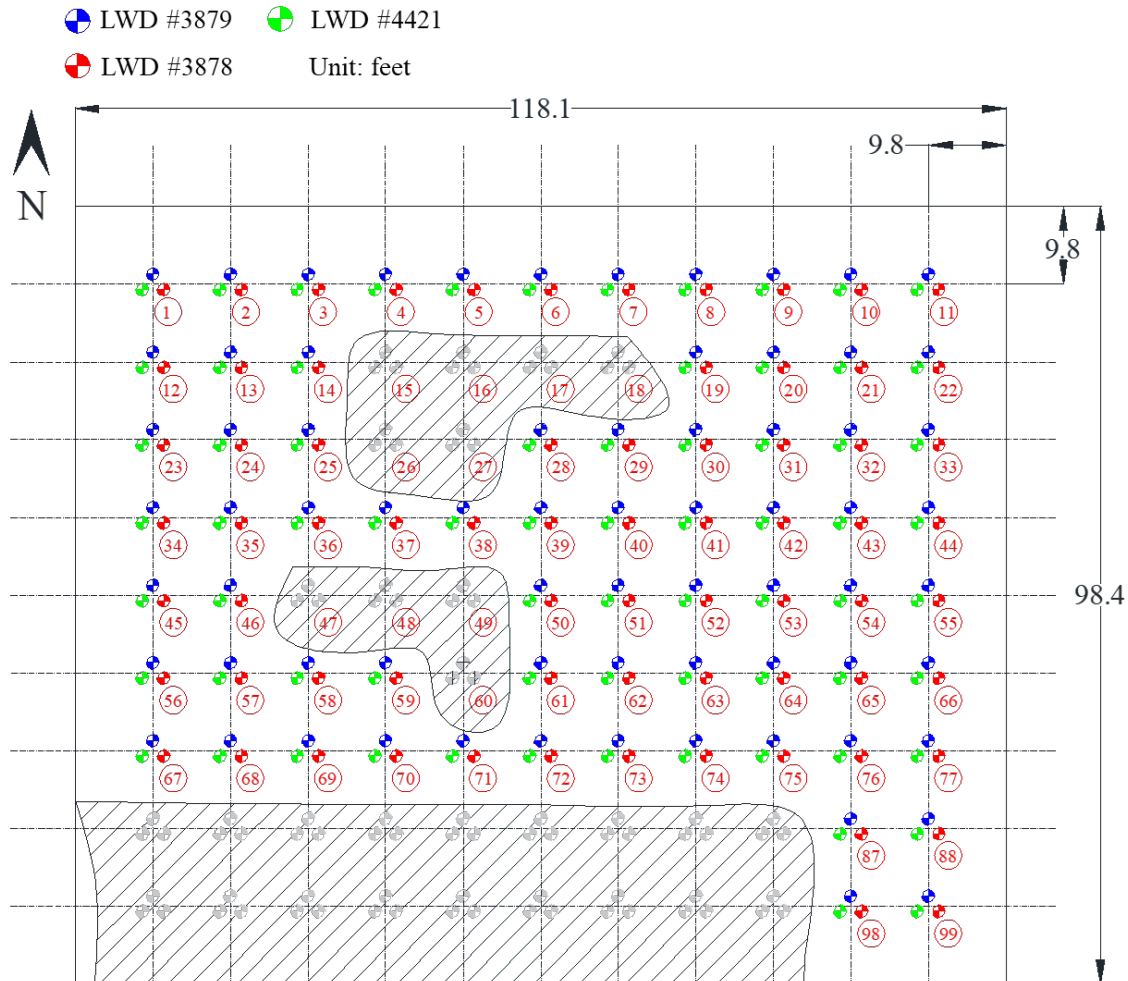


Figure 4.5 Points distribution at the silty clay site.


4.2.2 Testing Procedure

In order to collect as much data as possible from as many points as we can, multiple tasks were planned to be conducted in the field, in which the following equipment was used for either testing or assisting on testing at sites:

- Three Zorn ZFG 2000 LWD devices (numbered as 3878, 3879, 4421)
- NDG (available from the MoDOT team only at the WG and the silty clay sites)
- Kestrel 5000 Professional Construction Weather Tracker
- Fluke Infrared Thermometer
- Ohaus MB120 and generator
- Aggrameter

Table 4.3 lists the three LWD devices and their properties used in this project, which are the LWD 3878, 3879, and 4421. The LWD 3878 and 3879 have the same drop height (28.3 in, 720 mm) and loading plate diameter (11.8 in, 300 mm), while the LWD 4421 device has a drop height of 22.0 in (560 mm) and loading plate diameter of 7.9 in (200 mm). All the hammers have the same weight of 22.0 lbm (10 kg). Consequently, the LWD 3878 and 3879 have the same loading force of 1589.4 lbf (7.07 kN) and a resultant stress of 14.5 psi (100 kPa), while for the LWD 4421, the loading force and resultant stress are 1236.4 lbf (5.5 kN) and 25.4 lbf (175 kPa), respectively.

Table 4.3 Properties of LWD devices used in the field.

				
LWD	#	3878	3879	4421
Drop height	in	28.3	28.3	22.0
Plate diameter	in	11.8	11.8	7.9
Hammer weight	lbm	22.0	22.0	22.0
Loading force	lbf	1589.4	1589.4	1236.4
Resultant stress	psi	14.5	14.5	25.4

The weather tracker was set up as soon as the research team arrived at the sites. The collected weather data, including wind speed, air temperature, humidity, evaporation rate, humidity ratio, and station pressure, are shown in Appendix A. A generator was used to provide electric power for the Ohaus MB120 moisture analyzer in the field.

Testing points were selected according to site situation and shown in Figures 4.2 through 4.5. The points were first marked with color spray to facilitate the testing process. It is worth noting that there were significant variances in site surface flatness due to use of different compaction methods. For example, granular materials such as the well graded sand and base aggregate were compacted using vibratory rollers and had a relatively flat surface, while the lean clay and silty clay had very poor flatness after being compacted by sheep foot rollers. Therefore, extra efforts were needed to level testing surfaces to prepare the LWD tests for these sites.

LWD tests were subsequently conducted according to AASHTO TP 456-01 (Schwartz et al., 2017). The testing procedures are as follows. Firstly, the loading plate was positioned onto the interested area and rotated counterclockwise and clockwise for approximately 45 degrees to ensure that the testing plate and the soils beneath had good contact. Six drops were then performed according to the Zorn LWD operating manual, where the first three drops were used for conditioning purposes and the rest three drops were used for measuring purpose. After that, the device model, point numbering, deflection, and moduli were recorded using both the LWD devices and manual documentation on datasheets. In addition, default drop heights were used for the three LWD devices, which are shown in Table 4.3.

Field moisture content measurements were planned to conduct immediately after each individual LWD test using either the Aggrameter or Ohaus MB120 to reduce errors due to potential water evaporation. However, due to poor practicability of the two moisture content measurement devices, field samples were taken from the soil directly underneath the LWD loading plate, sealed into plastic bags, and brought back to the laboratory for moisture content determinations using the Ohaus MB120 and oven-drying method.

4.2.3 Determination of Field LWD Modulus

Calculating field LWD modulus is based on the concept of half-space Boussinesq equation with the assumption that the tested soil is an isotopically homogeneous and linear elastic semi-finite continuum, as shown in Equation (12) (Schwartz et al., 2017).

$$E_{field} = \frac{2k(1 - \nu^2)}{Ad} \quad (12)$$

where

E_{field} = field modulus (MPa),

k = soil stiffness, $k = F/\delta$,

F = maximum load (kN) applied by LWD device in the field,

δ = maximum deflection (mm) measured by LWD device in the field,

A = stress distribution factor obtained from Table 4.4,

ν = Poisson's ratio obtained from Table 3.11, and
 d = plate radius (m) of LWD device.

However, parameters A and Poisson's ratio were set as fixed values of $A = \pi$ and $\nu = 0.5$ in the three LWD devices, which need to be changed based on soil types following Tables 3.11 and 4.4 respectively. Thus, the actual E_{field} were determined by Equation (13) with input of target parameters and origin field LWD modulus. Values of A_2 in Equation (13) for the lean clay, well graded sand, base aggregate, and silty clay were selected as 4, $3\pi/4$, $3\pi/4$, 4, respectively. Values of A_2 in Equation (13) for the lean clay, well graded sand, base aggregate, and silty clay were selected as 0.4, 0.15, 0.35, and 0.4, where Poisson's ratio values for the two clay soils were different from those used in the data analysis for LWD tests on mold because the two clay soils in the field had much higher moisture contents than those tested in the lab.

$$E_2 = \frac{E_1 A_1 (1 - \nu_2^2)}{A_2 (1 - \nu_1^2)} \quad (13)$$

where

A_1 and A_2 are default and target stress distribution factors, respectively,

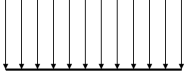
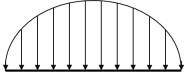
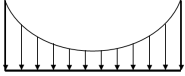
ν_1 and ν_2 are default and target Poisson's ratio, respectively,

E_2 is field LWD modulus (MPa) corrected with target parameters (A_2 and ν_2),

and

E_1 is field LWD modulus (MPa) calculated with default parameters ($A_1 = \pi$ and $\nu_1 = 0.5$).

Table 4.4 Stress distribution factors for different types of soils.

Soil type	Factor (A)	Stress distribution
Mixed soil (uniform)	π	
Granular material (parabolic)	$\frac{3\pi}{4}$	
Cohesive (inverse-parabolic)	4	

4.3 Evaluation of the Moisture Detection Devices in the Field

Two moisture determination devices, the Ohaus MB120 and Aggrameter, were intended to be used for rapidly measuring soil moisture content in the field. In addition, MoDOT project engineers helped perform NDG tests at the lean clay site of the I-270 North project and the silty clay of the Buck O'Neil Bridge project. The research team obtained the results to compare with those field moisture content measurements.

As discussed previously, the Ohaus MB120 is a mini in-field oven equipped with a built-in weight scale having 1851.9-gr (120-g) capacity and 0.0154324-gr (1-mg) readability. The analyzer requires strict working conditions such as leveled ground with no vibration,

disturbance, or magnetic field. However, these conditions are difficult to meet in the field because of wind, disturbance from rollers and other construction machines at the site, etc. Therefore, soil samples were dug out at each test point immediately after LWD testing and sealed in plastic bags, then returned to the lab for more accurate measurements.

Another field moisture content detecting device, the Aggrameter, does not have strict environmental requirements but has limited compatibility with some soil types. Specifically, the Aggrameter only works well with well graded sand, while getting constant readings from the base aggregate and clay soils regardless of moisture changes.

Figure 4.6 shows the comparison in moisture content results obtained by the oven-drying method and the Ohaus MB120 for the lean clay from the I-270 North project. The moisture content measurements from the oven-drying method can be viewed as the ground truth results, consequently, the line of equality as shown in Figure 4.6 represents 100% match of the ground truth. As shown in Figure 4.6, the Ohaus analyzer showed a consistent underestimation of moisture content for the lean clay within the measured moisture content range from 16% to 25%. The moisture content results obtained from the Ohaus (x in Figure 4.6) can be correlated to the results from the oven-drying method (y in Figure 4.6) using a straight line of $y=1.2635x$ with an R^2 of 0.9984. This indicates that the moisture content results obtained from the Ohaus MB120 had very high precision, but with low accuracy. By applying the correction coefficient of 1.2635, the Ohaus can provide moisture content measurements with both high precision and accuracy. Compared with the gain value of 1.20 obtained from the LWD test on Proctor mold, the gain of 1.2635 obtained from the field samples was slightly higher.

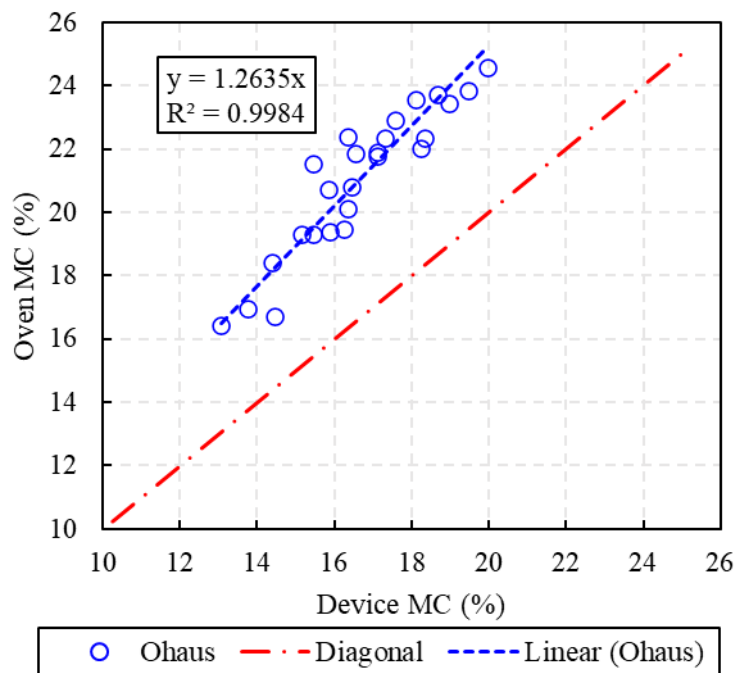


Figure 4.6 Moisture content measurement comparison between the Ohaus MB120 and oven for the lean clay.

Figure 4.7 shows the comparison in moisture content results obtained by the oven-drying method, the Aggrameter, the Ohaus device, and the NDG for the well graded sand from the I-270 North project. As shown in Figure 4.7, compared with the oven-drying method, the Ohaus device produced highly accurate and precise results for the well graded sand with a regression equation of $y=0.9936x$ and an R^2 of 0.9961, and the gain value 0.9936 was little lower than 1.1468 obtained from the lab compacted samples. The Aggrameter produced highly precise moisture content measurements but with relatively low accuracy. It was reflected by a high R^2 of 0.9909 and a straight line of $y=1.1848x$. The NDG results had lower accuracy and precision indicated by a regression equation of $y=0.8263x+0.7186$ and an R^2 of 0.8349.

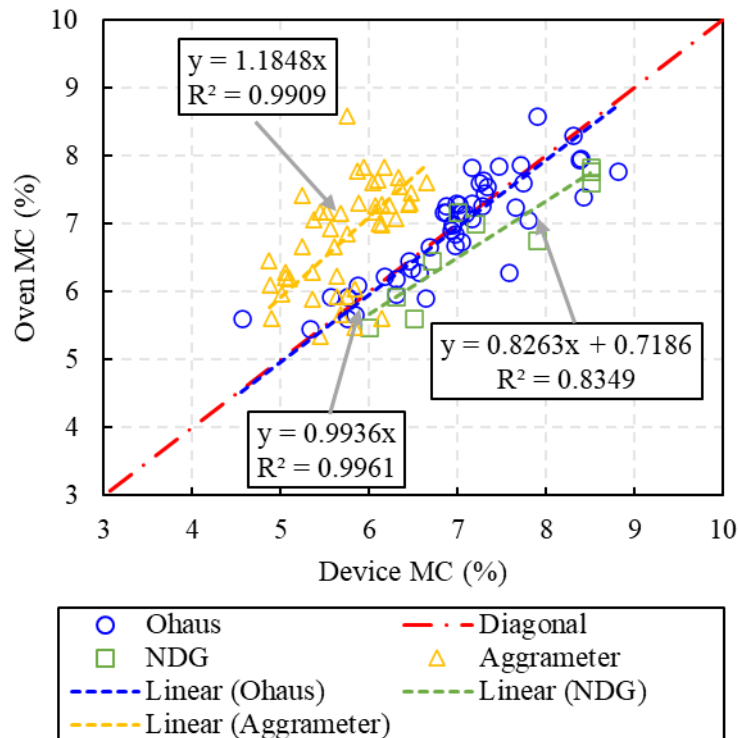


Figure 4.7 Moisture content measurement comparison between the Ohaus MB120, Aggrameter, NDG, and oven for the well graded sand.

Figure 4.8 shows the comparison in moisture content results obtained by the oven-drying method and the Ohaus MB120 for the base aggregate from the I-270 North project. The results were similar to those in Figure 4.7. Compared with the oven-drying method, the Ohaus device produced highly accurate and precise results for the base aggregate with a regression equation of $y=1.039x$ and an R^2 of 0.9956, which was quite similar to the gain value of 1.1737 obtained from lab compacted samples.

Figure 4.9 shows the comparison in moisture content results obtained by the oven-drying method, the Ohaus MB120, and the NDG for the silty clay from the Buck O'Neil Bridge project. The results from the Ohaus MB120 were similar to those as shown in Figure 4.6 for the lean clay. The Ohaus MB120 shows a consistent underestimation of moisture content for the silty clay with high precision. Its correlation with the oven-drying method (y in Figure 4.6) was approximated using a straight line of $y=1.2329x$ with an R^2 of

0.9989, which is close to the gain value of 1.2603 obtained from lab compacted samples. The results from the NDG were similar to those shown in Figure 4.7 for the well graded sand with low accuracy and precision. One difference is that the NDG overpredicts the moisture content for the well graded sand while underpredicts for the silty clay.

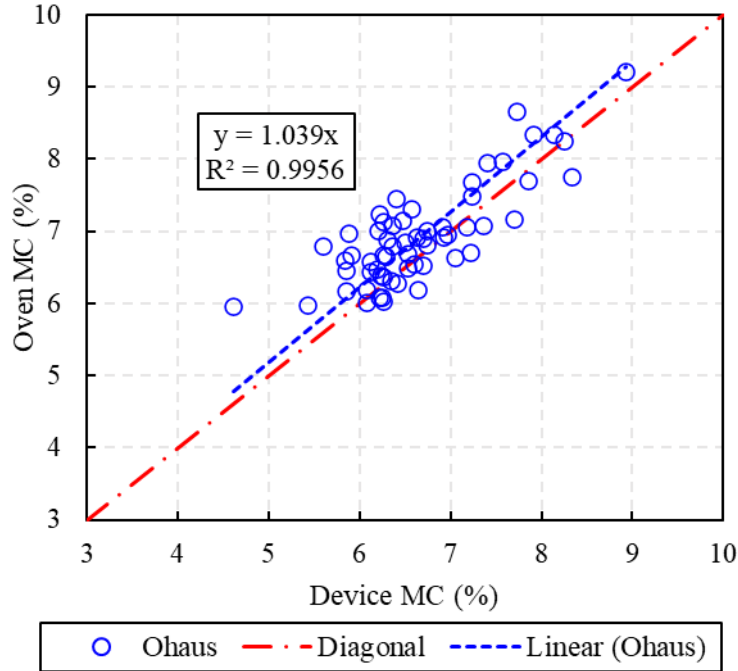


Figure 4.8 Moisture content measurement comparison between the Ohaus MB120 and oven for the base aggregate.

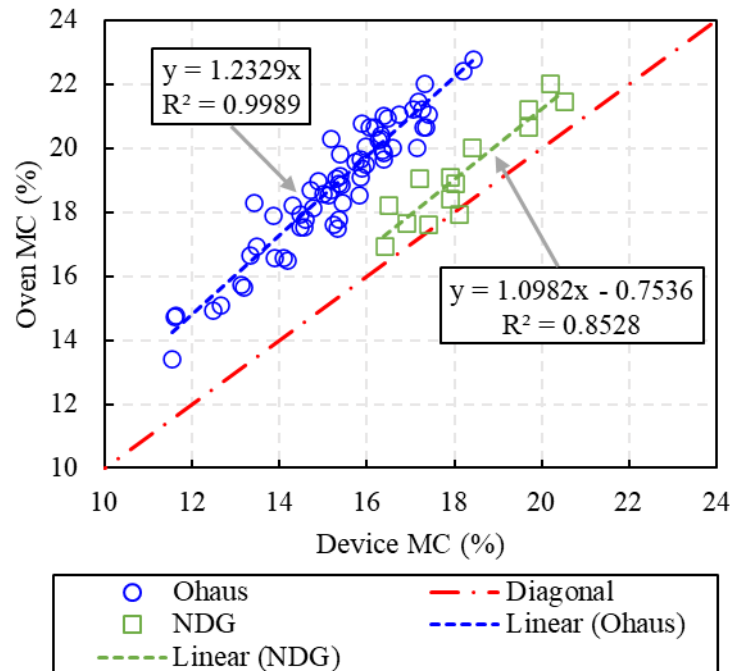


Figure 4.9 Moisture content measurement comparison between the Ohaus MB120, NDG, and oven for the silty clay.

4.4 Evaluation of LWD Devices in the Field

To investigate the correlation and consistency of the three different LWD device models, the LWD 3878, 3879, and 4421 were taken to the field and tested at as many points as possible. Testing points at sites were close but not overlapping with spacing around 6.6 ft to 13.1 ft (2 m to 4 m) to minimize the devices' impact on surrounding testing points, which were also kept 4.9 ft to 9.8 ft (1.5 m to 3 m) away from the edge of the site to avoid any boundary effects. The three LWD devices had the same falling height but different applied stresses due to the LWD 4421 had a loading plate 3.9 in (100 mm) smaller than other two devices in diameter.

To make sure that the testing conditions are all the same and the results are consistent for all tests, six students worked together to make measurements sequentially at the same time. The research team, consisting of six students, were divided into three groups with two people per group, each group was in charge of one LWD device and associated moisture content measurements. In this way, LWD tests and moisture content measurements (or sample collection) were conducted at the same time or at least within short intervals.

The correlations between the three LWD devices were determined based on corrected modulus as discussed in section 4.2.3. Graphs for three LWD devices at four construction sites are shown in Figures 4.10 through 4.13, and their R^2 are summarized in Table 4.5. R^2 values in the second column of Table 4.5 indicate that fair correlation existed between the LWD 3878 and 3879, even though the LWD 3878 and LWD 3879 are the same models of LWD ZFG 2000. High R^2 values between the LWD 3879 and 4421 (3rd column of Table 4.5) indicate there were good correlations between them for most soils. While that a good correlation between the LWD 3878 and 4421 existed only at the well graded sand site, which is indicated by an R^2 of 0.83. Moreover, Figures 4.10 through 4.13 show the points are scattered along the line of equality, indicating the fair correlations between the devices. In addition, as can be seen in Figures 4.10 through 4.13, points distributed around the line of equality scatter more when the measured moduli increase. It indicates that the three LWD devices had good correlation at points having relatively low LWD moduli, while their variation increased with increasing of LWD moduli they measured.

Table 4.5 R^2 for correlations between the three LWD devices

Field	3878 vs. 3879	3879 vs. 4421	3878 vs. 4421
Lean clay	0.44	0.83	0.46
Well grade sand	0.51	0.83	0.83
Base aggregate	0.58	0.78	0.52
Silty clay	0.50	0.64	0.58

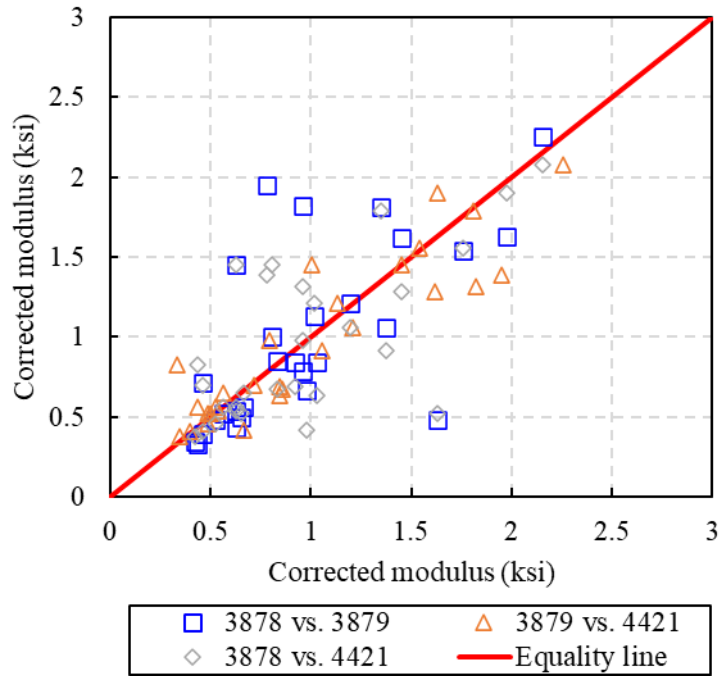


Figure 4.10 Correlations of LWD devices at the lean clay site.

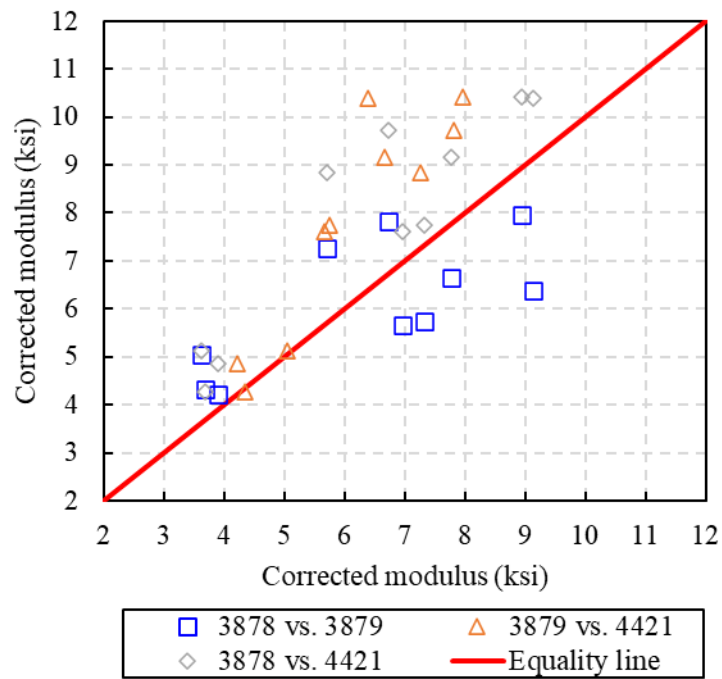


Figure 4.11 Correlations of LWD devices at the well graded sand site.

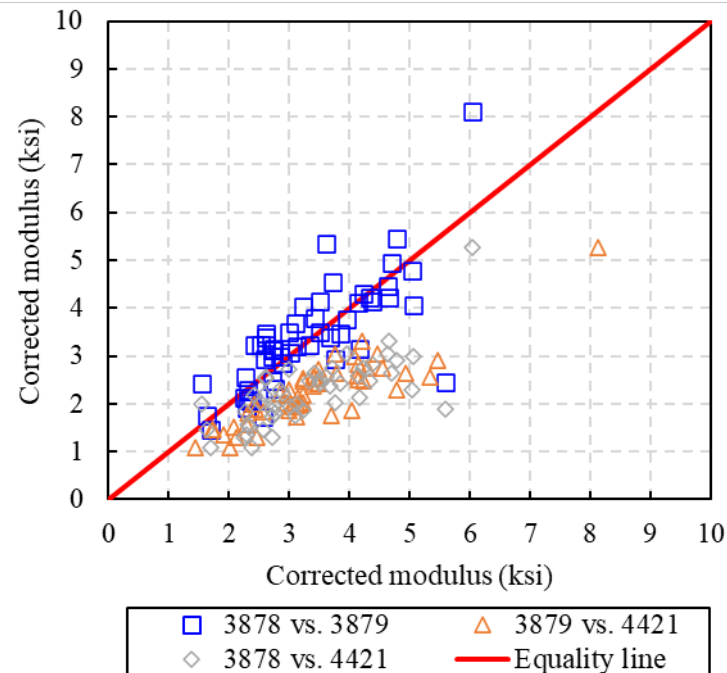


Figure 4.12 Correlations of LWD devices at the base aggregate site.

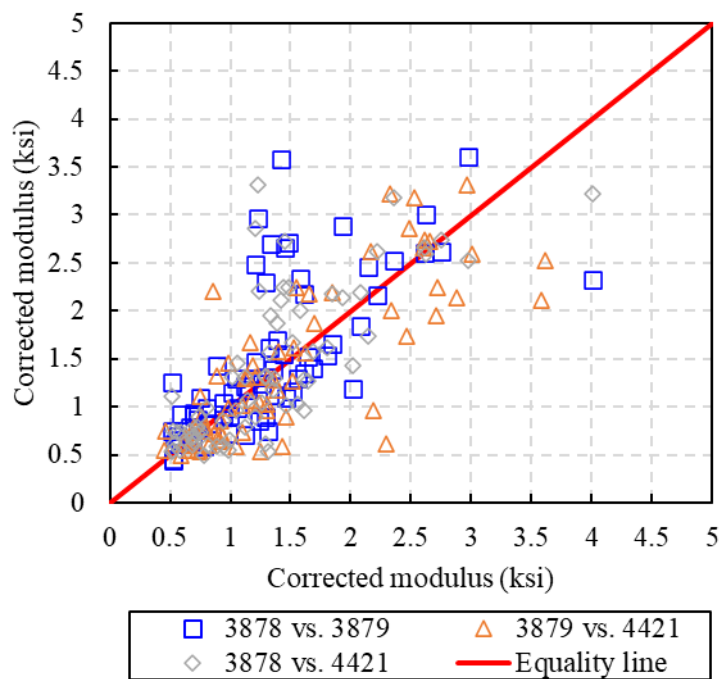


Figure 4.13 Correlations of LWD devices at the silty clay site.

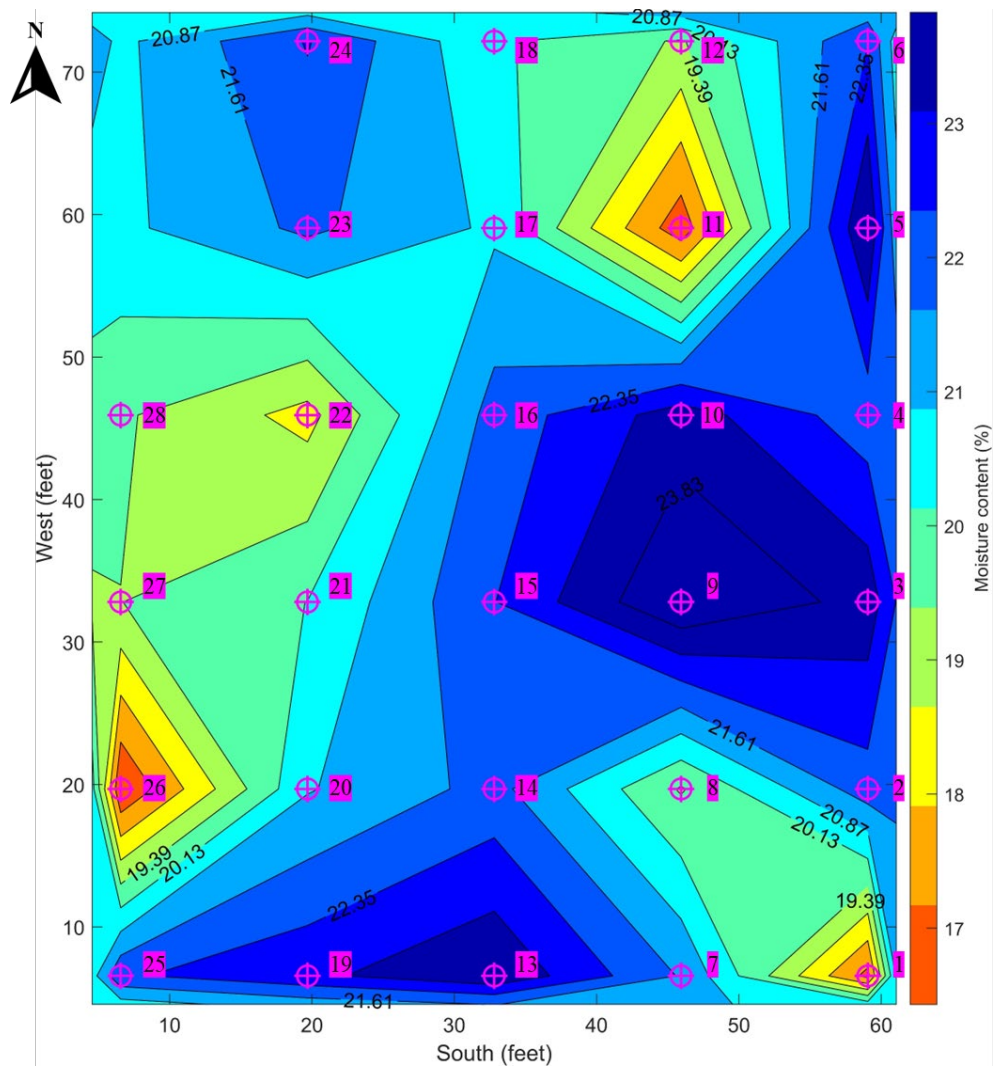
4.5 Evaluation of Moisture Content-Modulus Correlation in the Field

4.5.1 Relationship Between Moisture Content and LWD Modulus Right After Compaction

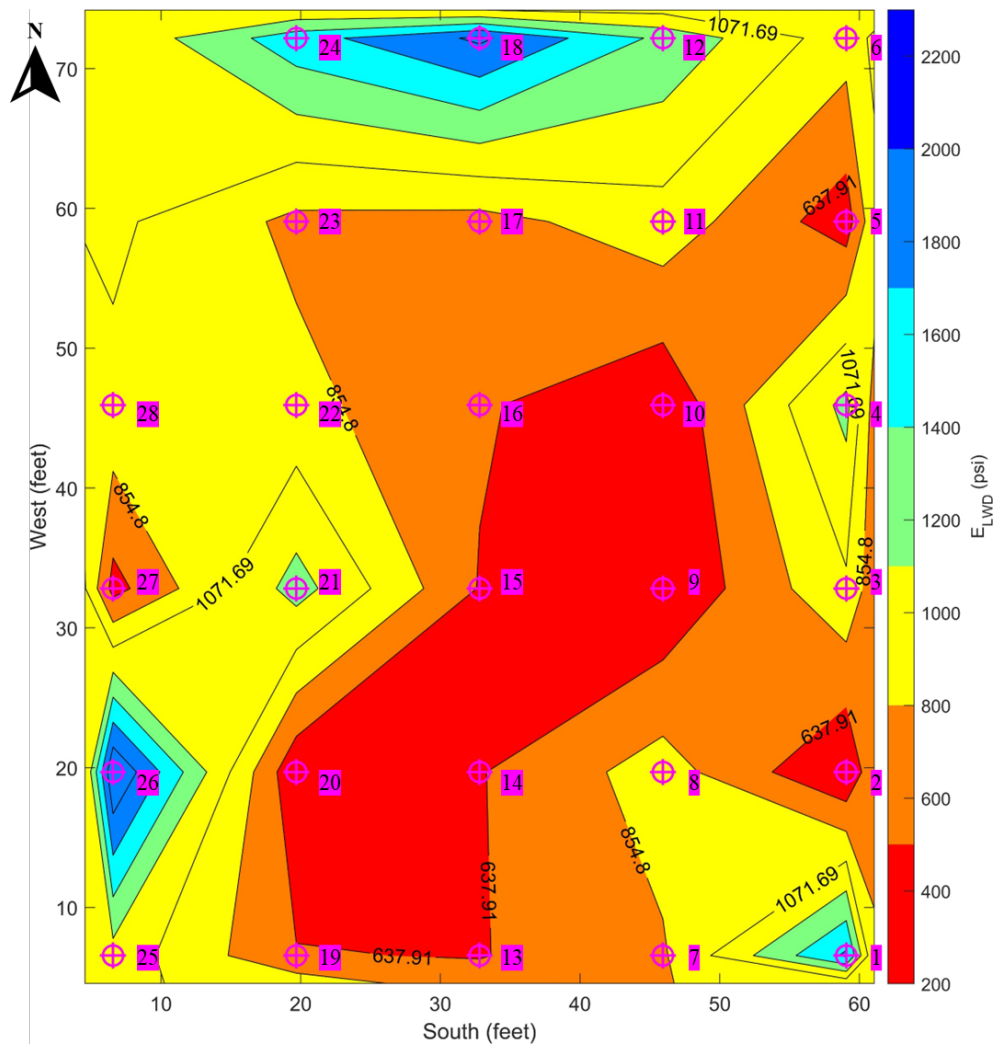
To analyze the relationship between the moisture content and LWD modulus in the field, the contours of moisture contents and field LWD moduli obtained from the three LWD devices were plotted, in which spatial distribution of testing points, moisture contents, and field LWD moduli from different sites were shown. The contours were plotted by linearly interpolating the moisture contents or LWD moduli between the testing points. The purpose of the contour plots was not to focus on the moisture content and LWD moduli at any individual testing point, but to get an overall picture of the moisture content and LWD moduli distributions and their correlations. For the following discussions about field results please refer to Figures 4.2 through 4.5 to reference point locations.

Figure 4.14a shows the moisture content contour for the lean clay at the I-270 North project site. As can be seen from Figure 4.14a, the moisture contents at all testing points were higher than 14.2%, which is the OMC of the soil. The moisture contents were extremely high along a diagonal band from southwest to northeast, which included points 3, 5, 9, 10, 15, 13, and 19 with moisture contents higher than 20%. There were three small areas that had fewer high moisture contents near points 1, 11, 22, and 26, whose moisture contents were around 17%.

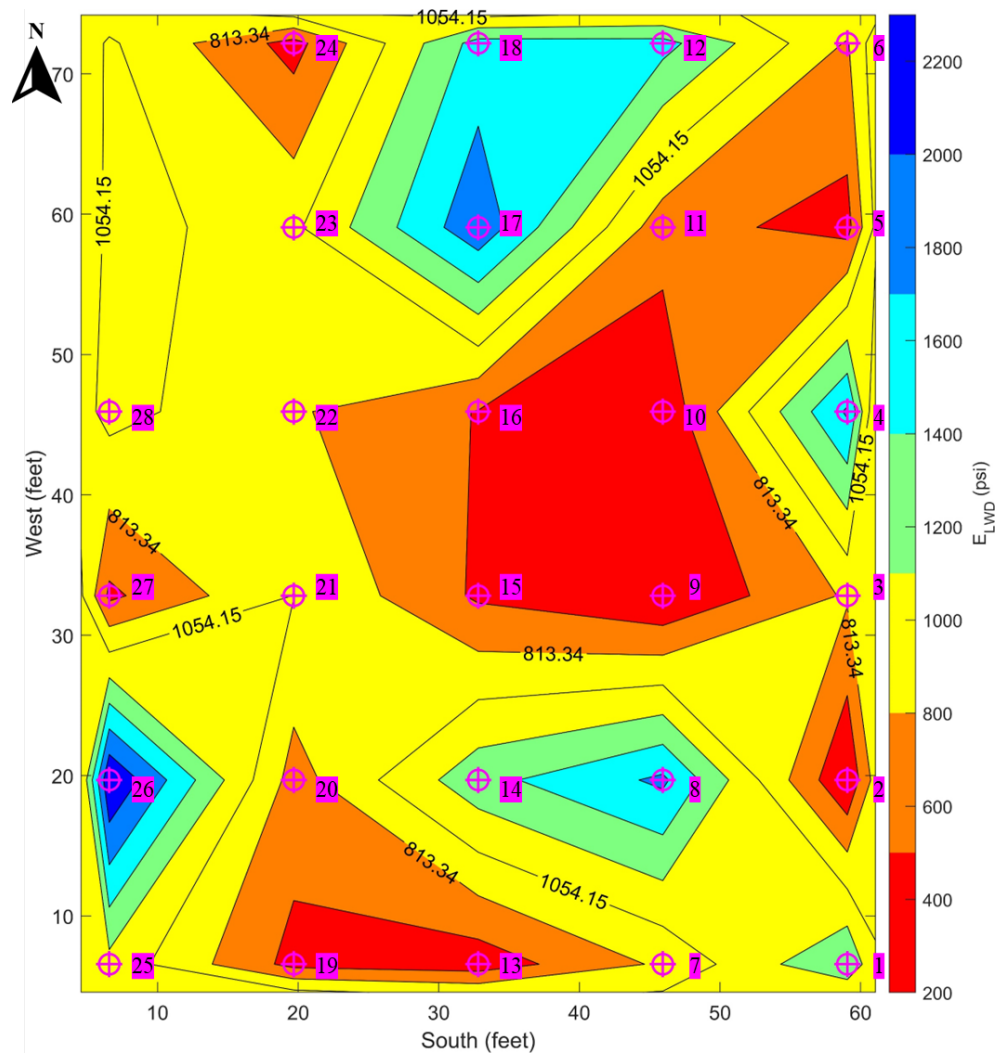
Figures 4.14b through 4.14d show the LWD modulus contours for the same site measured by LWD 3878, 3879, and 4421, respectively. It was found that there was a decent correlation between moisture contents and moduli obtained from the three LWD devices. For example, corresponding to the diagonal band from southwest to northeast having higher moisture contents in moisture content contour, LWD modulus contours also showed an almost the same diagonal band from southwest to northeast having lower LWD moduli. Specifically, at points 3, 5, 9, 10, and 13, where the moisture contents were high, the LWD moduli measured by the three devices were in the low range of 0.29-0.58 ksi (2-4 MPa). While at points 1, 12, and 26 where the moisture contents were less high, the moduli measured by the three LWD devices were in a high range of 1.31-1.74 ksi (9-12 MPa). By comparing Figure 4.14a with Figures 4.14b through 4.14d, it can be found that the LWD modulus generally decreases with the increase of soil moisture content. Although LWD moduli measured from different devices were different, they were closely related to the moisture contents and the measurements at the same locations have very similar trends in the modulus contours. This seems to indicate that the measurements from the three LWD devices are consistent and reliable for the lean clay.



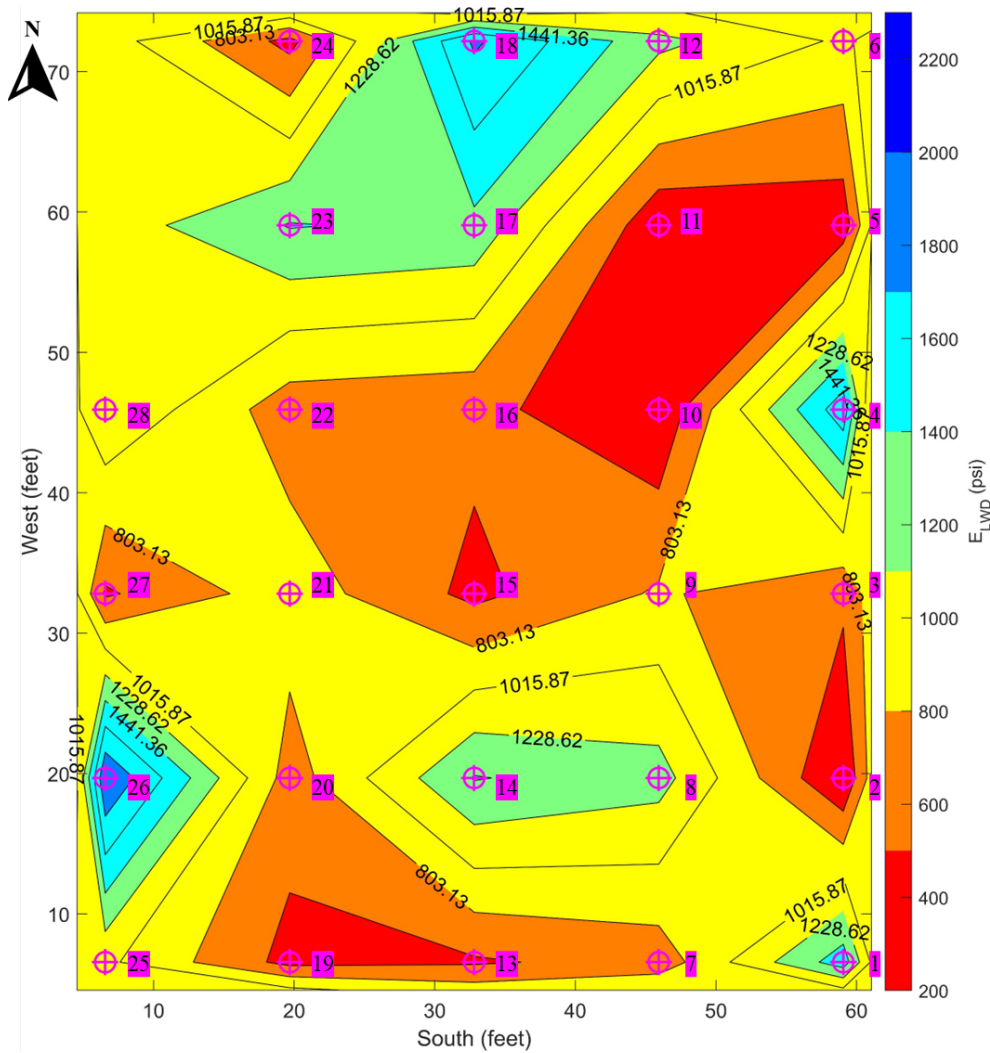
(a) Moisture content contour



(b) Modulus contour of LWD 3878



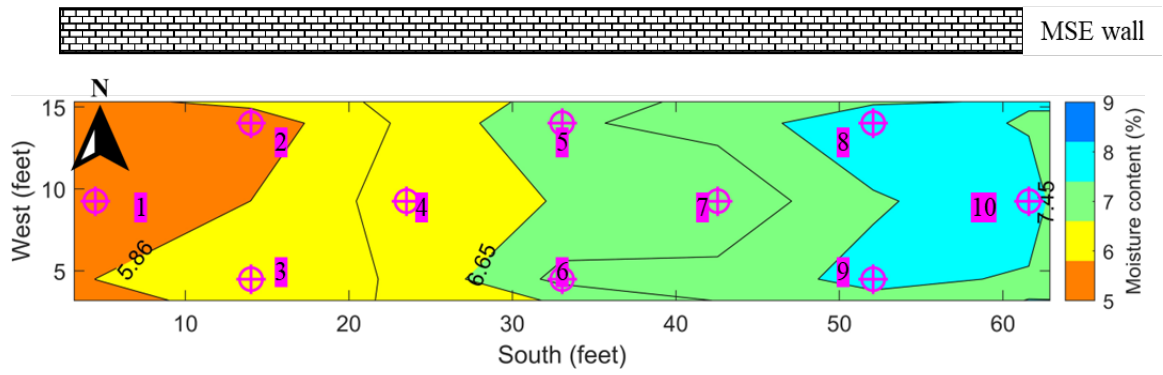
(c) Modulus contour of LWD 3879



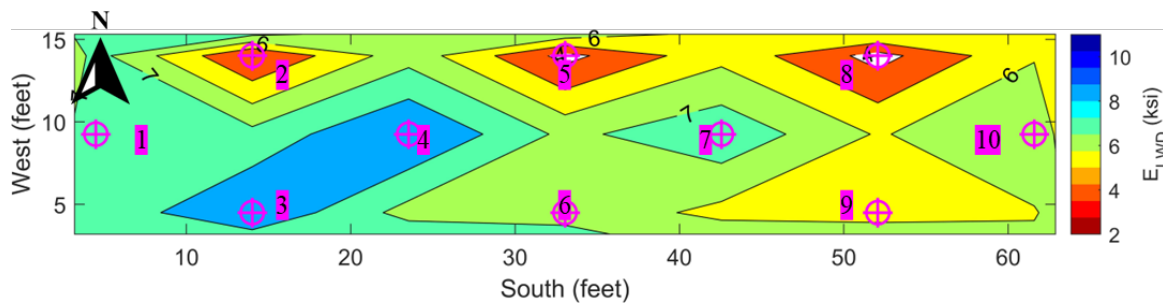
(d) Modulus contour of LWD 4421

Figure 4.14 Moisture contents and LWD moduli spatial distribution at the lean clay site.

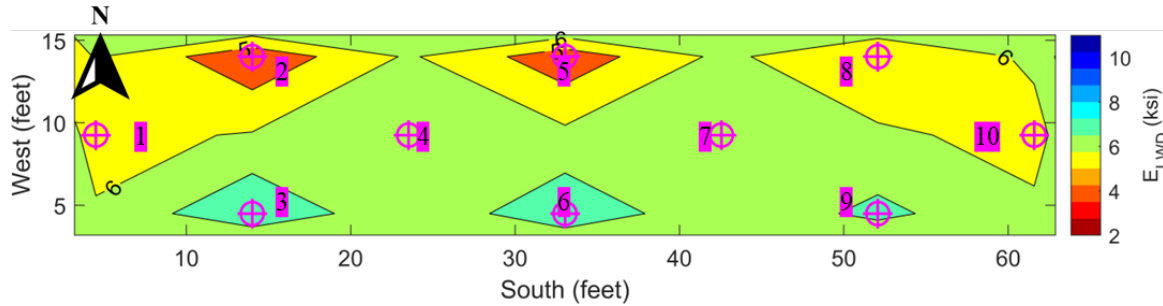
Figure 4.15 shows the contours for moisture contents and the LWD soil moduli measured using the three LWD devices at the section 1 of the well graded sand site from the I-270 North project. The well graded sand site was a retaining wall section as shown in Figure 4.1a. The OMC for the WG site was 9%. As shown in Figure 4.15a, the moisture contents at all points were lower than the OMC with a range from 5.5% to 8%. Figure 4.15a also indicates that the soils at the west end were around 5.8%, and gradually became wetter toward the east end (around 8%). The LWD moduli contours were generally consistent with the moisture content distribution, with lower moduli at the east end, while higher moduli at the west end. However, the trend was not obvious. Another finding was that the moduli along the MSE wall (east side of the test section) were consistently lower than that along the north side. Specifically, points 2, 5, and 8 in the first WG testing section show constant low LWD moduli even though the moisture contents decreased generally from points 8 to 2. This was attributed to a lower degree of compaction along the MSE wall where the soils were not compacted as dense as those inside.



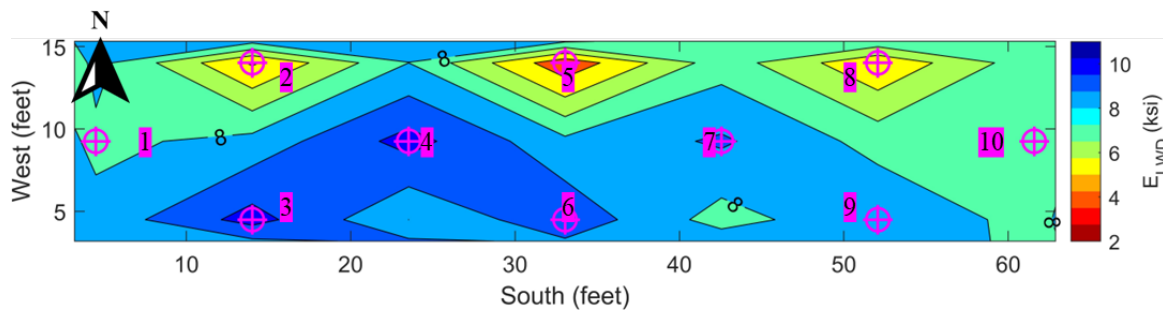
(a) Moisture content contour



(b) Modulus contour of LWD 3878



(c) Modulus contour of LWD 3879



(d) Modulus contour of LWD 4421

Figure 4.15 Moisture contents and LWD moduli spatial distribution of the well graded sand in section 1.

Figure 4.16 shows the contours for moisture contents and the LWD soil moduli measured using the LWD 3879 at the section 2 of the well graded sand site from the I-270 North project. As can be seen in Figure 4.16a, the section 2 had moisture contents ranged from 6% to 8%, and that most of region in the figure is in green indicates most moisture contents in the section 2 were around 7%. The explanation that poor compaction resulted into low LWD modulus can also be verified by results from the section 2 (as shown in Figure 4.16). 10 points including 13, 16, 19, 22, 25, 28, 31, 34, 37, and 40 that were along the MSE wall, showed consistently lower LWD moduli and poorer correlation with corresponding moisture contents shown in Figure 4.16a. Field observations also indicated that the soil near the MSE wall facing was less compacted during construction. In a summary, moisture content is an important influencing factor on the LWD moduli, but it is not the only influencing factor. Other factors such as degree of compaction also influence the LWD moduli. Consequently, the LWD modulus contours from the three devices shared a similar pattern with the moisture content contour, but they are not exactly the same.

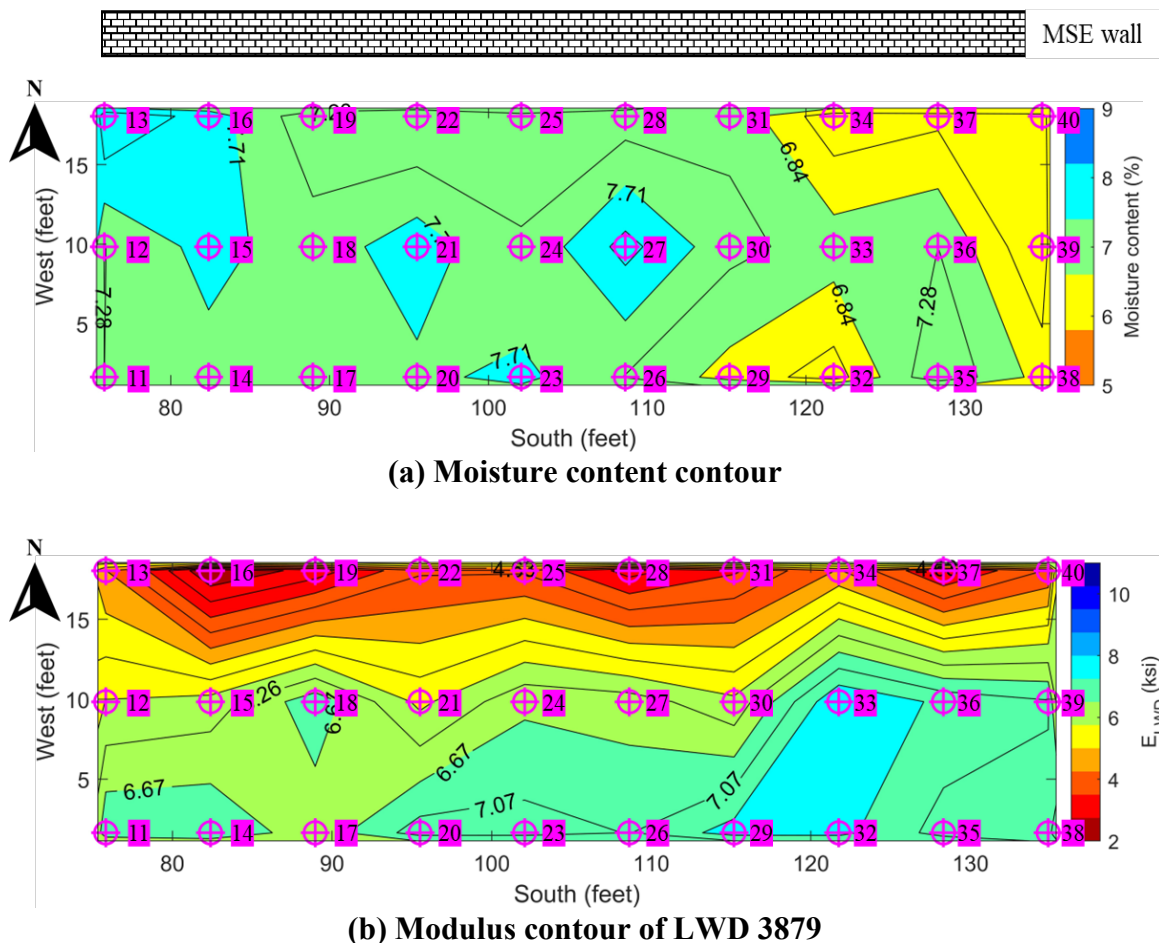
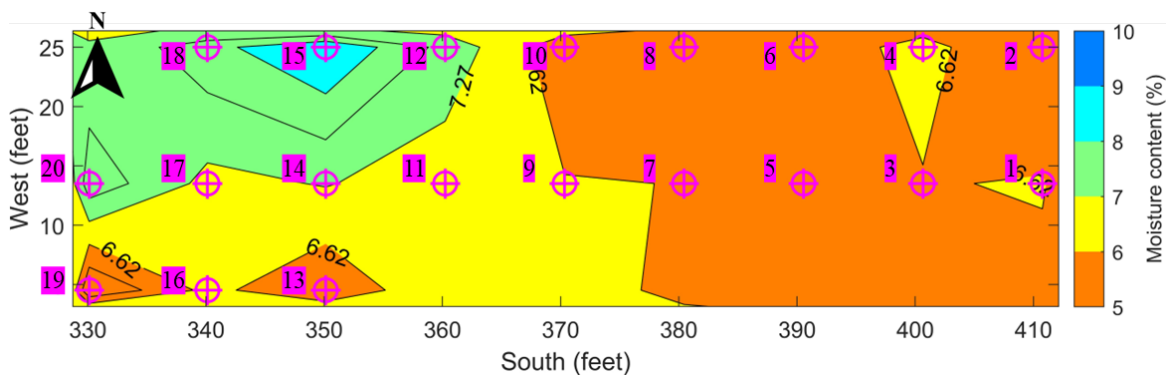


Figure 4.16 Moisture contents and LWD moduli spatial distribution of the well graded sand in section 2.

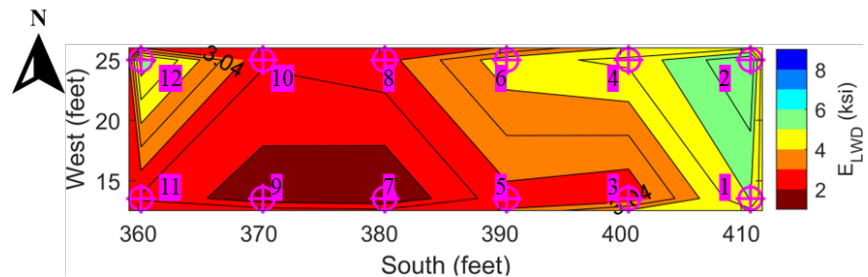
As discussed in Figure 4.4, there were three test sections at the base aggregate site. Figure 4.17 shows the test results for the test section 1 of the base aggregate site. As mentioned previously, although moisture content and LWD modulus tests were performed using the LWD 3879 for the whole area of the test section 1, due to the interruption from the construction process, LWD tests were not performed at part of west end using the LWD 3878 and 4421.

Figure 4.17a shows the moisture content contours for the test section 1. The OMC for the base aggregate was 7.5% and the acceptable moisture content range was 4.5% to 7.5%. As shown in Figure 4.17a, most points at this test section had moisture content ranging from 5.5%-8.5%. The east half of the test section in orange had moisture contents around 5.5%, while the west half had higher moisture contents at the north side, mostly ranging from 6.8% to 7.5%. At points 12, 15, 18, and 20, the moisture contents were higher than the acceptable upbound of 7.5%. In a summary, the moisture contents at this test section were generally well controlled within the acceptable range.

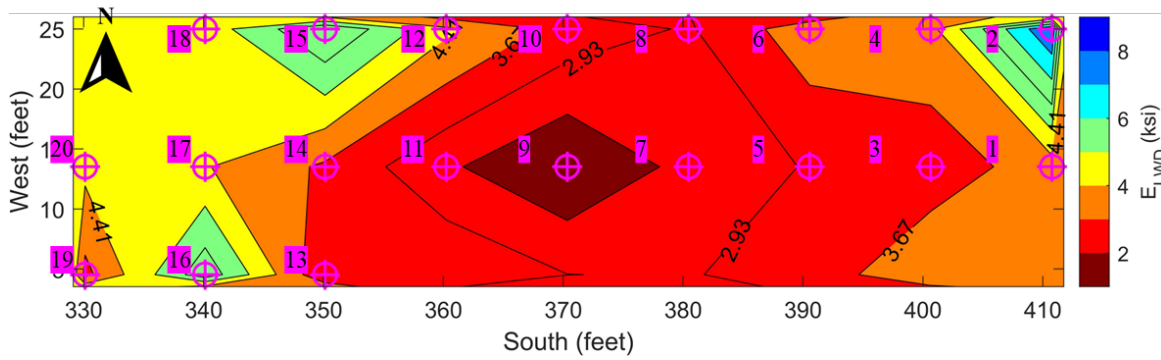
Figures 4.17b to 4.17d show the LWD modulus contours in the test section 1 measured by the LWD 3878, 3879, and 4421, respectively. As can be seen in these figures, the highest LWD modulus occurred at the northeast corner of test section, while lowest LWD modulus appeared at point 9 that located near the center of test section. However, the trend that the LWD modulus increased with decreasing of moisture content did not show much in this section. As shown in Figures 4.17b to 4.17d, the LWD moduli generally increased from the center part towards west and east ends separately, even though the moisture contents kept almost the same along the east direction and increased along the west direction. On the other hand, Figures 4.17b to 4.17d shared the similar distribution pattern of LWD moduli, which indicates some factors other than the moisture content had more impact on LWD modulus.



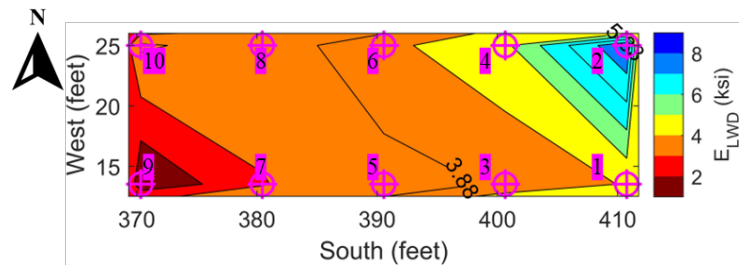
(a) Moisture content contour



(b) Modulus contour of LWD 3878



(c) Modulus contour of LWD 3879

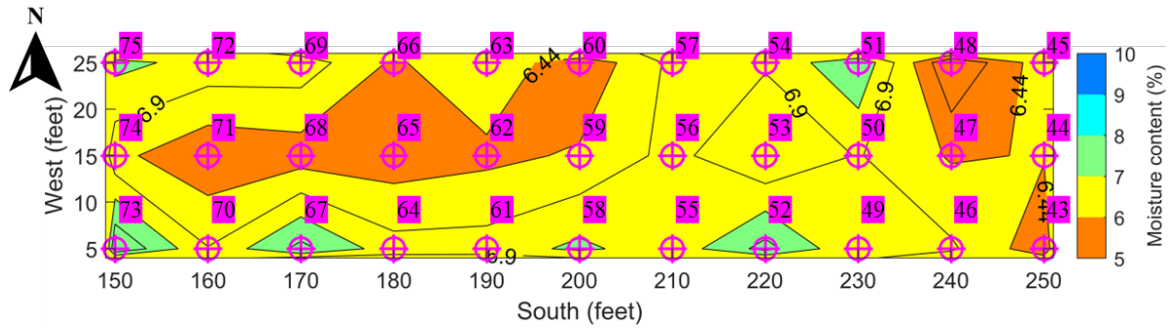


(d) Modulus contour of LWD 4421

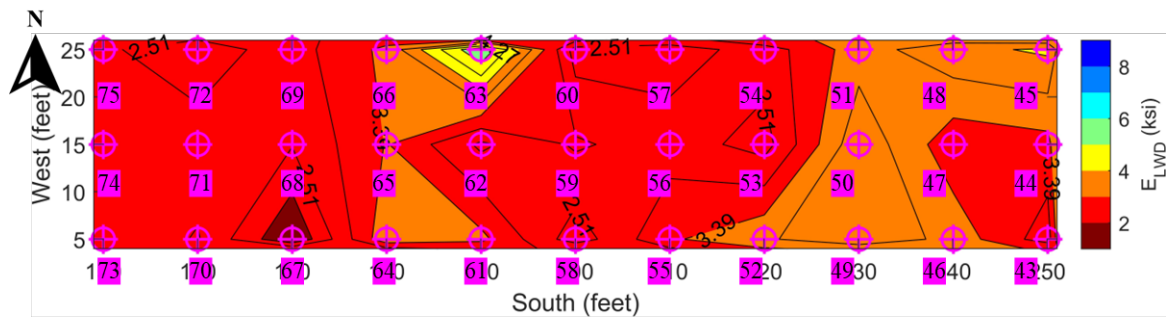
Figure 4.17 Moisture contents and LWD moduli spatial distribution of the base aggregate in section 1.

Figure 4.18a shows the moisture content contours for the test section 2 at the base aggregate site. As shown in the Figure 4.18a, the moisture contents of base aggregate were well controlled. Most of them fell into the range of 6.5% to 7.5%, with a few spots having lower moisture content, such as points 43, 44, 47, 48, 62, 65, 68, and 71, but they were still in the acceptable moisture content range of 4.5% to 7.5%.

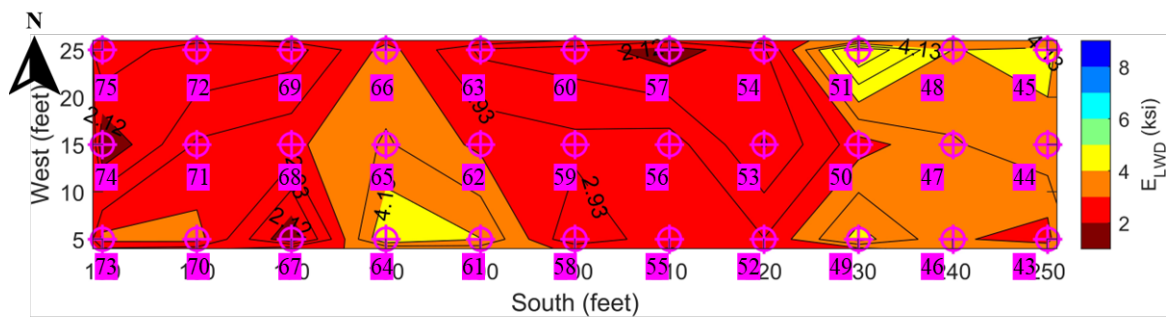
Figures 4.18b to 4.18d show LWD modulus contours in the test section 2 measured by the LWD 3878, 3879, and 4421, respectively. As can be seen in these figures, the LWD modulus contours showed a fluctuating trend that started with high moduli at the east end of the section, followed by low, high, and low moduli from east to west. This result, however, was barely consistent with the moisture content contour in Figure 4.18a. The trend that the LWD modulus increased with decreasing of moisture content occurred only at points 48, 58, and 67. On the other hand, similar to modulus contours in the test section 1, Figures 4.18b to 4.18d shared the similar distribution pattern of LWD moduli.



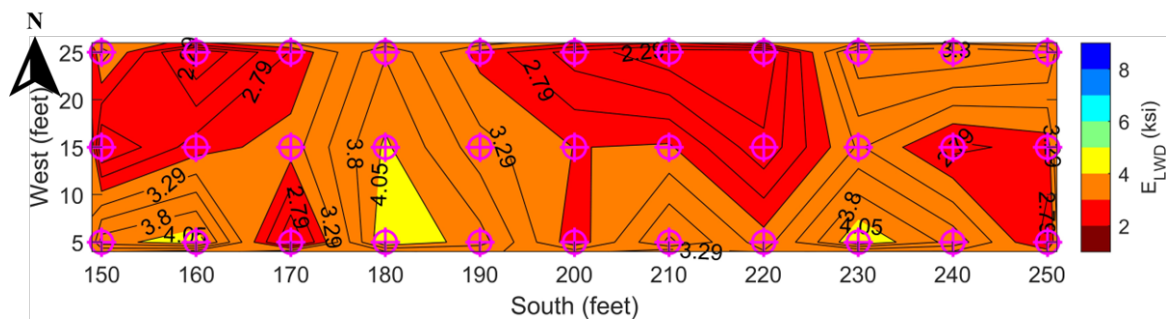
(a) Moisture content contour



(b) Modulus contour of LWD 3878



(c) Modulus contour of LWD 3879



(d) Modulus contour of LWD 4421

Figure 4.18 Moisture contents and LWD moduli spatial distribution of the base aggregate in section 2.

Figure 4.19a shows the moisture content contours for the test section 3 at the base aggregate site. As shown in the Figure 4.19a, the moisture contents of the base aggregate were well controlled, ranging from 5% to 7%. Most of the area had moisture content around 6.5%. At the west end, the moisture content change was the largest, varying from 5% from the south side to 7% to the north side. But they are still in the acceptable moisture content range of 4.5% to 7.5%.

Similar to the test sections 1, the moisture content and LWD modulus tests were performed using the LWD3879 for the whole area of test section 3. Due to the interruption from the construction process, LWD tests were not performed at part of west end using the LWD 3878 and 4421. Figures 4.19b through 4.19d present the LWD modulus contours measured by the LWD 3878, 3879, and 4421, respectively. It can be seen from those figures that although there was little change in moisture content in the east half of the test section, the LWD moduli decreased along east direction, which indicates some other factors other than the moisture content had more impact on LWD modulus. Moreover, the LWD moduli obtained from the three devices all showed the same pattern of lowest LWD moduli at the east end, while higher LWD moduli in the middle of the test section.

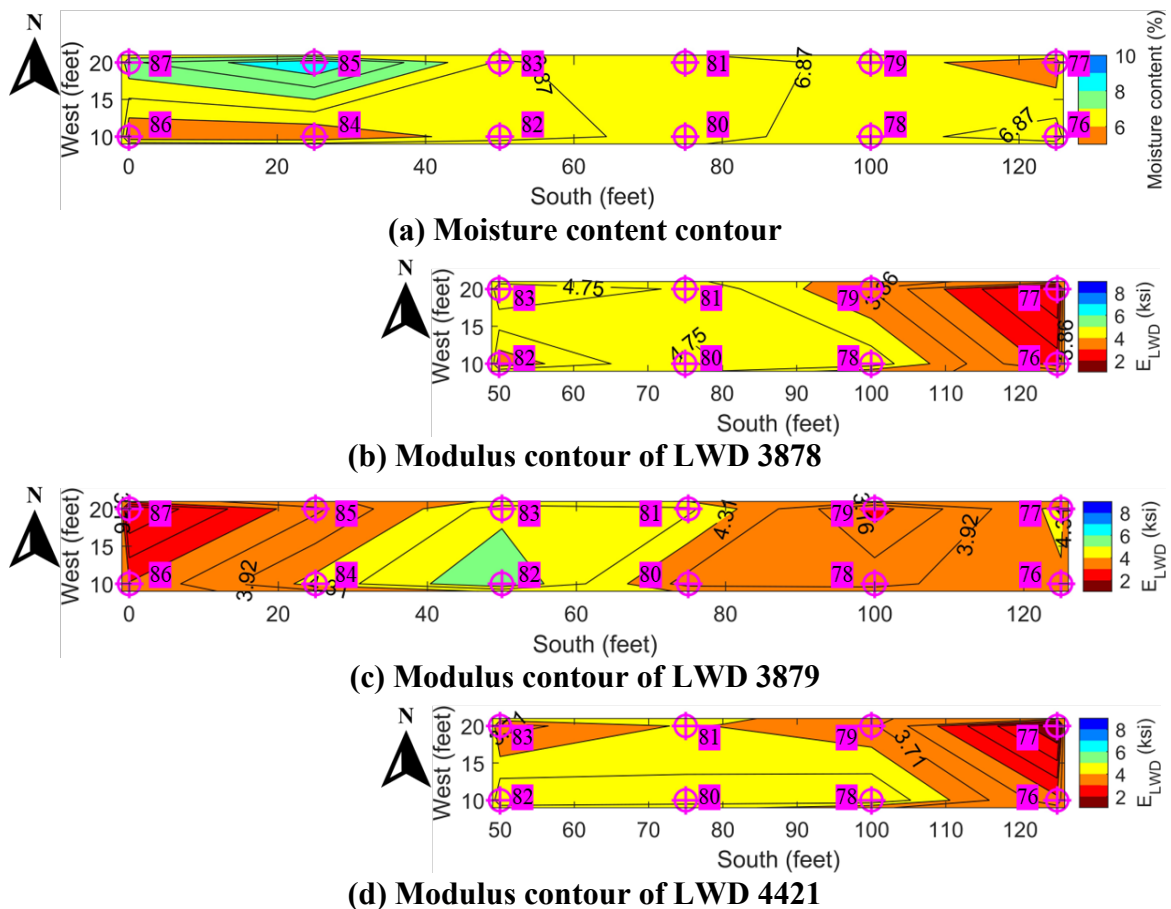
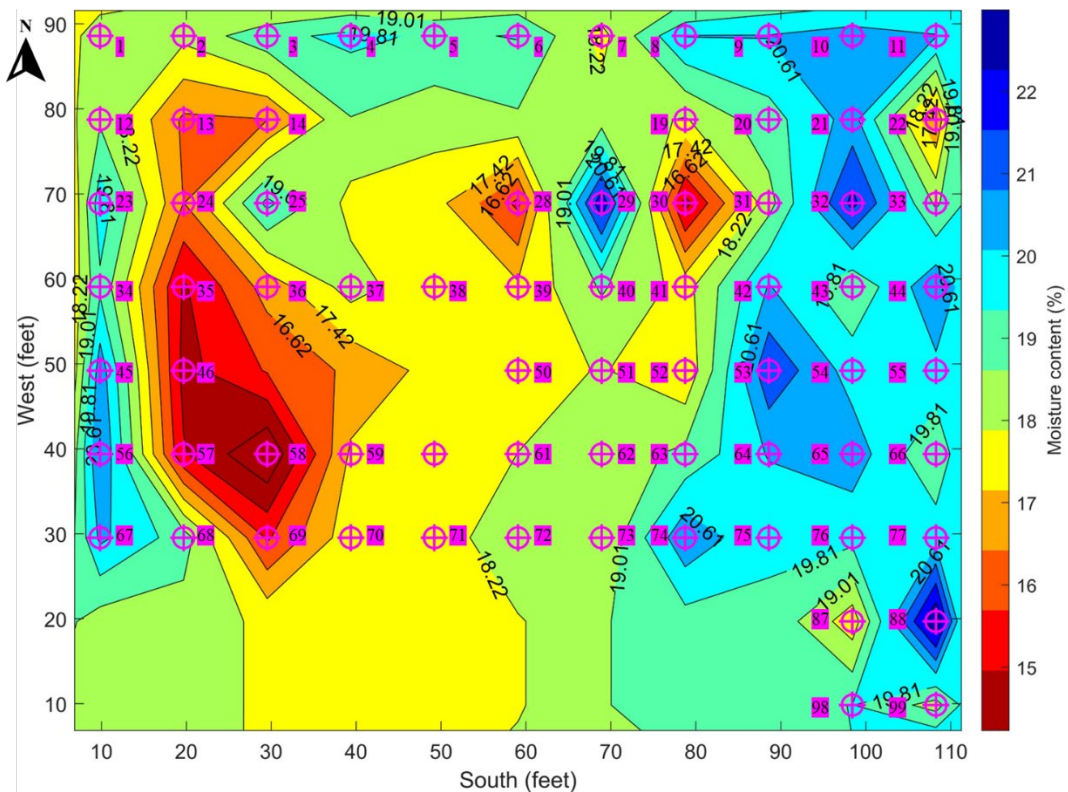


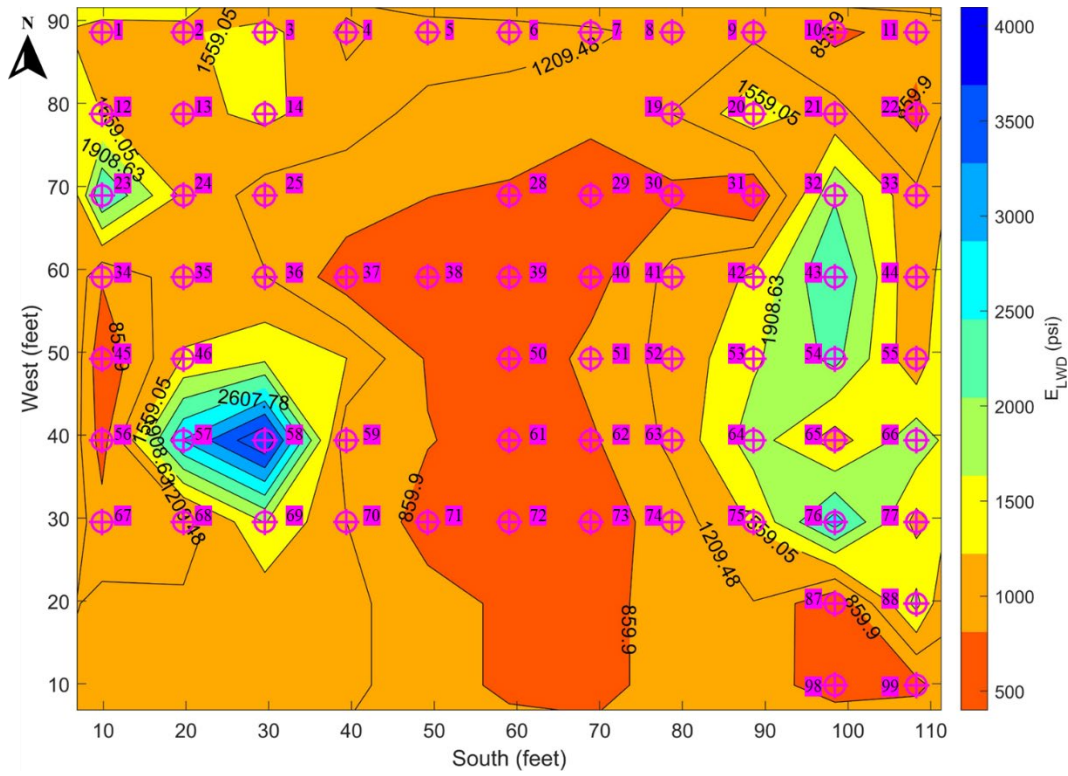
Figure 4.19 Moisture contents and LWD moduli spatial distribution of the base aggregate in section 3.

Figure 4.20a shows the moisture contours for the silty clay at the Buck O'Neil Bridge project. The OMC for the soil was 12.5%. Figure 4.20a indicates that the field moisture contents ranged from 13.4% to 23.8%, much higher than the OMC, with most of the area having moisture ranging from 17%-21%. This was attributed to the fact that all the tests at this site were performed 15 days after the completion of the construction and there were heavy rainfall events before the field trip. Please also note that there were three piles of waste soils at this test site as shown in Figure 4.5, where no test was performed. As shown in Figure 4.20a, four moisture content bands appeared along north to south direction, the moisture contents were lower in the center band, where fewer tests were performed (and less accurate), while higher in the west and east bands. There were three dry spots having moisture contents around 15%, they were points 28, 30, and 58.

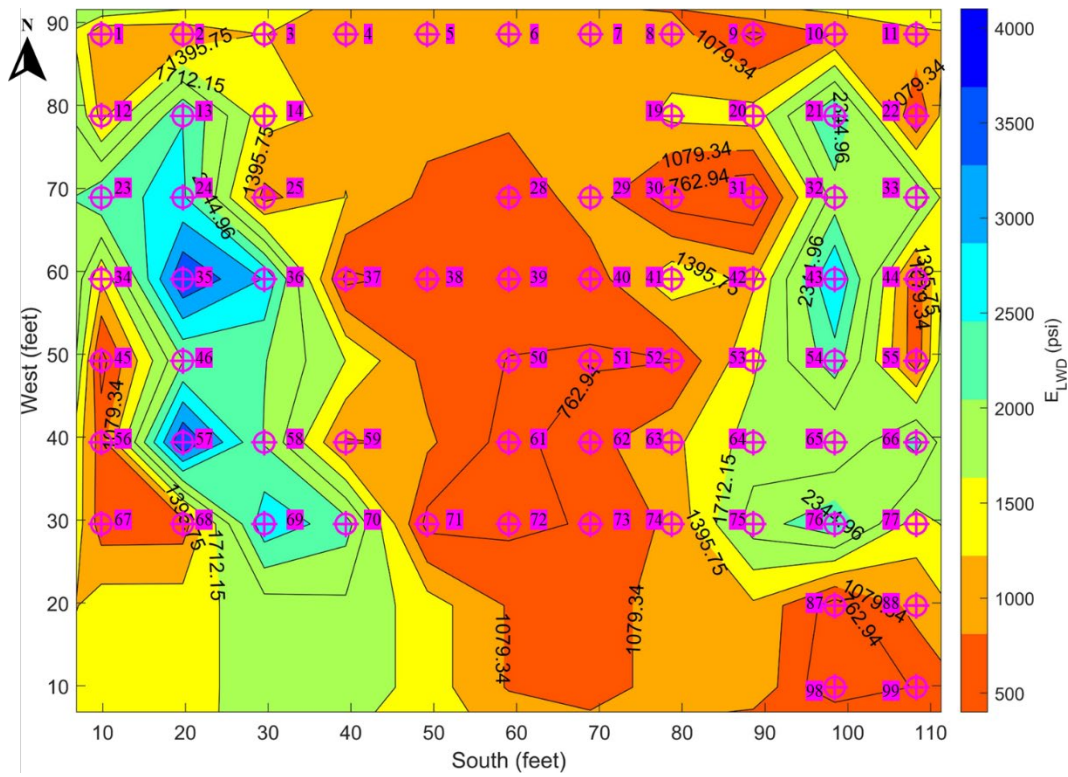
Figures 4.20b through 4.20d show the LWD moduli contours measured by the LWD 3878, 3879, and 4421, respectively. As can be seen from these figures, the LWD moduli obtained from the three devices were consistent with each other, as demonstrated by the similar patterns in the three figures. Moreover, LWD modulus contours also roughly showed four bands along north to south direction, those bands matched well with the moisture content bands where high moisture content bands corresponded to low LWD modulus bands except some points on the band at the east end. For example, at points 22 and 87 with lower moisture contents, the moduli measured by the three devices were consistently lower. It indicates that there were some factors other than moisture content that were influencing the soil stiffness.



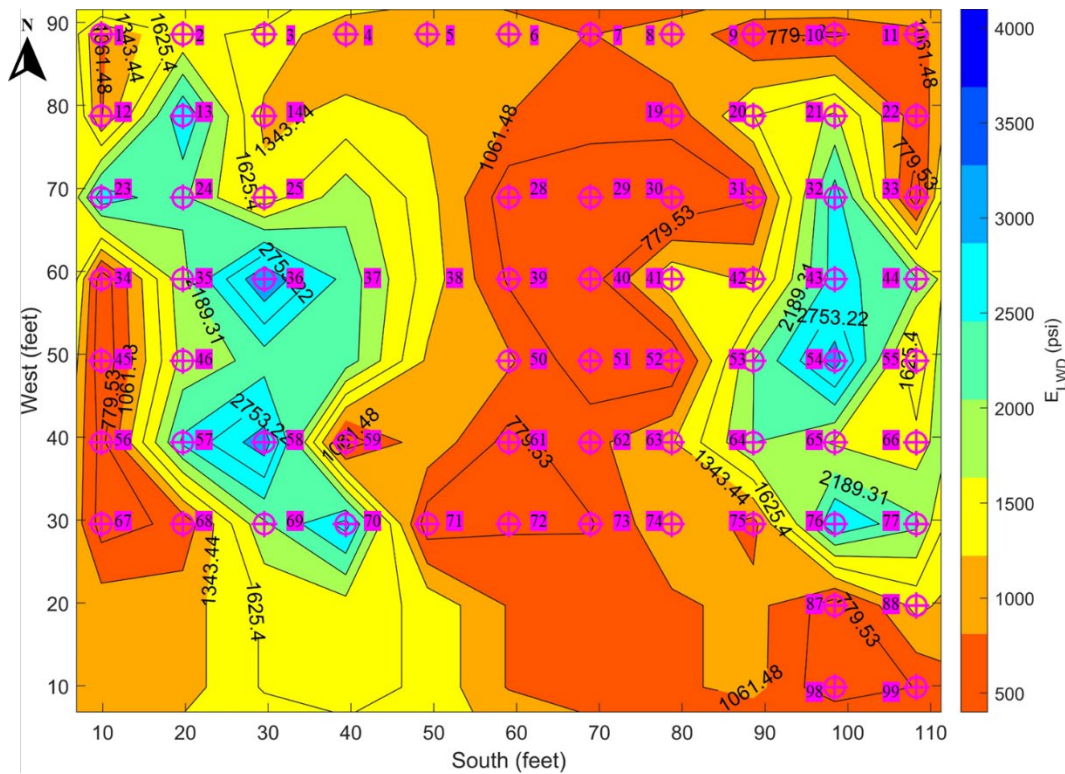
(a) Moisture content contour



(b) Modulus contour of LWD 3878



(c) Modulus contour of LWD 3879



(d) Modulus contour of LWD 4421

Figure 4.20 Moisture contents and LWD moduli spatial distribution at the silty clay site.

4.5.2 Relationship Between Moisture and LWD Modulus Two Hours after Construction

As mentioned in section 4.2.2, LWD tests were performed not only right after, but also two hours after compaction. Since all LWD tests had to be performed during the break or after working hours of the contractors, due to the limited access, the research team were only able to perform two-hour-after-compaction LWD tests at two of the four sites, one was the well graded sand site, and the other was the lean clay site.

Figure 4.21 compares the moisture contents and LWD moduli between right-after-compaction and two-hour-after-compaction at the WG site. As shown in Figure 4.21, the moisture contents at all test points experienced decreases, varying from 0.02% to 1.33% with an average of 0.7%. This was expected since evaporation can always result in loss of water from the compacted soil surface. The decreases in moisture contents generally caused slight increase in LWD moduli, excepting at points 3 and 8. The abnormal data might be caused by the random errors of the LWD measurements.

Figure 4.22 compares the moisture contents and LWD moduli between right-after-compaction and two-hour-after-compaction at the lean clay site. As shown in Figure 4.22, the moisture contents at all test points experienced consistent decreases, varying from 3.11% to 4.75% with an average of around 4%. The results were reasonable since unsaturated permeability for lean clay can be relatively high and make it easier for water

loss through evaporation. The decreases in moisture contents caused small or negligible increase in LWD moduli at all test points.

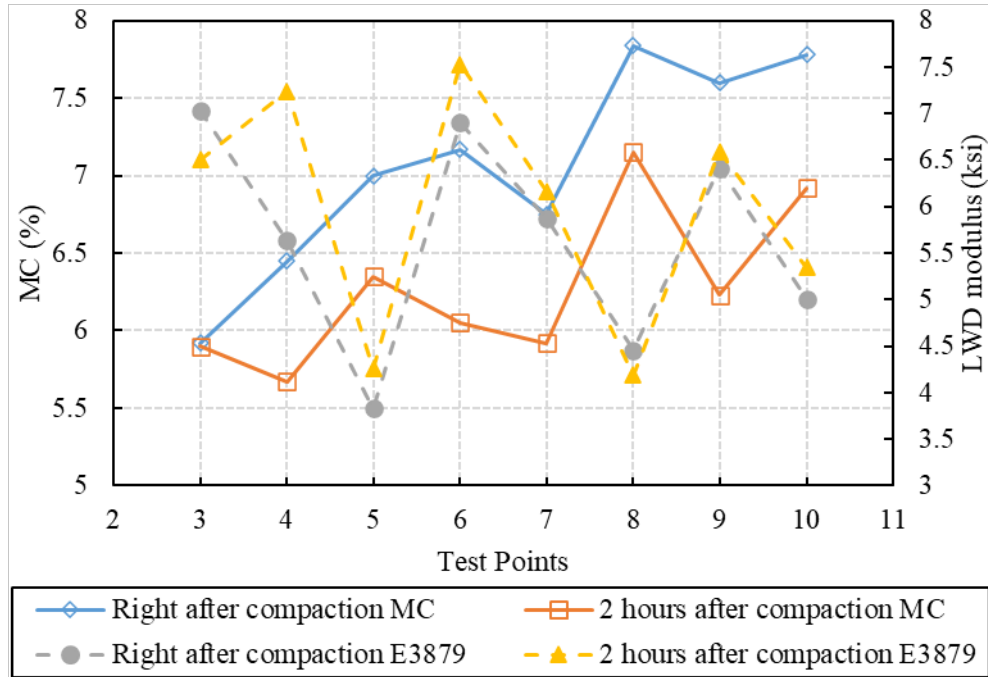


Figure 4.21 Instant and after-2h comparison of moisture contents and LWD moduli at the well graded sand site.

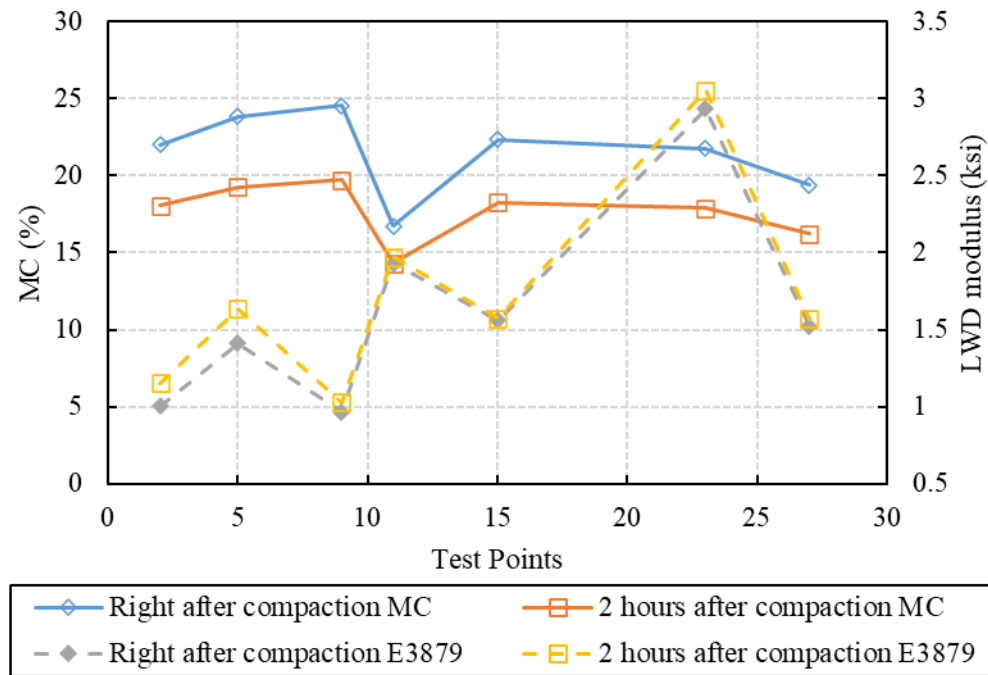


Figure 4.22 Instant and after-2h comparison of moisture contents and LWD moduli at the lean clay site.

4.6 Evaluation of Field Construction

4.6.1 Acceptance Criterion–Moisture Content

The moisture content undoubtedly plays an essential role in unbound granular material compaction. MoDOT specifies that the acceptable moisture content range for subgrade and base/subbase materials is from OMC-3% to OMC. Any moisture content beyond this range is not acceptable for QA/QC purposes.

Figures 4.23 through 4.26 show the moisture contents at all points at the four testing sites. The OMC and OMC-3% lines were also plotted in the figures to facilitate the discussions. As shown in the chapter 3, the OMCs for the lean clay and silty clay were 14.2% and 12.5%, respectively. As shown in Figures 4.23 and 4.26, all moisture contents at these two test sites were well above the OMC and thus the field compaction results were not acceptable.

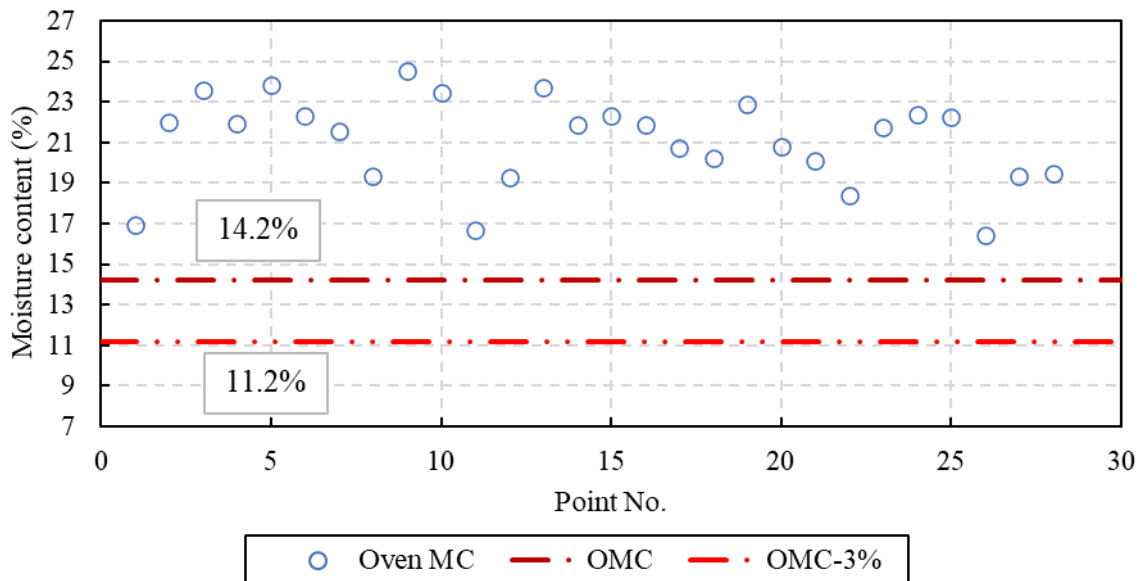


Figure 4.23 Moisture content range of testing points at the lean clay site.

Figure 4.24 shows the moisture content measurements at the well graded sand site. The OMC for the well graded sand was 9% and the acceptable moisture content range was 6%-9%. As can be seen in Figure 4.24, The well graded sand had a moisture content span of 5.5% to 8.6%, where 36 among 40 points fell into acceptable moisture content span.

Figure 4.25 shows the moisture content measurements at the base aggregate site. The OMC for the soil was 7.5% and the acceptable moisture content range was 4.5%-7.5%. As can be seen in Figure 4.25, The base aggregate had 65 testing points with a moisture content span of 5.3% to 9.2%, among which 55 points were in the acceptable range.

Consequently, compaction at the lean clay and silty clay sites were considered not acceptable due to failure to meet the moisture content requirements. Only those testing

points falling inside the acceptable moisture content ranges at the well graded sand and base aggregate sites were initially considered acceptable and kept for further modulus-based analyses as described in the following section.

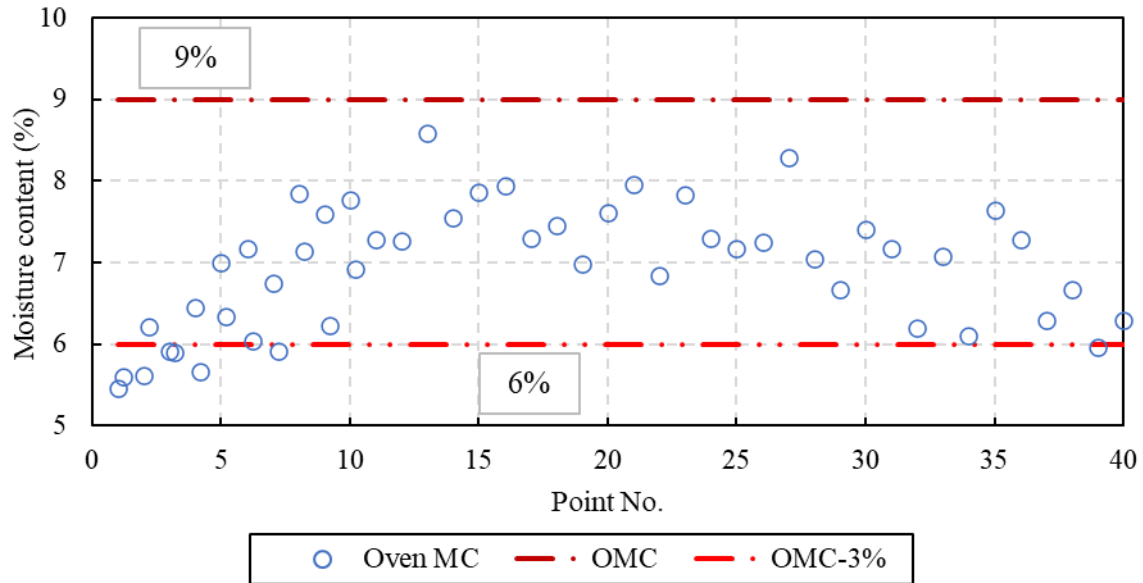


Figure 4.24 Moisture content range of testing points at the well graded sand site.

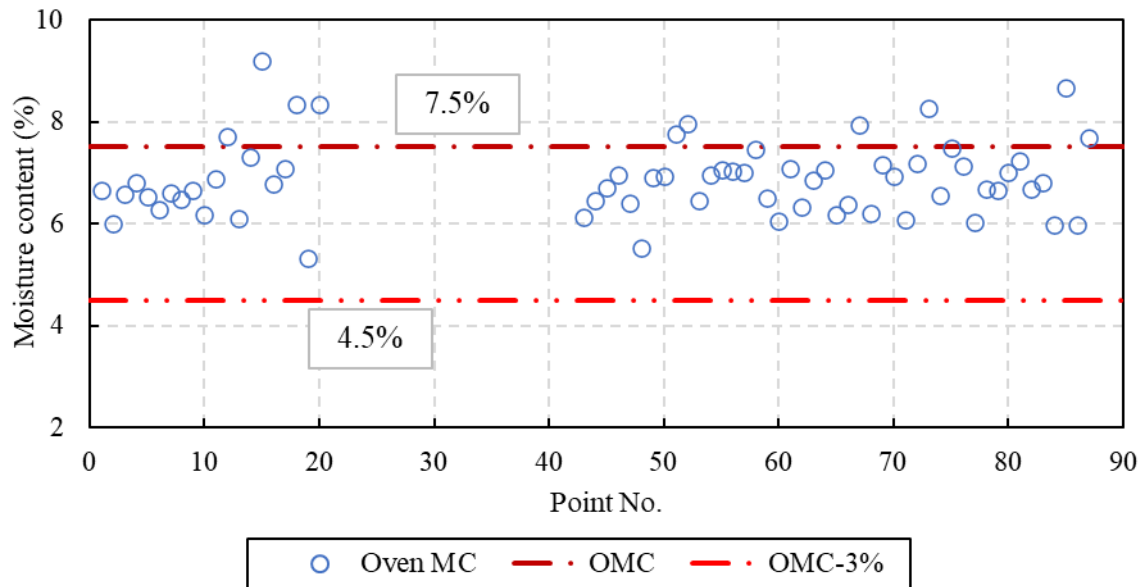


Figure 4.25 Moisture content range of testing points at the base aggregate site.

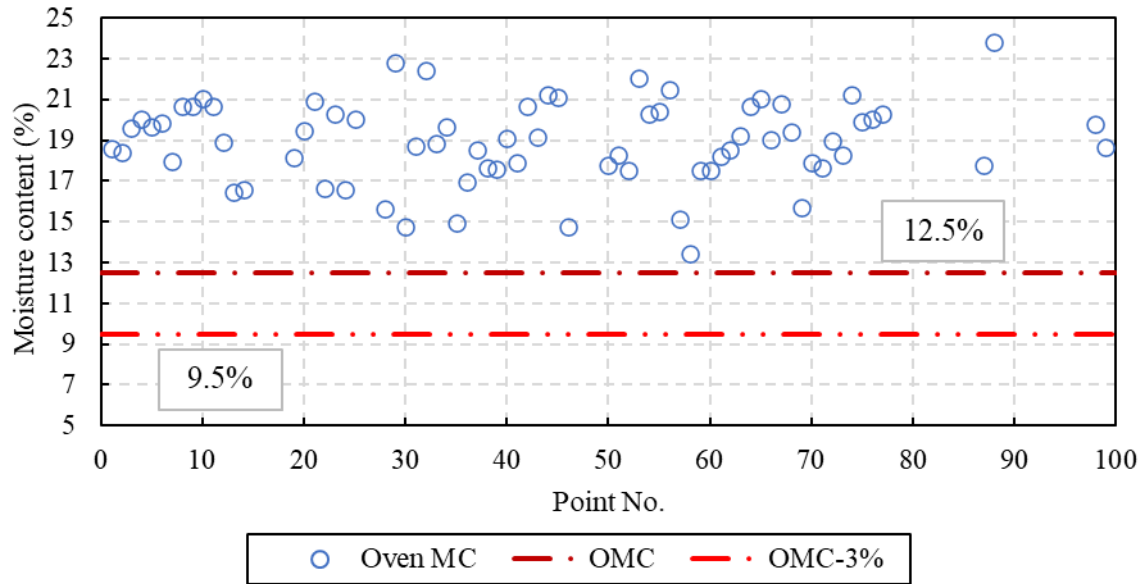


Figure 4.26 Moisture content range of testing points at the silty clay site.

4.6.2 Acceptance Criterion–Field to Target LWD Modulus Ratio

In the density-based method, dry density is another controlling factor for QA/QC criterion. Since the purpose of this project is to change from the density-based method to modulus-based method, LWD modulus will replace the dry density as an acceptance criterion. Specifically, the ratio of the field to target LWD modulus (E_{field}/E_{target}) takes the place of dry density ratio ($DD_{field}/DD_{lab-max}$) in modulus-based method to evaluate the quality of compaction.

As discussed in subsection 3.2.4, the target field LWD modulus for the well graded sand can be calculated by Equation (9) using the acceptable moisture content and the corresponding LWD applied stress in the field. Please note that the regression coefficients in Equation (9) were obtained by Equation (8) using the laboratory LWD test results within the acceptable moisture content range for the soil.

Figure 4.27 shows the field to target LWD modulus (E_{field}/E_{target}) ratios for all testing points at the well graded sand site with acceptable moisture contents. As shown in Figure 4.27, 11 out of 36 testing points (30.6%) had a modulus ratio under 100%. According to further inspection of Figures 4.3 and 4.27, it was found that all the points with unacceptable E_{field}/E_{target} (points 5, 8 in section 1, and 13, 16, 19, 22, 25, 28, 31, 34, 37, and 40 in section 2) were those points located right next to the MSE wall, which is a place that is usually difficult to compact. These results are also consisted with those shown in Figures 4.15 and 4.16. Figure 4.27 also indicates that the predictions from the three LWD devices are consistent. For point 5, all three devices predicted unacceptable results, while for points 4, 6, 7, 9, and 10, all three devices predicted acceptable results. There was only one exception, which is point 8. The LWD 3879 predicted acceptable result, while the LWD 3878 and 4421 predicted unacceptable results.

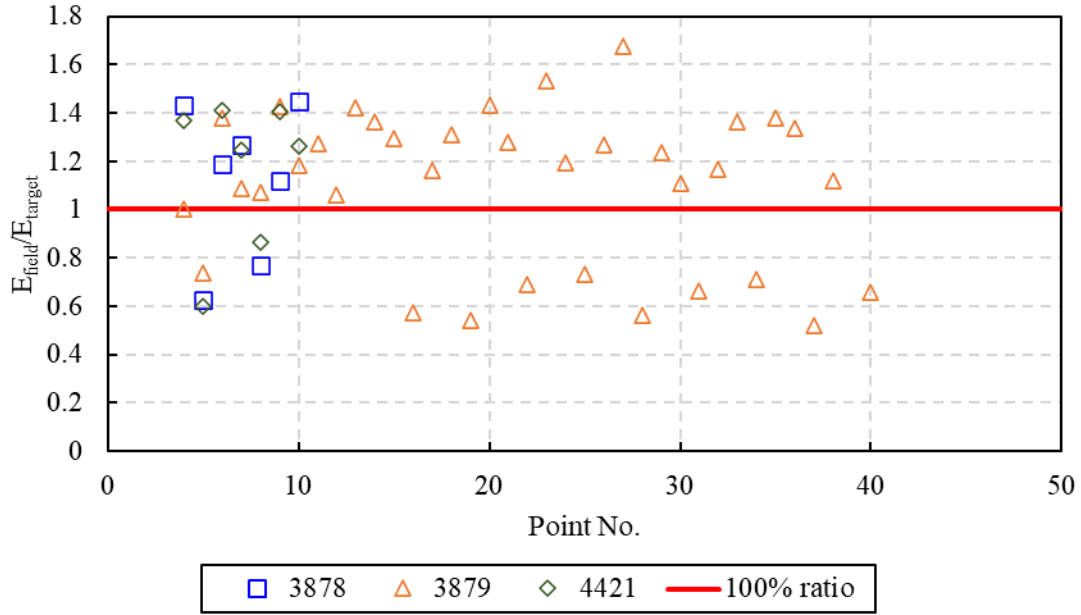


Figure 4.27 Field to target LWD modulus ratios of testing points at the well graded sand site.

Different from the well graded sand, the base/subbase layer is normally compacted on the top of a subgrade soil. As a result, the total surface deflection δ under LWD plate in Equation (12) is the summation of both top (base/subbase) and bottom (subgrade) layer. In order to obtain the correct field target LWD modulus of the base/subbase soils, the target field LWD modulus of base/subbase above the subgrade should be corrected using Equation (14) as follows:

$$E_{target-corr} = 1 / \left\{ \frac{1}{E_2 \left[\sqrt{1 + \left(\frac{h}{d} \sqrt{\frac{E_1}{E_2}} \right)^2} \right]} + \frac{\left[1 - \frac{1}{\sqrt{1 + \left(\frac{h}{d} \right)^2}} \right]}{E_1} \right\} \quad (14)$$

where

$E_{target-corr}$ = corrected target modulus (MPa) for the base material,

E_2 = modulus of the foundation (subgrade, or subbase plus subgrade) (MPa) measured by the LWD before base placement,

E_1 = target modulus (MPa) for the base material,

h = base layer thickness (m), and

d = LWD plate radius (m) used during field testing.

According to the information provided by MoDOT engineer, the subgrade soils for the aggregate base soils were lean clay with an average field LWD modulus of 2.9 ksi (20MPa) as determined in section 4.2.3 (E_2 in Equation (14)). The thickness of the

aggregate base soils was 4 inch (0.1 m) (h in Equation (14)). This information was used to corrected target field LWD modulus of base aggregate soil.

Figure 4.28 shows the field to target LWD modulus (E_{field}/E_{target}) ratios for all testing points at the base aggregate site with acceptable moisture contents. As shown in Figure 4.28, among 55 points satisfied with moisture content criterion, the LWD 3878, 3879, and 4421 tested 48, 55, and 47 points of them, respectively. As for each LWD device, the LWD 3878 had 22 out of 48 points (45.8%) having modulus ratios above 100% and were considered acceptable, the LWD 3879 had 35 out of 55 points (63.6%) were considered acceptable, and the LWD 4421 had 27 out of 47 points (57.4%) were acceptable. Figure 4.28 also indicates that the predictions from the three LWD devices were consistent. Among 47 points that all the three devices tested, 20 points including 1, 2, 4, 6, 45, 46, 48, 49, etc., were predicted acceptable by all the three devices, while for 14 points including 7, 9, 43, 53, 54, 57, 58, 59, 60, 69, 71, 72, 74, and 77, all the three devices predicted unacceptable results. It is also worth noting that 13 of the 47 points got different acceptance evaluation results from the three LWD devices. Among these points, the LWD 3878 rejected 6 points, the LWD 3879 rejected 7 points, and the LWD 4421 rejected 3 points. It seems that the LWD 4421 had a more lenient acceptance criterion. It is worth noting that 3 points of the LWD 3879 and 1 point of the LWD 4421 were higher than 200% modulus ratio, which might be attributed to over compaction at those points.

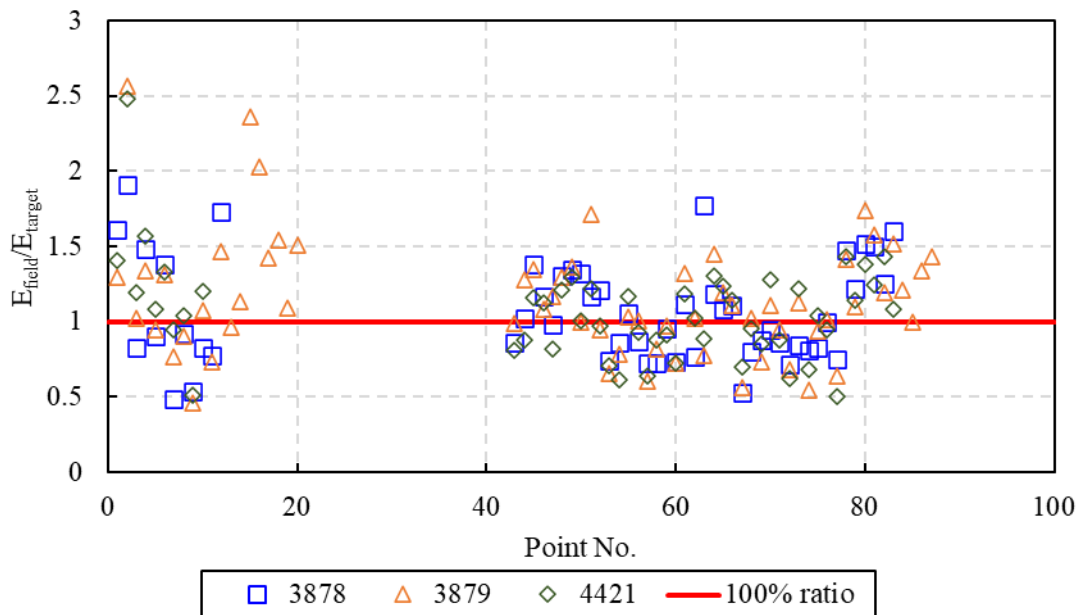


Figure 4.28 Field to target LWD modulus ratios of testing points at the base aggregate site.

CHAPTER 5 CONCLUSIONS

This research project investigates the feasibility of implementing a LWD on construction acceptance of unbound granular materials for MoDOT. An extensive literature review and industry survey among DOTs were performed. Different kinds of laboratory and field tests were conducted on four types of representative soils (e.g., lean clay, well graded sand, base aggregate, and silty clay) in Missouri state from two MoDOT construction projects, I-270 North and Buck O'Neil Bridge projects.

Laboratory testing includes 1) material characterization such as sieve analysis and hydrometer, Atterberg limits, and modified Proctor compaction tests, 2) moisture content measurements using the Aggrameter and Ohaus MB120 devices to evaluate their efficiency and practicability in field applications, 3) LWD tests on Proctor mold, as well as 4) repeated load triaxial tests. Several field trips were made to perform field LWD tests using three different devices. Besides performing field moisture content measurements, soil samples were also collected and brought back to the laboratory for standard moisture content measurement using the oven-drying method. Comprehensive data analyses were performed, from which the following conclusions were drawn:

1. Survey results showed that 6.5% of the responded state DOTs (3 out of 43 DOTs - Nebraska, Indiana, and Minnesota) implemented and used the LWD for compaction QC/QA of unbound materials. 63.0% of the respondents are unfamiliar with the LWD and never used it, even for evaluation or demonstration purposes. LWD tests were evaluated (in-house or through a university/consultant) or demonstrated in the rest of the DOTs. The Nebraska DOT specifies only the LWD for compaction QC and QA purposes.

2. Four representative soils from the I-270 North and Buck O'Neil Bridge projects were classified following AASHTO and ASTM soil classification. The OMC for the lean clay, the well graded sand, the base aggregate, and the silty clay were 14.2%, 9.0%, 7.5%, and 12.5%, respectively.

3. Four different methods were used to measure the moisture content for the soils in the laboratory and/or field, including the NDG, Ohaus MB120, Aggrameter, and the standard oven-drying method. It was found that the Ohaus moisture analyzer requires strict environmental conditions, for example, leveled ground without vibration, or disturbance, and or magnetic field, which were difficult to meet. In addition, it cannot be used for moisture content measurement of base aggregate since the minimum weight of 250 g for a maximum particle size of 19 mm is required in ASTM D2216-19. When the required conditions are met, the Ohaus moisture analyzer can be used to accurately measure the moisture content for different soils. With proper calibrations for each specific soil, the obtained moisture content results can be both accurate and precise.

4. The Aggrameter does not have strict environmental requirements but can only be used for certain types of soils. In this research project, the Aggrameter only worked well

with the well graded sand while getting erroneous results for both base aggregate and clay soils, regardless of moisture range.

5. When the LWD tests were performed in the Proctor mold, it was found that deflection increases with increases in the moisture content and the applied stress for all tested soils. The LWD modulus decreases with an increase in the moisture content. It was also found that when the moisture content keeps increasing, the LWD modulus for the lean clay and silty clay will decrease to a certain value and maintain as a constant value after that.

6. The repeated load triaxial tests confirmed that M_R decreased with increasing the moisture contents and deviatoric stresses. Another variable that affected the M_R value was the confining pressure. Generally, M_R increased with an increase in the confining pressure.

7. The MEPDG model on M_R only considered the impact of stress, while the influence of moisture content was not included. A new M_R prediction model was proposed in this report by modifying the MEPDG model to include the influence of moisture content changes on the M_R . Analyses indicate the proposed M_R model is robust and can provide better prediction of M_R for different types of soils.

8. The field LWD modulus measured from different devices were compared. It was found that there was a fair correlation between the results obtained from LWD 3878 and 3879, even though they share the same models of Zorn ZFG 2000. It was also found that there were good correlations between the results obtained from LWD 3879 and 4421 for all soil types. There was a good correlation between the results obtained from LWD 3878 and 4421 for the well graded sand only. While for other three soils, the correlations were fair.

9. LWD field tests were performed immediately after the compaction as well as two hours after the compaction. It was found that two hours after the compaction, the soil moisture normally decreased due to evaporation, and the LWD moduli increased accordingly. It was found that the moisture content changed more in fine-grained soils than coarse-grained soils, mainly attributed to a higher unsaturated permeability in fine-grained soils.

10. The contours of moisture contents and field LWD moduli obtained from different devices were plotted to analyze the relationship between the moisture content and LWD modulus in the field. It was found that the LWD modulus contours obtained from the three devices shared the same or similar patterns most of the time, indicating that all devices can correctly measure the trend of the LWD modulus. It was also found that the moisture content contours were closely related to the LWD modulus contours, but with large variations at many cases. This can be attributed to the fact that moisture content is an important influencing factor on the LWD moduli, but it is not the only influencing factor. Other factors such as degree of compaction also influence the LWD moduli.

Consequently, the LWD modulus contours from the three devices shared a similar pattern with the moisture content contour, but they are not the same.

11. The moisture contents at the lean clay and silty clay sites were found to be much higher than the acceptable moisture content ranges. Consequently, the compaction quality was not acceptable. The well graded sand and the base aggregate sites had acceptable moisture content and further analyses were performed to evaluate the LWD modulus acceptance.

12. Besides the moisture content, the ratio of the field to target LWD modulus was used to evaluate whether the LWD modulus results were acceptable. Due to the interruption caused by the construction process, there were only 10 points were tested by all three LWD devices at the well graded sand site. 3 of the 10 points had moisture contents outside the acceptable range, and only the rest 7 points were evaluated using the ratios of the field to target LWD moduli. Results indicated that for most cases, the three LWD devices predicted consistent results at the well graded sand site. Among the 7 points, 5 of them were evaluated as acceptable and one was considered unacceptable by all three devices. There was one point showed conflicting predicted results. The LWD 3879 predicted acceptable results, while according to the predictions by the LWD 3878 and 4421, the results were unacceptable. It was also found that nearly all the unacceptable testing points as predicted by the LWD 3879 were located right next to the MSE wall, which is a place that is usually difficult to compact.

13. Since the base/subbase layer is compacted on the top of a subgrade soil, the target field LWD modulus of base/subbase above the subgrade should be corrected to obtain the correct LWD modulus. Results from the base aggregate site were similar to those at the well graded sand site. It was found that the predictions from the three LWD devices were consistent. Among 47 points that all three devices tested, 20 points including were predicted acceptable by all three devices, while for 14 points, all three devices predicted unacceptable results. It is also worth noting that 13 of the 47 points got different acceptance evaluation results from the three LWD devices. Among these points, LWD 3878 rejected 6 points, 3879 rejected 7 points, and 4421 rejected 3 points. It seems that LWD 4421 had a more lenient acceptance criterion.

14. Overall, the results obtained from this study indicated that all three LWD devices can provide reasonable and consistent results for QA/QC for field compaction. The devices were easy to use, and the tests can be performed rapidly in the field with less interference with the compaction process. Since the moisture content at neither the lean clay nor the silty clay site was fallen in the acceptable moisture content ranges, the conclusions obtained from this study are only applicable for coarse-grained soils. More study is needed to evaluate the performance of the LWD test for fine-grained soils in Missouri.

REFERENCES

- AASHTO M 145. (1991). *Standard Specification for Classification of Soils and Soil-Aggregate Mixtures for Highway Construction Purposes*. American Association of State Highway and Transportation Officials.
- AASHTO T 265. (2015). *Standard Method of Test for Laboratory Determination of Moisture Content of Soils*. American Association of State Highway and Transportation Officials.
- AASHTO T 307. (1999). *Standard Method of Test for Determining the Resilient Modulus of Soils and Aggregate Materials*. American Association of State Highway and Transportation Officials.
- ASTM C127. (2016). *Standard Test Method for Relative Density (Specific Gravity) and Absorption of Coarse Aggregate*. ASTM International.
- ASTM D854. (2016). *Standard Test Methods for Specific Gravity of Soil Solids by Water Pycnometer*. ASTM International.
- ASTM D1557. (2021). *Standard Test Methods for Laboratory Compaction Characteristics of Soil Using Modified Effort (56,000 ft-lbf/ft³ (2,700 kN-m/m³))*. ASTM International.
- ASTM D2487. (2020). *Standard Practice for Classification of Soils for Engineering Purposes (Unified Soil Classification System)*. ASTM International.
- ASTM D4318. (2018). *Standard Test Methods for Liquid Limit, Plastic Limit, and Plasticity Index of Soils*. ASTM International.
- ASTM D7928. (2021). *Standard Test Method for Particle-Size Distribution (Gradation) of Fine-Grained Soils Using the Sedimentation (Hydrometer) Analysis*. ASTM International.
- ASTM E2835. (2021). *Standard Test Method for Measuring Deflections Using a Portable Impulse Plate Load Test Device*. ASTM International.
- Beshoy, R., Xiong, Z., & Jenny, L. (2021). *Implementing the LWD for MoDOT Construction Acceptance of Unbound Material Layers* (p. 102) [Interim Project Report]. Missouri University of Science and Technology.
- Bouazza, A., Zornberg, J. G., McCartney, J. S., & Nahlawi, H. (2006). Significance of unsaturated behaviour of geotextiles in earthen structures. *Australian Geomechanics*, 41(3), 133–142.
- Bryson, L., Jean-Louis, M., & Gabriel, C. (2012). Determination of in situ moisture content in soils from a measure of dielectric constant. *International Journal of Geotechnical Engineering*, 6(2), 251–259.
<https://doi.org/10.3328/IJGE.2012.06.02.251-259>
- Dai, S., & Kremer, C. (2006). *Improvement and Validation of Mn/DOT DCP Specifications for Aggregate Base Materials and Select Granular*.
- Fleming, P. R., Frost, M. W., & Lambert, J. P. (2009). Lightweight deflectometers for quality assurance in road construction. IN: Tutumluer, E. and Al-Qadi, IL (Eds). *Bearing Capacity of Roads, Railways and Airfields: Proceedings of the 8th International Conference (BCR2A'09)*, 809–818.
- Fredlund, D. G., & Rahardjo, H. (1993). An overview of unsaturated soil behaviour. *Geotechnical Special Publication*, 1–1.

- Fredlund, D. G., & Xing, A. (1994). Equations for the soil-water characteristic curve. *Canadian Geotechnical Journal*, 31(4), 521–532. <https://doi.org/10.1139/t94-061>
- Hick, R. G., & Monismith, C. L. (1971). Factors influencing the resilient response of granular materials. *Highway Research Record*, 345, 15–31.
- Hopkins, T. C., Beckham, T. L., Sun, C., & University of Kentucky Transportation Center. (2007). *Resilient modulus of compacted crushed stone aggregate bases* (KTC-05-27/SPR-229-01-1F). <https://rosap.nrl.bts.gov/view/dot/21627>
- Kalchey, I. V., & Hicks, R. G. (1973). A test procedure for determining the resilient properties of granular materials. *Journal of Testing and Evaluation*, 1(6), 472–479.
- Missouri highways and transportation commission. (2022). *Missouri standard specifications for highway construction*.
- Mohammad, L. N., Nazzal, M. D., Abu-Farsakh, M. Y., & Alshibli, K. (2009). Estimation of subgrade soils resilient modulus from in-situ devices test results. *Journal of Testing and Evaluation*, 37(3), 245–253.
- Nazarian, S., Mazari, M., Abdallah, I. N., Puppala, A. J., Mohammad, L. N., & Abu-Farsakh, M. Y. (2015). *Modulus-based construction specification for compaction of earthwork and unbound aggregate*. Transportation Research Board Washington, DC.
- Nazzal, M. (2014). *Non-nuclear methods for compaction control of unbound materials* (Issue Project 20-05, Topic 44-10).
- Schwartz, C. W., Afsharikia, Z., & Khosravifar, S. (2017). *Standardizing lightweight deflectometer modulus measurements for compaction quality assurance*. Maryland. State Highway Administration.
- TP BF-StB Part B 8.3. (2012). *Dynamic Plate Load Testing with the Light Drop-Weight Tester*.
- van Genuchten, M. Th. (1980). A Closed-form Equation for Predicting the Hydraulic Conductivity of Unsaturated Soils. *Soil Science Society of America Journal*, 44(5), 892–898. <https://doi.org/10.2136/sssaj1980.03615995004400050002x>
- Vanapalli, S. K., Fredlund, D. G., & Pufahl, D. E. (1999). The influence of soil structure and stress history on the soil–water characteristics of a compacted till. *Geotechnique*, 49(2), 143–159.
- Witczak, M. W., & Uzan, J. (1988). The universal airport pavement design system. *Report I of V: Granular Material Characterization, Department of Civil Engineering, University of Maryland, College Park, MD*.
- Zhao, G., Yao, Y., Li, S., Jiang, Y., & Purdue University. Joint Transportation Research Program. (2018). *Maximum Allowable Deflection by Light Weight Deflectometer and Its Calibration and Verification* (FHWA/IN/JTRP-2018/21). <https://doi.org/10.5703/1288284316866>

APPENDIX

A. Weather Condition of Four Sites During Testing

A.1 Soil surface temperature and weather conditions of lean clay.

No.	Fluke thermo meter reading (°F)	Wind speed (mi/h)	Air temperature (°F)	Humidity (%)	Evaporation rate (gr/ft ² /hr)	Humidity ratio (gr/lbm)	Station pressure (psi)
1	85.1	2.67	83.1	41.6	15.98	70.98	14.51
2	81.9	0.00	96.6	26.5	7.99	69.16	14.50
3	75.2	4.66	91.0	25.7	31.97	56.42	14.50
4	73.4	3.79	87.6	27.3	29.30	53.69	14.49
5	78.8	1.68	94.8	24.2	17.32	59.85	14.49
6	74.5	1.18	93.6	23.7	15.98	56.28	14.48
7	79.3	2.11	93.4	24.3	21.31	57.26	14.48
8	77.4	2.11	91.9	25.3	15.98	57.19	14.47
9	76.3	1.12	92.7	23.5	11.99	54.32	14.47
10	77.9	0.00	92.3	24.5	18.65	55.86	14.47
11	81.1	1.62	91.0	25.5	10.66	56.07	14.47
12	77.4	0.00	89.4	27.1	14.65	56.56	14.47
13	77.4	0.87	89.6	27.4	15.98	57.47	14.47
14	77.4	1.18	83.7	34.7	14.65	60.55	14.46
15	77.4	1.30	87.8	35.4	7.99	70.35	14.47
16	77.4	2.67	83.1	41.6	15.98	70.98	14.44
17	77.4	0.00	96.6	26.5	7.99	69.16	14.48
18	77.4	4.66	91.0	25.7	31.97	56.42	14.48
19	77.4	3.79	87.6	27.3	29.30	53.69	14.49
20	77.4	1.68	94.8	24.2	17.32	59.85	14.50
21	77.4	1.18	93.6	23.7	15.98	56.28	14.50
22	77.4	2.11	93.4	24.3	21.31	57.26	14.49
23	77.4	2.11	91.9	25.3	15.98	57.19	14.49
24	77.4	1.12	92.7	23.5	11.99	54.32	14.48
25	77.4	0.00	92.3	24.5	18.65	55.86	14.48
26	77.4	1.62	91.0	25.5	10.66	56.07	14.47
27	77.4	0.00	89.4	27.1	14.65	56.56	14.47
28	77.4	0.87	89.6	27.4	15.98	57.47	14.47
29	77.4	1.18	83.7	34.7	14.65	60.55	14.47
30	77.4	1.30	87.8	35.4	7.99	70.35	14.47
Avg.	77.7	1.62	90.6	27.78	17.32	59.5	14.48

A.2 Soil surface temperature and weather conditions of well graded sand.

No.	Fluke thermo meter reading (°F)	Wind speed (mi/h)	Air temperature (°F)	Humidity (%)	Evaporation rate (gr/ft ² /hr)	Humidity ratio (gr/lbm)	Station pressure (psi)
1	85.5	4.04	82.9	42.5	18.65	73.15	14.41
2	88.5	2.49	82.6	43.6	13.32	74.06	14.40
3	84.4	0.00	84.6	40.4	6.66	73.01	14.40
4	87.3	2.36	84.7	40.9	13.32	74.41	14.40
5	86.9	0.75	86.2	37.5	9.32	71.33	14.40
6	87.1	0.00	84.4	39.5	6.66	70.91	14.40
7	88.7	2.30	86.2	37.5	14.65	71.33	14.40
8	88.3	1.30	85.5	39.6	10.66	73.92	14.41
9	87.1	0.81	89.8	33.9	9.32	72.45	14.39
10	84.7	0.00	93.2	34.3	5.33	81.62	14.41
11	85.6	0.00	93.7	34.3	5.33	83.3	14.40
12	85.6	0.00	93.0	31.3	6.66	73.78	14.40
13	87.3	1.93	85.3	32.2	18.65	59.43	14.40
14	86.9	1.18	86.5	31.6	14.65	60.55	14.40
15	91.0	1.30	86.9	29.6	15.98	57.4	14.40
16	87.6	0.00	87.8	29	10.66	58.1	14.40
17	85.6	1.68	89.1	28.1	17.32	58.17	14.40
18	84.7	1.93	85.6	29	19.98	53.9	14.40
19	85.1	0.75	87.8	28.5	14.65	56.98	14.40
20	86.5	2.05	86.7	28.3	21.31	54.53	14.40
21	84.0	2.30	85.3	26.8	23.98	49.28	14.40
22	86.7	2.17	84.9	27.2	23.98	49.35	14.40
23	87.6	2.24	84.7	29.3	22.64	52.92	14.40
24	88.0	0.00	87.4	29.9	10.66	59.22	14.40
25	85.1	1.49	86.9	27.1	18.65	52.36	14.40
26	86.7	1.18	85.8	28.1	17.32	52.64	14.40
27	86.2	0.75	84.7	28.1	15.98	50.75	14.40
28	85.1	1.24	84.6	31	15.98	55.86	14.40
29	86.0	1.55	85.3	30.2	18.65	55.79	14.40
30	87.1	2.80	85.8	27.9	25.31	52.15	14.40
Avg.	86.6	1.35	86.6	32.57	14.65	62.79	14.40

A.3 Soil surface temperature and weather conditions of base aggregate.

No.	Fluke thermo meter reading (°F)	Wind speed (mi/h)	Air temperature (°F)	Humidity (%)	Evaporation rate (gr/ft ² /hr)	Humidity ratio (gr/lbm)	Station pressure (psi)
1	66.7	0.00	78.8	46	7.99	68.25	14.51
2	67.5	1.68	78.8	47.5	11.99	70.56	14.50
3	68.4	1.12	78.8	48.3	10.66	71.82	14.49
4	66.7	1.99	79.0	49.2	11.99	73.78	14.49
5	67.8	1.43	80.2	48.2	10.66	75.11	14.49
6	68.4	1.68	80.2	45.7	11.99	71.12	14.49
7	66.6	1.24	80.2	47.4	10.66	72.31	14.48
8	67.3	0.93	79.5	47.9	9.32	74.27	14.48
9	68.0	1.06	79.5	47.9	9.32	73.85	14.48
10	67.1	0.99	79.9	46.8	9.32	75.39	14.47
11	68.9	3.11	80.6	46.6	15.98	72.31	14.47
12	69.3	0.87	81.3	46.1	7.99	75.11	14.47
13	66.7	6.46	80.4	45	25.31	73.99	14.46
14	68.4	2.42	82.2	44.8	10.66	79.1	14.46
15	68.5	0.00	81.9	46.8	5.33	79.38	14.46
16	66.4	4.23	82.6	45.6	17.32	76.37	14.46
17	66.6	0.87	83.5	44.1	7.99	77.63	14.46
18	66.6	2.11	83.3	46.3	11.99	75.53	14.45
19	66.4	1.68	82.4	45.9	10.66	76.86	14.45
20	66.7	2.73	81.9	47.7	11.99	78.05	14.45
21	67.1	1.86	81.1	47.8	9.32	78.4	14.45
22	66.7	2.30	81.5	48.4	10.66	78.61	14.45
23	67.1	1.74	81.3	48.4	10.66	76.79	14.45
24	67.6	1.43	82.8	46.3	9.32	75.88	14.46
25	66.4	0.00	81.3	47.3	5.33	75.88	14.46
26	66.9	7.52	79.5	49.5	26.64	74.76	14.46
27	67.5	3.11	79.5	51	13.32	76.51	14.46
28	66.2	0.81	78.6	51.3	7.99	76.86	14.45
29	66.4	0.99	78.6	52.2	7.99	75.53	14.46
30	67.3	0.00	78.1	52.3	7.99	75.53	14.46
31	66.7	1.49	78.3	53.5	6.66	75.88	14.46
32	67.3	3.85	78.3	54.8	10.66	75.04	14.46
33	67.6	3.29	77.2	55.4	15.98	74.48	14.46
34	67.5	5.84	76.5	55.5	15.98	75.32	14.46
35	67.3	2.42	75.9	56.1	22.64	73.92	14.46
Avg.	67.3	2.09	80.1	48.67	11.99	75.18	14.47

A.4 Soil surface temperature and weather conditions of silty clay.

No.	Fluke thermo meter reading (°F)	Wind speed (mi/h)	Air temperature (°F)	Humidity (%)	Evaporation rate (gr/ft ² /hr)	Humidity ratio (gr/lbm)	Station pressure (psi)
1	52.2	1.18	66.9	38.7	22.64	38.99	14.26
2	50.4	1.18	73.4	29.7	22.64	37.38	14.26
3	50.0	2.11	72.3	29.4	29.30	35.56	14.26
4	53.1	1.99	72.9	31.3	27.97	38.71	14.26
5	52.7	0.00	72.9	31.9	14.65	39.48	14.26
6	50.0	2.11	72.3	30.3	29.30	36.82	14.26
7	50.5	1.37	71.2	31.9	23.98	37.31	14.26
8	50.4	1.06	70.5	32.7	22.64	37.24	14.26
9	50.5	2.17	70.9	32.3	29.30	37.31	14.26
10	52.7	0.00	71.6	32.3	14.65	38.29	14.26
11	52.0	1.37	71.4	32.2	23.98	37.87	14.25
12	50.4	0.00	70.9	33	14.65	38.29	14.26
13	50.7	0.00	70.2	33.6	14.65	37.8	14.26
14	46.8	1.06	70.0	33.3	22.64	37.24	14.26
15	50.0	1.06	70.7	33.7	21.31	38.64	14.26
16	50.4	1.06	69.4	35	21.31	38.5	14.26
17	48.2	0.00	68.0	36.7	14.65	38.43	14.26
18	50.2	0.93	68.9	35.5	21.31	38.43	14.26
19	50.0	1.68	68.5	36.1	25.31	38.57	14.26
20	50.4	0.00	68.5	36.3	14.65	38.78	14.26
21	48.6	0.87	68.0	36.6	19.98	38.36	14.26
22	50.0	0.00	67.6	37	14.65	38.08	14.27
23	50.0	0.81	67.8	36.6	19.98	37.94	14.27
24	50.9	0.00	66.4	38.3	14.65	37.59	14.27
25	49.1	0.00	66.0	38.5	14.65	37.52	14.27
26	48.4	0.00	66.9	37.2	14.65	38.15	14.27
27	49.6	0.00	65.7	39.5	14.65	39.48	14.27
28	50.0	0.00	64.6	42.5	14.65	39.97	14.27
29	51.4	0.00	64.0	43.7	14.65	39.48	14.27
30	50.2	0.00	63.3	44.5	14.65	39.41	14.27
31	50.9	0.00	63.1	44.7	14.65	40.32	14.27
32	49.1	0.00	64.0	44.3	14.65	38.64	14.28
33	48.4	0.00	62.6	44.5	14.65	39.34	14.27
34	49.6	0.00	63.3	44.3	14.65	39.27	14.27
35	50.0	0.00	62.2	45.8	14.65	39.27	14.27
36	50.7	0.00	60.4	48.8	14.65	39.34	14.28
37	46.8	0.00	59.5	50.5	14.65	39.76	14.28
38	50.0	0.00	58.6	53.5	14.65	39.69	14.28
Avg.	50.2	0.58	67.5	37.81	18.65	38.43	14.27

B. Guideline of Implementing LWD Devices on QC/QA for Unbound Material Layers

xxx.x.x.xx TM-xx, Modulus-based Construction Acceptance Testing of Unbound Material Layers with a Light Weight Deflectometer

xxx.x.x.xx.1 Apparatus

- Zorn ZFG Lab 3 lightweight deflectometer (LWD) with 6 in (150 mm) loading plate
- Zorn ZFG 2000 LWD with either 7.78-in (200-mm) or 12-in (300-mm) loading plate
- Ohaus MB120 moisture analyzer
- Other devices related to 6 in (150 mm) diameter Proctor test

xxx.x.x.xx.2 Procedure

This test method consists of two parts of tests and data analysis:

- Determination of regression coefficients via LWD test on Proctor mold
- Measurement of moisture content (MC) and LWD modulus in the field
- Acceptance evaluation of moisture content and field to target LWD modulus ratio

Determination of regression coefficients via LWD test on Proctor mold

The LWD test on Proctor mold test is an add-on testing to the Proctor test of compaction characteristics of soils. The following steps shall be used for performing an LWD test on Proctor mold.

Step 1. Based on optimal moisture content (OMC) obtained from the soil compaction characteristics test, plan a moisture content span for the acceptance criteria, such as OMC-3% to OMC. In addition, a series of dropping heights need to be decided according to the applied stress of the LWD device to be used in the field. For example, the Zorn ZFG 2000 LWD having 12-in (300-mm) loading plate applies 14.5 psi (100 kPa), while the same model that equipped with 7.78-in (200-mm) loading plate applies 25.4 psi (175 kPa).

Step 2. By following the planned target moisture contents, compact a specimen using modified compaction energy in method B or D as described in AASHTO T 180.

Step 3. Rest the mold on a stable solid foundation or concrete floor. Reattached collar to a trimmed specimen to help align placement of LWD plate. Carefully place the LWD with a 12-in (150-mm) diameter loading plate on top of the mold sample and rotate approximately 45° back and forth to seat the plate. Any lateral movement of the plate with successive drops should be minimized.

Step 4. Hold the rod as vertically as possible to make sure the falling height of weight represents the target applied stress P_{lab} . Apply six drops with falling weight by raising it to the designated LWD falling height and allowing the weight to fall freely without lateral movement. The first three drops are conducted for the seating purpose, while the rest three are measurement drops. The specimen after testing is considered disturbed and should not be used for other mechanical property related tests.

Step 5. Record data including deflections, applied stress, and LWD modulus (E_{lab}) on the datasheet or export them from the data logger.

Step 6. Extrude the specimen from the mold and take three representative soil samples from the top, middle, and bottom of the specimen, respectively, to measure the moisture content of the tested specimen (MC_{lab}) by oven-drying method.

Step 7. With E_{lab} , MC_{lab} , and P_{lab} obtained from the LWD test on Proctor mold conducted at designated applied stress and moisture content span, determine regression coefficients a_i for

regression Equation (2) by putting them into Equation (1). The Solver in MS Excel may be helpful in doing regression for this step.



LWD test on Proctor mold

$$E_{lab} = a_0 + a_1 \times MC_{lab} + a_2 \times MC_{lab}^2 + a_3 \times P_{lab} + a_4 \times P_{lab}^2 \quad (1)$$

$$E_{target} = a_0 + a_1 \times MC_{field} + a_2 \times MC_{field}^2 + a_3 \times P_{field} + a_4 \times P_{field}^2 \quad (2)$$

where

E_{lab} = LWD modulus determined by LWD test on Proctor mold (LWD lab test), (kPa),

a_0, \dots, a_4 = regression coefficients,

MC_{lab} = moisture content of the sample in LWD lab test, (%),

P_{lab} = applied stress in LWD lab test, (kPa),

E_{target} = target LWD modulus in the field, (kPa),

MC_{field} = moisture content of the sample in the field, (%), and

P_{field} = applied stress in LWD lab test (kPa).

Measurement of moisture content and LWD modulus in the field

A series of testing points should be planned and marked at the construction site, on which both moisture content and LWD modulus measurements are to be conducted by following the steps listed below. Most importantly, the LWD device to be used in the field should be consistent with the device referred in the LWD test on Proctor mold.

Step 1. Arrange and mark testing points in the spacing of at least 10 ft (3 m) at the construction site with color spray.

Step 2. Level and smoothen an area approximately larger than that of the LWD plate at the testing point. Carefully place the loading plate of LWD ZFG 2000 onto the flat soil and rotate approximately 45° clockwise and counterclockwise to seat the plate, then dock the LWD onto its loading plate.

Step 3. Hold the rod vertically and then apply six drops with dropping weight, three seating drops followed by three measurement drops, by raising the falling weight to the designated LWD height and allowing it to fall freely without lateral movement. The falling height corresponds to applied stresses P_{field} .



LWD test in the field



Ohaus MB120

Step 4. Record data including deflection, applied stress, and LWD modulus (E_{field}) on the datasheet or export them from the data logger.

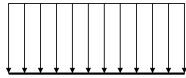
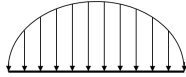
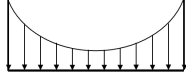
Step 5. Collect the soil sample with a sealable container from the location where the LWD plate was placed immediately after finishing the LWD test, so that the water in the soil can be kept as much as possible. Then put the collected soil sample into the Ohaus MB120 for moisture content (MC_{field}) measurement.

Step 6. Correct measured LWD modulus via Equation (3) with correct parameters including the stress distribution factor A and Poisson's ratio ν obtained from Tables 1 and 2 based on the type of tested soil.

Table 1 Typical Poisson's ratio values for different geomaterials from MEPDG.

Material	Range of values	Typical value
Untreated granular materials	0.30-0.40	0.35
Cement-treated granular materials	0.10-0.20	0.15
Cement-treated fine-grained soils	0.15-0.35	0.25
Lime-stabilized materials	0.10-0.25	0.20
Loose sand or silty sand	0.20-0.40	0.30
Dense sand	0.30-0.45	0.35
Saturated soft clays	0.40-0.50	0.45
Silt	0.30-0.35	0.32
Clay (unsaturated)	0.10-0.30	0.20
Sandy clay	0.20-0.30	0.25
Coarse-grained sand	0.15	0.15
Fine-grained sand	0.25	0.25

Table 2 Typical Poisson's ratio values for different geomaterials from MEPDG.

Soil type	Factor (A)	Stress distribution
Mixed soil (uniform)	π	
Granular material (parabolic)	$\frac{3\pi}{4}$	
Cohesive (inverse-parabolic)	4	

$$E_2 = \frac{E_1 A_1 (1 - \nu_2^2)}{A_2 (1 - \nu_1^2)} \quad (3)$$

where

A_1 and A_2 = default and target stress distribution factors, respectively,

ν_1 and ν_2 = default and target Poisson's ratio, respectively,

E_2 = field LWD modulus (MPa) corrected with target parameters (A_2 and ν_2), and

E_1 = field LWD modulus (MPa) calculated with default parameters ($A_1 = \pi$ and $\nu_1 = 0.5$).

Acceptance evaluation of moisture content and field to target LWD modulus ratio

Modulus-based acceptance criteria start with moisture content evaluation. Only the moisture content of soil falls into the target moisture content range will the soil proceed to be evaluated with the field to target LWD modulus ratio.

Step 1. Compare moisture contents of testing points measured from the field with acceptable moisture content range. Testing points having moisture contents within acceptable moisture content

range are considered qualified, while points with moisture contents beyond the range are considered unqualified.

Step 2. Calculate the target modulus (E_{target}) of qualified points in Step 1 via Equation (2).

Importantly, the target moduli need to be corrected if the soil is compacted as a base course above subgrade, by entering the initial target modulus and thickness of base material, modulus of underlying subgrade, and radius of LWD loading plate into Equation (4), E_{target} is corrected to $E_{target-corr}$.

Step 3. Determine the field to target LWD modulus ratio for qualified points in Step 1, and evaluate soil compaction quality based on the modulus ratio for testing points.

$$E_{target-corr} = 1 / \left\{ \frac{1}{E_2 \left[\sqrt{1 + \left(\frac{h}{d} \sqrt{\frac{E_1}{E_2}} \right)^2} \right]} + \frac{\left[1 - \frac{1}{\sqrt{1 + \left(\frac{h}{d} \right)^2}} \right]}{E_1} \right\} \quad (4)$$

where

$E_{target-corr}$ = corrected target modulus (MPa) for the base material,

E_2 = modulus of the foundation (subgrade, or subbase plus subgrade) (MPa) measured by the LWD before base placement,

E_1 = target modulus (MPa) for the base material,

h = base layer thickness (m), and

d = LWD plate radius (m) used during field testing.